

Investigation of hydrocarbons in the naphthenic and paraffinic froth treatment tailings

by

Anagha Kiran

A thesis submitted in partial fulfillment of the requirements for the degree of

Master of Science

in

Chemical Engineering

Department of Chemical and Materials Engineering
University of Alberta

© Anagha Kiran, 2020

Abstract

The oil sands reserves in Northern Alberta is the primary energy source for many consumers. The production of saleable oil sands generates large amounts of tailings waters, which are stored in dykes or ponds due to the zero-discharge policy. As global demand increases, oil production increases, leading to the storage of large volumes of tailings. This results in an increase in the overall emissions and impacting a facility's environmental footprint.

The surface mining production process relies on the froth treatment process, which is responsible for producing two main streams: diluted bitumen froth and the waste tailings stream, known as froth treatment tailings (FTT). The addition of a paraffinic diluent or naphthenic diluent reduces the viscosity of the crude oil, the tailings streams from these processes are known as the paraffinic froth treatment tailings (PFT) and naphthenic froth treatment tailings (NFT). Paraffinic froth treatment process uses a mixture of alkanes while naphthenic froth treatment use a mixture of aliphatic, aromatic and naphthenic compounds. The focus of this thesis was on the froth treatment tailings (FTT) as this stream is known to have higher concentrations of hydrocarbons with trace amounts of solvents, despite the froth treatment tailings comprising 2% - 4% of the total tailings discharged by volume of the overall tailings. As well, this diluent is often found in the tailings stream.

While current industrial practices rely on naphthenic froth treatment tailings, individual operators are choosing to rely on the alternative, which utilizes paraffinic diluents to reduce the viscosity. Based on the previous studies performed, there was a need for

characterization studies of the hydrocarbons within this stream. Specifically, an understanding that the hydrocarbons exist in both the aqueous phase and the solids phases. Both tailings samples were centrifuged for separation into the aqueous and organic phases. Therefore, the separate studies on the filtered aqueous phase and the centrifuged solids were conducted.

Chloroform was used to extract the hydrocarbons from the aqueous phase. The pH (3.0, 2.0, 1.0) and temperature (20 °C, 40 °C and 60 °C) was varied for the liquid-liquid extractions. Attenuated Total Reflectance - Fourier Transform Infrared Spectroscopy (ATR-FTIR) was used to identify the functional groups of the hydrocarbons extracted. An increase in temperature led to slight increases in the O—H peaks for NFT and the PFT between 20 °C to 40 °C however, at 60 °C, the increase in temperature drove evaporation rather than the transfer of the acids from one phase to another.

Toluene and heptane extracted the hydrocarbons for the solids phase of the tailings. The extractions were performed at 20°C, 40°C and 60°C and for 0.5 hours, 1 hour, 2 hours, 4 hours and 6 hours. Ultraviolet-Visible Spectroscopy confirmed presence of metal porphyrins as all samples corresponding to the Soret bands and certain extraction conditions showed indications of the etioporphyrin or the octethylprophyrin groups. NMR studies showed the presence of aromatic and aliphatic groups in the extracts, as well as clusters of peaks in the aliphatic and the aromatic regimes. This analysis is better understood by obtaining NMR spectra using a high-resolution NMR. Overall, the estimates of the hydrocarbons from the centrifugation and the TGA studies for the NFT and PFT are 83.3% and 73.1%.

Acknowledgements

I am incredibly grateful for having Dr. Gupta as a supervisor through my master's journey. I want to thank him for including me in his group. Essentially, I am thankful for his patience, knowledge, positive and encouraging attitude, without which this journey would be arduous. I am incredibly grateful for Dr. Prasad's help and guidance throughout my masters. As well, I would not be able to perform a large portion of my experiments without the help of Dr. de Klerk. I appreciated your support and just pure enthusiasm for science and analytical techniques. I would like to thank Alberta Environment and Parks for providing the funding for the masters project which I have worked on.

I am thankful for the members of both my team and Dr. de Klerk's research group as they provided constant suggestions, feedback and many jokes. I would especially like to thank Dr. Deepak Pudasainee for your valuable advice and input with my work.

I want to thank Dr. Md Khan for showing me how to use the LECO TGA and the Rotary Evaporator, Cibebe, with the NMR, Priscilla with Ultraviolet-Visible spectroscopy and Dr. Kaushik Sivaramakrishnan for the FTIR. I want to thank Ankit, Garima, Lina, Felix and Adrianna for providing many experimental suggestions with my work. Of course, I would like to thank Dr. Natalia Montoya Sanchez for giving me an introduction in a research lab, her kindness and guidance.

I want to thank several of my friends inside and outside grad school as they have been a source of constant encouragement, coffee breaks and fun times! Especially, I would like to thank (in no particular order): Sanjula, Khyati, Reza, Hareem, Wasel, Himanshi, Aakanksha, Shruti, Lina, Akash, Gustavo, Nilesh, Shweta, Manika, Omnath, and Animesh for all your support.

I want to thank my parents and my extended family for providing me unconditional support. I wanted to thank my younger cousins as they kept asking me, "what are you learning today?" motivating me to keep learning and pushing to meet my goals.

Contents

Abstract	ii
Acknowledgements	iv
List of Figures	vii
List of Tables	x
List of Abbreviations	xii
1. Introduction	1
1.1. Overview of Oil Sands Mining Operations	1
1.2. Motivation	6
1.3. Thesis Outline	6
1.4. Objectives	7
2. Literature Review	8
2.1. Characterization of the froth treatment tailings	8
2.2. Overview of Solvent Extraction	10
2.3. Extraction methods for the liquid phase tailings	10
2.3.1. Description of the organic compounds in the tailings fluid	10
2.3.2. Extraction methods conducted in literature	12
2.3.3. Important parameters for the extraction of Acid Extractable Organics	16
2.3.4. Spectroscopic method to analyze these hydrocarbons	18
2.4. Characterization for the centrifuged solids in froth treatment tailings	18
2.4.1. History of studies performed on the centrifuged tailings solids	22
2.4.2. Solvent choices for the studies with centrifuged solids from the FTT	23
2.4.3. Analyzing the tailings solids post extractions	24
2.4.4. Analyzing the liquids post solvent extraction	25
2.5. Hypotheses	27
2.5.1. Hypothesis for liquid-liquid extractions	28
2.5.2. Hypothesis for solid phase extractions	28
2.6. Proposed Methods	29
2.6.1. Methods for the liquid phase extractions	29
2.6.2. Methods for the solid phase extractions	29
3. Analytical Techniques	30
3.1. Reagents and Materials Used	30
3.2. Equipment and Procedures	34
3.2.1. Rotary Evaporator	34
3.2.2. Mass Balance for Froth Treatment Tailings and their centrifuged solids	34
3.2.3. Centrifugation of the Froth Treatment Tailings	36
3.2.4. Procedure used for liquid-liquid extractions	39
3.2.5. Procedure used for solid-liquid extractions	40
3.3. Analyses Methods	41
4. Results and Discussion	46
4.1. Compositional breakdown from TGA experiments	46
4.2. Analysis for the aqueous phase for froth treatment tailings	51

4.3. Analysis of extracted centrifuged tailings solids	58
4.3.1. <i>Solid liquid extractions for the centrifuged solids from NFT.....</i>	58
4.3.2. <i>Solid liquid extractions for the centrifuged solids from PFT.....</i>	67
4.4. H-NMR studies for the froth treatment tailings.....	73
5. Summary and Conclusions	83
6. Recommendations for Future Work.....	85
Bibliography	87
Appendix A	91
A.1. Mass Balance using the TGA for FTT tailings	91
A.1.2. TGA experiments for the naphthenic froth treatment tailings	92
A.1.3. TGA Experiments for the Centrifuged Solids from NFT	94
A.1.4. TGA experiments for the PFT	96
A.1.5. TGA Experiments for the centrifuged solids from the PFT.....	98
A.2. Summary of the centrifugation experiments	100
A.3. IR spectra for the various samples.....	102
A.4. Diluted NMR spectra for the toluene and the heptane extracts	104

List of Figures

Figure 1.1. Overview of in-situ mining extraction process for bituminous deposits in Northern Alberta ^{1,2,7-9}	2
Figure 1.2. Detailed description for the in-situ mining process based on the process flow diagram of the oil sands mining facilities ^{1,10}	3
Figure 2.1. Reaction mechanism for the monocyclic carboxylic acids which influence the corrosion of the metal surfaces. R refers to the alkyl parents hydrocarbon chains ²¹⁻²⁵	11
Figure 2.2. Naphthenic acid structures from Athabasca bitumen, where R is the alkyl chain, Z is the hydrogen deficiency and m is the number of peripheral methyl units preceding the acidic group ²⁰	12
Figure 2.3. The chemical structures for the (a) chlorophyll precursor (b) heme precursor (c) general porphyrin structure (d) vanadyl octethylporphyrin (e) vanadyl etioporphyrin (f) vanadyl deoxophylloerythroetioporphyrin (DPEP) (g) vanadyl benzoetioporphyrin (h) vandyl mesotetraphenylporphyrin (i) nickel etioporphyrin (j) nickel deoxophyllerythroetioporphyrin ^{5,37,38,40}	21
Figure 3.1. The scheduled experiments for the naphthenic froth treatment tailings.....	32
Figure 3.2. The scheduled experiments for the paraffinic froth treatment tailings.....	33
Figure 3.3. LECO Thermogravimetric Analyzer – TGA 701 Instrument.....	35
Figure 3.4. (left) The Eppendorf Centrifuge 5430 used in the centrifugation for the separation of the components of the froth treatment tailings, (right) rotor used alongside the centrifuge for the separation of the tailings.....	37
Figure 3.5. Detailed experimental schematic describing the separation of the two types of the froth treatment tailings leading to the solid-liquid and liquid-liquid extractions..	37
Figure 3.6. Vacuum filtration set-up with: (1) glass pipette to insert samples (2) Millipore 0.45 micron filter paper (3) Buchner funnel with glass sample holder (4) clamp used to hold the flask and the Buchner funnel together (5) stopper to close the side arm of the funnel (6) Erlenmeyer flask used to collect the filtrate (7) vacuum pump.....	39
Figure 3.7. Detailed experimental schematic for the liquid-liquid extractions of the filtered aqueous naphthenic and paraffinic froth treatment tailings with chloroform at 20 °C, 40 °C and 60 °C, where the orange dots are representative of the polar hydrocarbons.....	40
Figure 3.8. Detailed experimental schematic for the solid-liquid extractions of the filtered aqueous naphthenic and paraffinic froth treatment tailings emulsion with heptane and toluene, performed at different temperatures and contact times. Blue dots are representative of the asphaltene aggregates.	41
Figure 3.9. ATR-FTIR used for the qualitative analysis of the chloroform extracts for various experimental conditions.....	43
Figure 3.10. (left) The Shimadzu UV-2700 Spectrophotometer used for the qualitative analysis of the toluene and heptane analysis; (right) interior of the spectrophotometer, with the back position for the baseline cuvette (highlighted in blue) and for the sample (highlighted in green).....	44
Figure 3.11. (left) Nanalysis 60 MHz NMReady – 60 Nuclear Magnetic Resonance (NMR) Spectrometer, (right) heating area for the samples used. The temperature set point was 30 °C.	45
Figure 4.1. Thermogram for the tailings emulsion under nitrogen atmosphere up to 350 °C, followed by a combustion period under air environment from 350 °C to 650 °C.	47
Figure 4.2. Thermogram for the tailings solids under nitrogen atmosphere upto 350 °C, followed by a combustion period under air environment from 350 °C to 650 °C.....	49

Figure 4.3. Derivative weight loss and temperature for: (a) PFT and NFT tailings emulsion from 25 °C to 650 °C; (c) PFT and NFT solids.....	50
Figure 4.4. Relative transmittance for the chloroform extracts from NFT collected at differing temperature: (a) T = 20 °C, (b) T = 40 °C and, (c) T = 60 °C.....	52
Figure 4.5. Relative transmittance for the chloroform extracts from NFT collected at differing pH: (a) pH = 3.0 (b) pH = 2.0 and (c) pH = 1.0.	53
Figure 4.6. Relative transmittance for the chloroform extracts from PFT collected at: (a) pH = 1.0 (b) pH = 2.0 and (c) pH = 3.0	55
Figure 4.7. Relative transmittance for the chloroform extracts from PFT collected at: (a) 20 °C, (b) 40 °C, (c) 60°C	55
Figure 4.8. UV Visible spectra for the toluene extracts of the NFT centrifuged solids (a) the spectra obtained at 7% dilution with pure toluene and (b) the spectra obtained at 30% dilution with pure toluene.....	60
Figure 4.9. UV Visible spectra for the toluene extracts for increasing contact time (a) the spectra obtained at 7% dilution with pure toluene and (b) the spectra obtained at 30% dilution with pure toluene.....	62
Figure 4.10. UV Visible spectra for the heptane extracts for increasing temperature (a) the spectra obtained at 7% dilution with pure toluene and (b) the spectra obtained at 30% dilution with pure heptane.....	64
Figure 4.11. UV-Visible spectra for the heptane extracts for increasing contact time (a) the spectra were obtained at 7% dilution with pure toluene and (b) the spectra obtained from undiluted samples.....	66
Figure 4.12. UV-Visible spectra for the toluene extracts for increasing temperature (a) the spectra obtained at 7% dilution with pure toluene and (b) the spectra obtained at 30% dilution with pure toluene.....	68
Figure 4.13. UV Visible spectra for the toluene extracts for increasing temperature (a) with 1% dilution and (b) the spectra obtained at 10% dilution with pure toluene	70
Figure 4.14. UV-Visible spectra for the heptane extracts for increasing temperatures (a) with 20% dilution (b) the spectra obtained without dilution.	72
Figure 4.15. UV-Visible spectra for heptane extracts with increasing time (a) 20% dilution with pure heptane and (b) the spectra obtained without dilution.	73
Figure 4.16. Low resolution H-NMR spectra for (a)NFT toluene extract for increasing temperatures, (b) NFT toluene extract for increasing contact times, (c) NFT heptane extract for increase temperatures, (d) NFT heptane extract for increasing contact times.	75
Figure 4.17. Low resolution H-NMR spectra for (a)PFT toluene extract for increasing temperatures, (b) PFT toluene extract for increasing contact times, (c) PFT heptane extract for increase temperatures, (d) PFT heptane extract for increasing contact times.	77
Figure 4.18. Aromatic-to-aliphatic ratios for the toluene extracts collected with increasing temperatures.	78
Figure 4.19. Aromatic-to-aliphatic ratio for the toluene extracts collected with increasing contact times.	79
Figure 4.20. Aromatic-to-aliphatic ratio for the heptane extracts collected at increasing temperatures.....	80
Figure 4.21. Aromatic-to-aliphatic ratio for the heptane extracts collected at increasing contact times.	81

Figure A. 1. The weight loss and the first derivatives for the naphthenic froth treatment tailings emulsion.....	92
Figure A. 2. The weight loss and the first derivative for the centrifuged solids from the naphthenic froth treatment tailings (performed in triplicate).....	94
Figure A. 3. The weight loss and the first derivative for the paraffinic froth treatment tailings emulsion, performed in triplicate.....	96
Figure A. 4. Thermograms for the centrifuged solids from the paraffinic froth treatment tailings performed in triplicate.	98
Figure A. 5. Infrared spectra for the comparison for the paraffinic and the naphthenic froth treatment tailings	102
Figure A. 6. IR spectra for the standard solutions for pure toluene, chloroform, distilled water and acetic acid.	103
Figure A. 7. NMR spectra with NFT toluene at different temperatures.....	105
Figure A. 8. NMR spectra for the NFT toluene extracts at different contact times	105
Figure A. 9. NMR spectra for the NFT heptane extracts at different temperatures.....	106
Figure A. 10. NMR spectra for NFT heptane extracts collected at different contact times	106
Figure A. 11. NMR spectra for PFT toluene extracts collected at different temperatures	107
Figure A. 12. NMR spectra for PFT toluene extracts at different contact times.....	107
Figure A. 13. NMR spectra for PFT heptane extracts at different temperatures	108
Figure A. 15. NMR spectra for PFT heptane extracts collected at different contact times.	108

List of Tables

Table 1.1. The components from several important streams in the mining operations (shown in Figure 1.2) of sand, fines, bitumen and water. All compositions were reported in weight percent ¹⁰ .	4
Table 1.2. Composition of froth treatment tailings from the naphthenic and the paraffinic processes used ^{1,2} .	5
Table 2.1. Summary of the feed conditions for different operators for the naphthenic froth treatment processes ¹ .	9
Table 2.2. Summary of the feed conditions for the various operators using paraffinic froth treatment processes ¹ .	9
Table 2.3. Summary of various extraction studies, and their conclusions ²⁸⁻³² .	14
Table 2.4. Various solvents used and their physical properties ³³ .	17
Table 2.5. Summary of the solubility parameters for the different solubility class in bitumen froth ³⁴ .	19
Table 2.6. The solvent properties for various classes of hydrocarbons used to extract asphaltenes from the solids ³³ .	24
Table 2.7. Soret bands for the vanadyl and nickel porphyrins from various sources ^{5,38,47} .	26
Table 2.8. Absorption Spectra for the different peripheral groups in organic solutions from the UV-Visible Spectra ^{46,48,49} .	27
Table 3.1. Summary of the composition of the naphthenic froth treatment tailings, paraffinic froth treatment tailings, organic solvents and acid properties used in this study.	31
Table 3.2. Multi-step heating method used for the thermogravimetric experiments on the froth treatment tailings samples.	36
Table 3.3. Compositional breakdown for the aqueous and the solids phases in the froth treatment tailings.	38
Table 4.1. Composition of the naphthenic and the paraffinic froth treatment tailings from the thermogravimetric studies.	47
Table 4.2. The composition of the centrifuged solids from the naphthenic and the paraffinic froth treatment tailings from the thermogravimetric studies.	48
Table 4.3. Composition for the NFT and PFT emulsion after centrifugation.	51
Table 4.4. Relative intensities for the chloroform extracts obtained at different pH and temperature for the naphthenic froth treatment tailings.	54
Table 4.5. Relative intensities for the chloroform extracts obtained at different pH and temperature for the paraffinic froth treatment tailings.	56
Table A. 1. The multistep heating method used for the TGA experiments for the naphthenic and paraffinic froth treatment tailings and their centrifuged solids.	91
Table A. 2. Initial and final masses for the naphthenic froth treatment tailings.	92
Table A. 3. Summary of the weight loss for the naphthenic froth treatment tailings emulsion and the average weight loss for the triplicates.	93
Table A. 4. Complete mass balance for the naphthenic froth treatment tailings.	93
Table A. 5. The sample names along with the initial and final masses for the TGA experiments using the centrifuged NFT solids.	94
Table A. 6. Summary of the weight loss for the centrifuged solids from the naphthenic froth treatment tailings.	95
Table A. 7. Mass balance for the centrifuged solids from the naphthenic froth treatment tailings.	95

Table A. 8. The sample names, alone with the initial and final masses for the TGA experiments using the paraffinic froth treatment tailings.....	96
Table A. 9. The summary of the weight loss for the paraffinic froth treatment tailings....	97
Table A. 10. Mass balance for the centrifuged solids for the paraffinic froth treatment tailings.....	97
Table A. 11. The sample names with the initial and final masses for the centrifuged solids from the paraffinic froth treatment tailings	98
Table A. 12. Weight loss for the individual and average for the centrifuged solids from the paraffinic froth treatment tailings performed in triplicates.....	99
Table A. 13. Mass balance for the centrifuged solids from the paraffinic froth treatment tailings.....	99
Table A. 14. Mass balance for the naphthenic froth treatment tailings and the paraffinic froth treatment tailings before and after the centrifugation experiments.	101

List of Abbreviations

AEO	Acid extractable organics
ATR-FTIR	Attenuated total reflectance - fourier transform infrared spectra
DCM	Dichloromethane
FTT	Froth treatment tailings
GHG	Greenhouse gases
H-NMR	Proton nuclear magnetic resonance
LLE	Liquid-liquid extraction
NA	Naphthenic acids
NAFC	Naphthenic acid fraction components
NFT	Naphthenic froth treatment
NRU	Naphtha recovery unit
OSPW	Oil sands process waters
PAW	Process affected water
PFT	Paraffinic froth treatment
SAGD	Steam assisted gravity drainage
SPE	Solid-phase extraction
TGA	Thermogravimetric analysis
TSRU	Tailings solvent recovery unit
UV-Vis	Ultraviolet visible spectroscopy

1. Introduction

1.1. Overview of Oil Sands Mining Operations

Heavy oil and bitumen resources are estimated at approximately 890 Gm³ (5.6 trillion barrels), with over 80% of the world's resources situated in Canada¹. The largest deposits are located in Alberta and are approximately 70% of the world's in-place bitumen estimates^{1,2}. There are three primary deposits: namely, Athabasca, Cold Lake and Peace River, and have an "in situ viscosity of > 1 Pa*s" and density around 1000 kg/m³ at reservoir conditions^{1,3}.

Crude bitumen found as oil sands ore, is a mixture of rocks, mineral matter, and natural gases. Due to the biogenic and abiogenic processes of marine life, and the bacterial degradation of the trapped subsurface liquids, the amounts of alkanes found in the reservoirs have depleted, increasing the concentrations of heavier and higher molecular weight hydrocarbons⁴. As a result, greater sulphur content, heavy minerals (such as vanadium, nickel and magnetite) and metalloporphyrins are observed^{1,5,6}.

Due to the viscous nature of the deposits of the Alberta oil sands, there are two methods of production, namely: (1) Steam Assisted Gravity Drainage (SAGD) and (2) Surface Mining. This thesis will focus on the reject tailings stream from the surface mining operations. The production of crude bitumen from surface mining operations, described in Figure 1.1 was patented initially by Dr. Karl Clark is the Clark Hot Water Extraction, which relies on adding caustic hot water to liberate the hydrocarbons from the reservoir matrix, which is processed downstream^{1-3,7}.

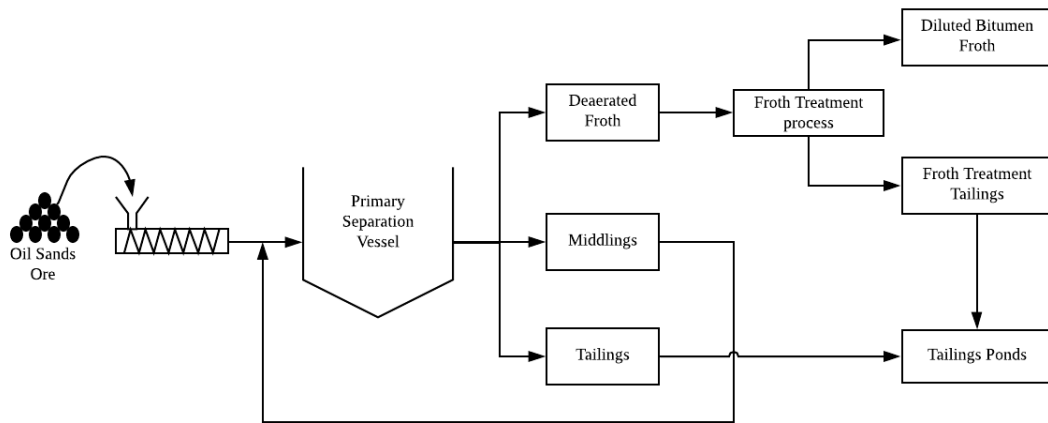


Figure 1.1. Overview of in-situ mining extraction process for bituminous deposits in Northern Alberta^{1,2,7-9}.

The detailed process flow diagram for surface mining facility is shown in Figure 1.2, with the compositional breakdown in Table 1.1. As shown, the crushed ore is mixed with hot water and strong base, producing an emulsion of the organic and the inorganic phases. Caustic reagents like sodium hydroxide, increases the surfactants in the bitumen froth, facilitating the liberation of the hydrocarbons from the ore^{1,7,9}. The surfactants, the operating pressure and agitation in the Primary Separation Vessel (PSV), enhances the liberation of bitumen from the ore^{1,9}.

This emulsion contains dissolved salts that are detrimental for construction materials used in upgrading and refining operations that occur downstream of the oil extraction². This emulsion is processed in the froth treatment process to create a pipeline-ready diluted bitumen product transported to the end consumer. The froth treatment process is a multi-step process that is responsible for removing the impurities (such as the clays and water) in the bitumen for final sale. Here, the first step is the addition of a lighter hydrocarbon diluent to bitumen to provide a density difference between the aqueous and oil phases, facilitating the gravity separation process².

The froth treatment process uses a lighter hydrocarbon as a diluent to deaerated bitumen froth. This diluted bitumen is further processed downstream with a variety of the separation equipment, producing the saleable product bitumen and a waste stream called the Froth Treatment Tailings (FTT)¹⁻³. This tailings from the Primary Separation Vessel (PSV) is steam stripped to recover any residual diluent and hydrocarbons from the water and solid mixture. The froth is then processed to reduce viscosity and for the removal of entrained solids and water^{1-3,7}. This recovered diluent stream is often reused in the upstream processes.

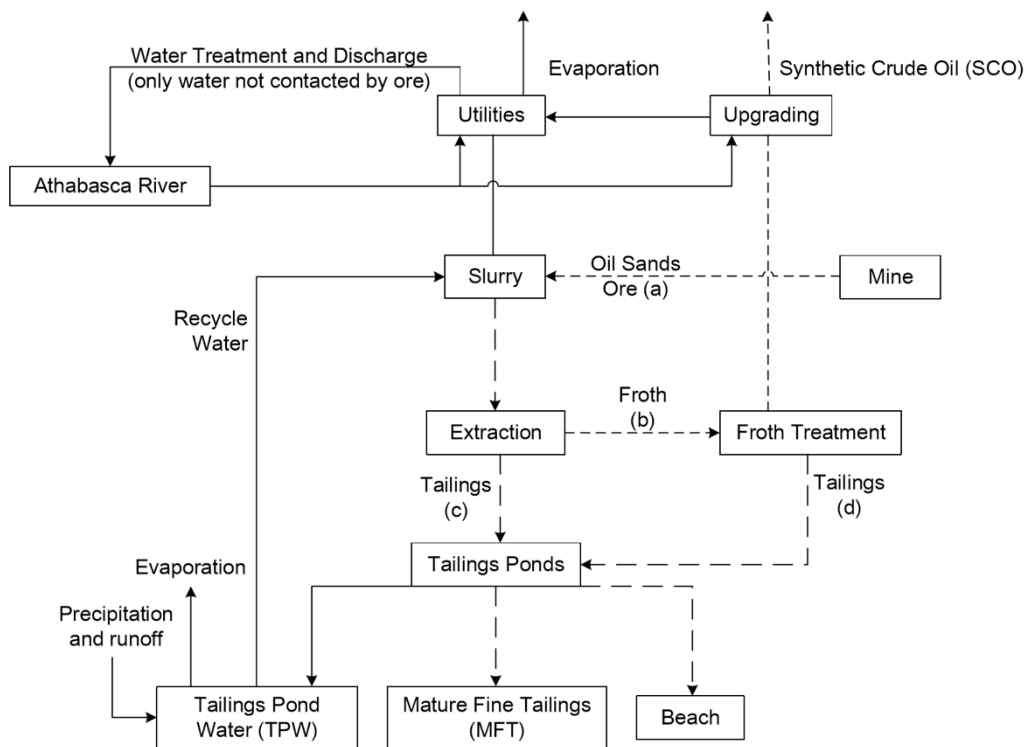


Figure 1.2. Detailed description for the in-situ mining process based on the process flow diagram of the oil sands mining facilities^{1,10}.

Table 1.1. The components from several important streams in the mining operations (shown in Figure 1.2) of sand, fines, bitumen and water. All compositions were reported in weight percent¹⁰.

Component/Stream	Oil Sands Ore (a) ^a	Froth (b) ^a	Tailings (c) ^a	Froth Treatment Tailings (d) ^a
Sand	70.4 %	3.4 %	45.0 %	6.6 %
Fines	15.1 %	10.9 %	8.3 %	20.4 %
Bitumen	11.1 %	47.8 %	0.7 %	3.1 %
Water	4.0 %	37.9 %	45.9 %	69.9%

^aAll compositions are reported in weight percent.

The diluent type for the froth treatment process influences the composition of the produced tailings. The two main types of froth treatment are the naphthenic froth treatment (NFT) and paraffinic froth treatment (PFT)^{1-3,8}. The NFT process uses naphtha as a diluent, while the PFT process relies on a light paraffin mixture^{1,2}. Naphtha diluents are the industrial convention employed to reduce the density of the oil, as it is produced alongside the extraction operations, eliminating the need to ship the diluent over vast distances¹. This diluent is a mixture of aliphatic, aromatic and naphthenic solvents. The optimal ratio of the diluent-to-bitumen is 0.6 - 0.8².

Paraffinic diluents are mixtures of lighter alkanes and olefins^{1,2}. These diluents result in the precipitation of asphaltene flocs (when added in sufficient volumes) and considered as an alternative to the conventional naphthenic diluents. One drawback of using the paraffinic solvents are the large volumes required, increasing operating costs¹¹.

Specifically, the Tailings Solvent Recovery Unit (TSRU) is responsible for the final removal of the diluent and the hydrocarbons before storage onsite due to the zero-discharge policy¹². Table 1.2 summarizes the compositional properties for the FTT from the naphthenic and the paraffinic froth treatment processes prior to the recovery units.

Table 1.2. Composition of froth treatment tailings from the naphthenic and the paraffinic processes used^{1,2}.

Components	Naphthenic froth treatment tailings (NFT), (%) ^a	Paraffinic froth treatment tailings (PFT), (%) ^a
Water	76.5 – 78.1	55.1 – 68.1
Bitumen	0.63 – 4.50	7.9 – 17.6
Mineral Solids	17 – 20	16.6 – 21.9
Diluent	1.27 – 2.00	2.8 – 11.8

^a The compositions are reported in weight percent.

The production of synthetic crude oil requires large volumes of fresh and recycled water, which can result in the discharge of 0.1 – 0.2 m³ of waste tailings per tonne of oil sands processed¹². Currently, these tailings are discharged into (ponds or dykes) where they are stored in atmospheric conditions, increasing the environmental footprint of oil sands industries^{1,2,12}. As the projected oil production increases, the increase in tailings results in higher volumes discharged into the tailings ponds. To combat increased water usage, the tailings water is recycled upstream in the process (also known as process-affected water or PAW). As PAW is recycled continuously from the tailing ponds, the concentrations of the residual hydrocarbons in the ponds increase, increasing the inherent hazards of the tailings stored in these ponds¹³. While a surface mining facility discharges a variety of tailings, this thesis will focus on the tailings from the froth treatment unit due to the nature of the compounds present. This is due to high concentrations of sulphide minerals, low levels of radioactive material and various aromatic and volatile compounds. Additionally, the percentage of FTT to the overall tailings is approximately 2% - 4% by volume of the overall tailings discharged^{8,13}.

Following the investigations performed by Pudasainee et al.¹⁴, through the thermogravimetric (TGA) studies. The objectives were increasing solvent recovery, predict the fugitive greenhouse gas (GHG) emissions and the quantification of trace elements and rare earth elements from paraffinic and naphthenic froth treatment tailings. From the TGA analyses, there were higher concentrations of lighter hydrocarbons in the NFT, lower amount of bituminous residue, and the rotary evaporator experiments yielded higher amounts of moisture. Trace element analysis documented a

lower concentration of Vanadium in the NFT, while a lower amount of Nickel in the NFT than the PFT¹⁴. Further experiments focussing on the polyaromatic hydrocarbon concentrations and asphaltenes in the FTT. Also, it identified the need for further analyses dedicated to the extraction of hydrocarbons.

1.2. Motivation

Recent policy changes that advocate for climate change is driving researchers to focus on various environmental concerns surrounding the tailings ponds. As identified by Small et al.¹², several gaps in literature that need to be addressed are (1) emission monitoring, (2) emission parameter estimation, (3) characterization of hydrocarbons and extraction of specific compounds. Referencing the gaps identified by Small et al.¹², and Pudasainee et al.¹⁴, the main focus of this investigation will be the recovery of the hydrocarbons from the aqueous and the solids phases of the tailings. While the study by Pudasainee et al. focussed greenhouse gas emissions, upgrading of the residual bitumen and quantification of rare earth and trace elements¹⁴. The focus of this thesis is to better understand the hydrocarbons from the tailings streams.

The purpose of this study is to apply various extraction techniques combined with qualitative analyses techniques to characterize the two different kinds of froth treatment tailings: the naphthenic froth treatment process and the paraffinic froth treatment process. The extractions for the aqueous and solid phases will be used for the characterization of the hydrocarbons.

1.3. Thesis Outline

In the first chapter, an overview of the oil sands mining operations, as well as the tailings produced by the froth treatment process, is presented. The significance of the current work, followed by the objectives, will be outlined.

The second chapter will focus on a literature review on the extraction techniques, along with the gaps which exist in literature.

The third chapter will summarize the materials used, the experimental procedures and the analysis methods used.

The fourth chapter will focus on the results and discussions from the extraction of the hydrocarbons from the aqueous phase, and solids phases for the naphthenic and the paraffinic froth treatment tailings.

The fifth chapter will summarize the findings from this thesis.

The last chapter has a section summarizing any recommendations for the experiments performed. There will be an Appendix which will summarize any other pertinent experimental information and data obtained.

1.4. Objectives

As the tailings streams contain various classes of hydrocarbons as shown by Pudasainee et al., a study that further extracting the hydrocarbons from the separate phases after centrifugation need to be performed¹⁴. Specifically, hydrocarbons such as naphthenic acids, and asphaltene residues will be focused upon.

In characterizing the solids and liquids phases of the tailings, the following investigations have been performed:

- To extract the hydrocarbons from the aqueous phases for the naphthenic and the paraffinic froth treatment tailings
- To extract the hydrocarbons from the solids phases for the naphthenic and paraffinic froth treatment tailings.

2. Literature Review

This section reviews the pertaining published literature for the extraction of hydrocarbons from the solid and the aqueous phases of the froth treatment tailings. This literature review begins by focussing on the contaminants within the aqueous phases, extraction methods used along with any identified gaps in the literature. Similarly, the second portion of the literature review focusses on the presence of asphaltenes within the bitumen froth and the tailings, followed by a review of the current methods and identified gaps in literature. The review of the literature and gaps identified will be followed by a summary of the hypotheses as well as the proposed methods.

2.1. Characterization of the froth treatment tailings

Surface mining process uses water to extract bitumen from the oil matrix. As a result, there are a variety of tailings produced differing based on the unit operations within the oil sands plant, the ore used as well as day-to-day operational variability^{1,2,15}. While there are a variety of different types of tailings with varying compositions depending on upstream process conditions, reservoir conditions, this thesis will focus on the froth treatment tailings.

The froth treatment tailings has a higher concentrations of the contaminants found in the froth treatment tailings (FTT) despite the lower volumes of FTT produced (~2% - 4% of the overall tailings disposed)^{13,15}. These include trace amounts of diluent, and bituminous residues such as asphaltenes¹⁶. The degradation of the diluents forms the volatile organic compounds (VOCs) resulting in the emissions surrounding the tailings ponds¹⁶. The discharge temperature of the FTT regardless of diluent choice is approximately 80 °C^{1,9}. Higher temperatures degrades the diluent into the VOCs.

Aside from the solvents, the tailings ponds contain traces of organic matter such as isoprenoids, terpenoid acids, and metalloporphyrins¹. Additionally, polar hydrocarbons such as carboxylic acids - isoprenoids, steroids, amino and naphthenic acids and polycyclic aromatic compounds are observed in groundwater surrounding these facilities^{1,15,17}.

The variation of the feed to the solvent recovery unit determines the composition of the FTT produced. The summary for the feed conditions is found in Table 2.1 and Table 2.2. The main assumption made in estimating these are a single flash drum and a three-phase accumulator to recovery and recycle diluent¹.

Table 2.1. Summary of the feed conditions for different operators for the naphthenic froth treatment processes¹.

	Suncor	Syncrude	Canadian Natural Resources Limited (CNRL)
Average ore content (%)	10.9	10.9	10.9
Temperature (°C)	Between 80 °C – 100 °C		
Composition (%)			
Water	78.1	76.5	90.6
Bitumen	0.6	4.5	1.4
Mineral solids	20	17	8
Diluent	1.3	2.0	0.05

In comparison with NFT, the paraffinic diluents are responsible for higher asphaltene precipitation once the optimal ratio of the solvent to bitumen is surpassed¹. However, this requires higher amounts of diluents required by the process, increasing the cost and, consequently, the environmental footprint of the facility. The precipitation of the asphaltenes within the FTT results in the solids and liquids phases which are comprised of water, mineral solids, free diluent, residual bitumen and asphaltene aggregates^{1,2,9,13}. The difference in the PFT and the NFT streams are the asphaltenes and maltenes or the residual bitumen in the tailings stream¹.

Table 2.2. Summary of the feed conditions for the various operators using paraffinic froth treatment processes¹.

	Shell (Albian)	Suncor (Fort Hills)	Total (Joslyn)	Imperial Oil (Kearl)
Average ore composition (%)	10.9	10.9	10.1	12.0
Temperature (°C)	80	77	93	90
Composition (%)				
Water	55.5	68.1	59.4	57.0
Bitumen	7.9	11.4	8.9	17.6
Mineral solids	16.6	17.7	19.8	21.9
Diluent	20	2.8	11.8	3.5

The regulatory requirements ensures that the facilities operate under a zero-discharge policy, therefore, the waste tailings are stored in dykes or ponds^{1,15}. As a result, there are over one billion tailings water collected in Northern Alberta¹⁵. As the tailings are deposited under open atmospheric conditions, emissions arising from the tailings ponds potentially add to the overall carbon footprint of each operating facility^{12,15}.

2.2. Overview of Solvent Extraction

Solvent extraction is the process which separates the compound or solute of interest to a favourable phase for further analysis or other industrial applications¹⁸. The variety of the solvent class are segregating according to their ability to solvate hydrocarbons of interest. The choice of solvent for the extractions are dependent on the affinity of polar hydrocarbons for certain solvent classes¹⁸. The parameters which affect solvent extraction are pH, temperature, solvent ratio to sample ratio, type of extraction experimental setup, stirring rate, contact time, and the contact time of solvent extraction for the sample^{18,19}.

2.3. Extraction methods for the liquid phase tailings

2.3.1. Description of the organic compounds in the tailings fluid

The aqueous phase of the tailings comprises of water and various types of dissolved organic matter. Recent research on the Oil Sands Process Water (OSPW) has documented of carboxylic acids, phenols, and other polyaromatic hydrocarbons^{15,20}.

Other contaminants present in the tailings ponds include benzene, toluene, xylene, phenolics, carboxylic compounds, alcohols, organic sulfides^{1,5,15}. Notably, carboxylic acids such as formic, propionic, butyric and acetic acids are observed regularly in the process affected waters (PAW) of crude oil extractions or upgrading^{4,5,17}. Additionally, heteroatomic organic molecules with nitrogen and sulfur such as sulfoxides, thiophenes, quinolines and pyridines have also been observed⁵. As well, metal salts are present with concentrations as high as 1000 ppm of both calcium and sodium ions⁹. The presence of these ions are indicative of the clay and fine solids dispersion⁹. As well, the sodium ions may be present as the carboxylate bases of the above mentioned acids.

Another property that influences the composition of the organic compounds in the aqueous phase is the pH of the water solution. If the solution is slightly basic (pH is approximately 8.0), the likelihood of observing carboxylates is higher. This observation is also applicable to longer chains (C14 to C30) alkanolic chains in the formation waters follow the same phenomenon⁵. The presence of carboxylic acids in the tailings stream leads to the corrosion of the steel alloys, comprising their structure integrity and shortening their lifetime, where the corrosion mechanism is described in Figure 2.1^{20,21-24}. The corrosion reaction is between the iron found in the steel alloys used in the refinery and the hydrogen sulphide present in the crude oils. This reaction results in the production of a metal carboxylate coating the metal's surface, and exacerbating the rate of corrosion²³⁻²⁵.

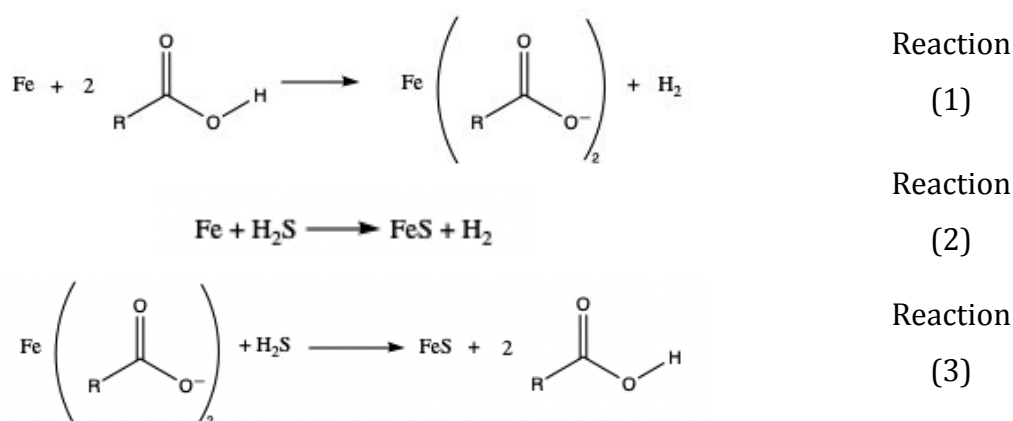


Figure 2.1. Reaction mechanism for the monocyclic carboxylic acids which influence the corrosion of the metal surfaces. R refers to the alkyl parents hydrocarbon chains²¹⁻²⁵.

Out of the earlier mentioned contaminants, off specific concern are naphthenic acids. These are naturally occurring “complex mixture[s] of the alkyl-substituted acyclic and cycloaliphatic carboxylic acids” carboxylic acids, which may contain fused or bridged structures, as shown in Figure 2.2²⁰. While there are evolving definitions of components of NA, the classical definition of NA that will be referred to in the thesis is the chemical formula for $\text{C}_n\text{H}_{2n+Z}\text{O}_2$. Here, n refers to the number of carbon atoms in the molecule, and Z refers to the hydrogen deficiency as a result of ring structures in the parent chain²⁰. Naphthenic acids are as a subset of a larger class of polar hydrocarbons, which synonymously known as “naphthenic acid fraction components” (NAFC) or “acid extractable organics” (AEO)²⁶. These are naturally occurring compounds when reservoirs

have not completely undergone catagenesis, or when the reservoirs undergo biodegradation by bacteria²¹. The presence of naphthenic acids has been documented in the groundwater surrounding oil sands developments^{1,51,5,15}.

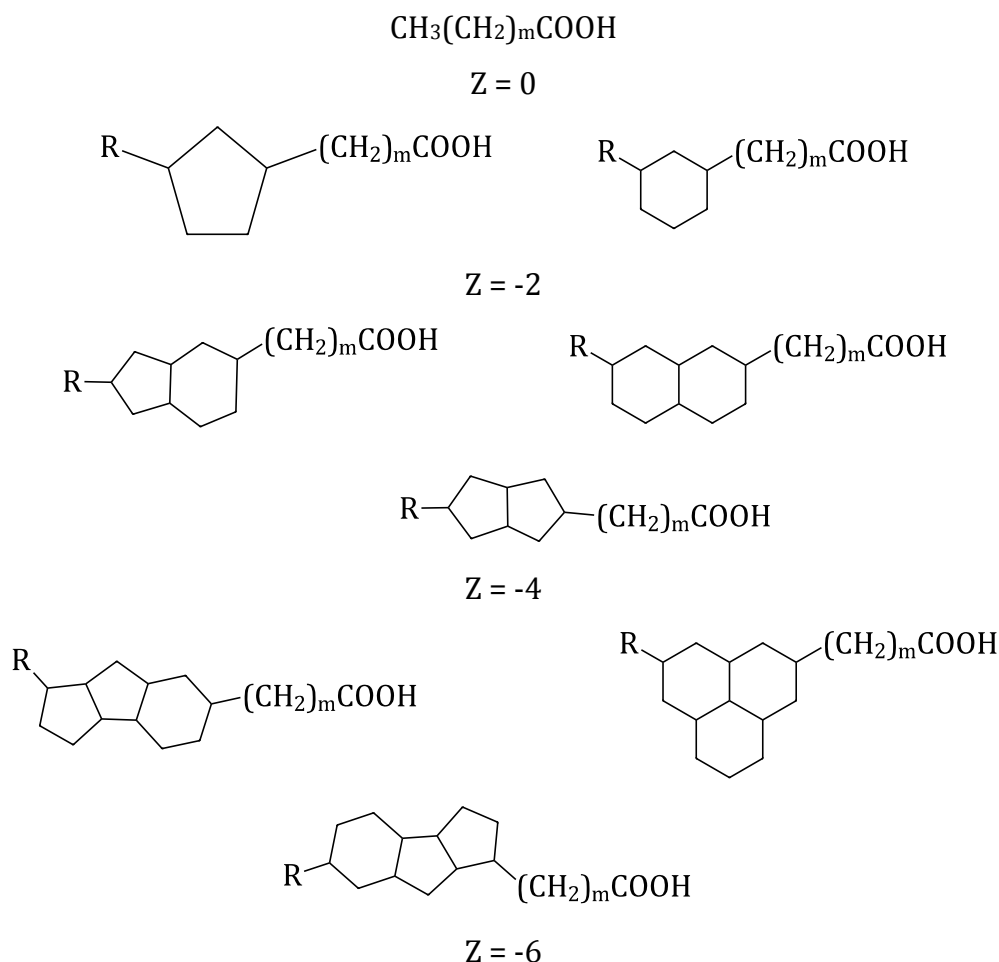


Figure 2.2. Naphthenic acid structures from Athabasca bitumen, where R is the alkyl chain, Z is the hydrogen deficiency and m is the number of peripheral methyl units preceding the acidic group²⁰.

2.3.2. Extraction methods conducted in literature

Separation of compounds between different phases can occur in a multitude of ways. The main separation of the acidic extractable organic compounds in aqueous phases are solid-phase extraction (SPE) and liquid-liquid extractions (LLE)^{18,19}. This mechanism is dependent upon solubilities of the solute in organic solvents, relative densities of solvents, and nature of the solute^{18,19}. The partitioning of the compound from one phase to another can be driven faster by altering pH, temperature and salinity. The relative

impacts of these factors can vary between different systems. These variables are important as they potentially increase the solubility of the polar acidic compounds in the organic solution.

Solid-phase extraction (SPE) is critical for the isolation of isomers of acidic compounds, and more minute analysis^{18,19}. SPE relies on the adsorption of the contaminant from the aqueous phase onto a solid surface^{18,19}. On the other hand, liquid-liquid extraction uses two immiscible solvents creating a concentration gradient, where the solute partitions into the preferred phase, until the chemical potentials in both phases are equal. Another widely applied technique for the analysis of carboxylic acids is the derivatization of the acidic compounds into ester forms, ensuring that these compounds are in their most stable phase^{13,27}. The stability of the compounds allows for better fragmentation of the ions for analysis with mass spectrometry analysis^{13,27}. Derivatization is used primarily for detailed chromatographic analysis^{13,27}, which at this stage will not be pursued. Since one of the objectives is to try to isolate these acidic fractions from the aqueous state, only liquid-liquid extraction procedures will be considered in this work. Table 2.3 summarizes relevant literature in the field, their feedstock, extraction methods, research outcomes and main learnings.

Table 2.3. Summary of various extraction studies, and their conclusions²⁸⁻³².

Feed source	Method of extraction	Analysis method	Conclusions	Ref.
Industrial OSPW samples were compared with standard solution of naphthenic acids	<ul style="list-style-type: none"> LLE with toluene, dichloromethane, hexane, ethyl acetate, and chloroform at room temperature 	Negative-ion electrospray orbitrap mass spectroscopy	Hexane selectively extracts oxygenated compounds better.	[28]
	<ul style="list-style-type: none"> Solid phase extraction using ENV + 	Negative-ion electrospray orbitrap MS	Better for less selective extraction of certain functional groups and is better for the full extraction of all the compounds	
OSPW from the Syncrude Oil Sands Development Areas	LLE (using dichloromethane) was performed after OSPW was adjusted to 2.5 with sulfuric acid using dichloromethane at room temperature	Fourier Transform Infrared spectroscopy	<ul style="list-style-type: none"> Semi-quantification was performed by following Jivraj et al. at different concentrations. Extracted NA and possibly other polar hydrocarbons affecting the results, which are assumed to be humic and fulvic acids. 	[29]
OSPW from the fluid fine tailings of the Syncrude Mildred Lake's oil sands development areas	LLE (using dichloromethane) was performed after OSPW was adjusted to 2.5 with sulfuric acid at room temperature	Mass spectrometry through GC X GC/TOFMS	Identified indane, tetralin, thiophenic, cyclohexanoic and adamantane type carboxylic acids.	[30]

OSPW from various oil sands development areas	Performed and compared computational calculations with varying the temperature, pH and the salinity of the samples to observe the extraction conditions in order to isolate the naphthenic acids	Comparison of experimental data and theoretical calculations.	<ul style="list-style-type: none"> • As pH increases the acidic components will partition into the water phase. • As salinity increases, the log (K_{NOW}) and log H increases resulting in an increase to the partitioning into the octanol phase. A reduction in solubility is noticed with an increase in salinity. 	[31]
OSPW from Albertan oil sands	Investigated the solvent type and the extraction pH for various other conditions for extracting acidic compounds	Performed liquid-liquid extractions with pentane, hexane, cyclohexane, dichloromethane, ethyl ether, ethyl acetate and water at pH of 2.0, 8.5 and 12.0.	<ul style="list-style-type: none"> • At pH 12.0, ethyl acetate has the highest extraction efficiency. • At pH 8.5, all solvents show the same extraction of the hydrocarbons. • At pH 2.0, there is improved extraction of the acidic compounds. 	[32]

As outlined in Table 2.3, the extraction parameters studied were limited to the pH and the solvent chosen. The effect of temperature, a critical parameter that governs the migration of polar organic compounds between phases, has yet to be extensively studied for this feedstock. As indicated by Kislik (2013), a rise in temperature between 50°C and 90 °C have slightly increased the extraction using solvents such as benzene and chloroform^{18,19}. This greatly has to do with an increased solubility of the acids at higher temperatures^{18,19}. While the studies with salinity indicate potential to increase partitioning between phases, this direction was not pursued.

The liquid-liquid extractions performed in Table 2.3 primarily used OSPW samples from the tailings ponds and did not use filtered FTT samples. The conclusions from the variety of studies in Table 2.3 may be replicated for the FTT. However, concentrations may be subject to change. A review of the effects of pH and temperature must be conducted. The AEO extracts is analyzed by either spectroscopic or chromatographic method for the characterization of hydrocarbons. While there are a variety of chromatographic techniques used for the separation of analytes from samples, the first step is confirming the presence of carboxylic compounds in the organic phases. Spectroscopy might be used in the identification of the polar hydrocarbons in the organic extracts. The next phase of studies involves further quantification, extensive chromatographic studies, which will not be performed for these tailings samples.

2.3.3. Important parameters for the extraction of Acid Extractable Organics

Solvent choice plays a vital role in the ability extract or dissolve the desired compounds from the samples used. One metric to assess this solvation ability is the Hildebrand Solubility parameter^{1-3,5,33,34}. Solubility parameter are functions of the total van der Waals forces, which affects the solvent properties of compounds in any solvent. Additionally, the relative polarity affects the compound's ability to migrate from one phase into another. A comparison of the physical properties of various organic solvents used in reviewed investigations (as summarized previously in Table 2.3) and other commonly used solvents are summarized in Table 2.4.

Table 2.4. Various solvents used and their physical properties³³.

Solvent Name	Chemical structure	Boiling point (°C)	Polarity	Solubility parameters (cal ^{1/2} cm ^{-3/2})
Water	<chem>H-O-H</chem>	100	100	23.4
Dichloromethane (DCM)	<chem>Cl-CH2-Cl</chem>	39.6	30.9	9.7
Chloroform	<chem>Cl-CHCl2</chem>	61.2	25.9	9.3
Ethyl Acetate	<chem>CC(=O)OCC</chem>	77.1	23.0	9.1
Ethyl Ether	<chem>CCOCC</chem>	34.6	11.7	7.4
Cyclohexane	<chem>C1CCCCC1</chem>	80.8	0.6	8.2
Toluene	<chem>Cc1ccccc1</chem>	110.6	9.9	8.9
n-Hexane	<chem>CCCCCC</chem>	69	0.9	6.9
n-Pentane	<chem>CCCCC</chem>	36	0.9	7.0

As the temperature played an essential role in extractions, the solvent's boiling point was to be below the highest temperature for their extractions. While dichloromethane was the solvent of choice for a few studies, due to the low boiling point, the extractions at higher temperatures may be performed. From parameters described in Table 2.4, chloroform was chosen as a solvent due to the similarities between chloroform and dichloromethane for its properties. The sample pH and temperature will be manipulated prior to the extractions.

2.3.4. Spectroscopic method to analyze these hydrocarbons

Once extracted, the compounds can be analyzed by a variety of spectroscopic and chromatographic methods. As NAFC found in extracts have a boiling point of above 200 °C, conventional gas chromatographic methods may not be suitable for the tailings samples. The spectroscopic methods are chosen, as it can be used for confirming the presence of certain hydrocarbons, which may be further analyzed by the above chromatographic studies. Prior to isolation of the individual compounds, the FTIR with a fixed path length, is used for the confirmation and the quantification of the carboxylic acids in the samples samples³⁵. The underlying principle relies on the absorption of photons of light, corresponding to the vibrational or the stretching bonds for the functional groups present in the molecule. The characteristic stretching peaks for carboxylic acids are at 1700 cm⁻¹ for the carbonyl bond and at 3000 cm⁻¹ for the hydroxyl bonds³⁶. Once the presence of carboxylic acids can be confirmed, quantitative studies may be performed.

Due to the time constraints, further analysis of the extracts has not been performed. Additionally, as there is a limited number of studies using FTT as a feedstock, it would be beneficial to study the extraction parameters rather than the detailed chromatographic analyses.

2.4. Characterization for the centrifuged solids in froth treatment tailings

Bitumen froth contains various kinds of hydrocarbons of different hydrocarbons classes such as: saturates, aromatics, resins and asphaltenes (SARA fractions), classified based on solubility of the compounds within the crude oils. The classes differ by the functional groups present and molecular weight, with the asphaltenes being the largest hydrocarbon class and the most complex concerning chemical structure and composition. The classes are often differentiated using the solubility parameters, as summarized in Table 2.5.

Table 2.5. Summary of the solubility parameters for the different solubility class in bitumen froth³⁴.

Solubility class of bitumen	Hildebrand solubility parameter (MPa ^{1/2})
Saturates	17
Aromatics	19
Resins	18 – 20
Asphaltenes	20 – 24

Asphaltenes are solid heterogeneous mixtures which precipitate in n-alkanes and not in aromatic solvents like benzene or toluene^{1,2,5,34}. They are comprised of 14% to 20% of the bitumen^{1,2,34}. Asphaltenes are characterized with the highest molecular mass due to the complex structures^{2,5}. The aggregates form flocs in solution with a minimal diameter of 0.3 µm, if the concentration of the asphaltenes reaches the critical concentrations³⁴.

The reported molecular masses for the precipitated asphaltenes range between 850 Da and 1240 Da^{1,2,34}. For instance, the asphaltenes precipitated with pentanes, hexanes and heptanes differ in quality³⁴. A higher molecular weight of the solvent results in the extraction of 'stickier' asphaltenes; further divided into two blocks on the basis of their boiling points: small blocks (boiling point below 538 °C) and large blocks (boiling point above 538 °C)³⁴. In certain conditions, the asphaltene compounds form aggregates in solution which behave like polymers and are strongly adsorbed to solids in the crude bitumen².

These aggregates contain aromatic, cyclic, aliphatic and traces of metalloporphyrins, composed of sulfur, nitrogen, oxygen and metallic ions of compositions (0.3% – 10.35%), (0.3% – 4.8%) and (0.6% – 3.3%), respectively^{1,2,5,34}. These metal elements such as iron, nickel and vanadium in small concentrations^{5,37,38}. The presence of the metallic cations are due to the primary and the secondary process from the chlorophyll and heme precursors^{37,39}. The primary process are the process in the source rock during diagenesis and secondary processes are the processes are in the sedimentary rocks surrounding the reservoir formation³⁷. The secondary processes focus on the degradation of the reservoir, where more thermal maturity decreases the concentrations of the porphyrins observed^{37,39}.

During the maturation process, the metalloporphyrins decomposes to become more complexed as they become parts of asphaltene functionality or may get adsorbed onto polar hydrocarbons such as naphthenic acids or a metal sulphide molecule^{5,37,39}.

The metals observed in crude oils are iron, lithium, potassium, sodium, strontium, copper, silver, vanadium, manganese, tin, lead, cobalt, titanium, gold chromium and nickel. The heavy metals in crude oils are found in porphyrin or non-porphyrin forms^{5,34,40}. Zinc, titanium, calcium and magnesium present themselves alongside the naphthenic acids as soaps (basic naphthenate salt) form. On the other hand, vanadium, nickel and copper naturally occur in porphyrin and non-porphyrin compounds alike^{5,37,40}. While there have been certain studies which focussed on the isolation of the non-porphyrin trace metal compounds, isolation of the individual metalloporphyrins weren't studied. The main focus was the identification of the nickel and vanadium porphyrins, which may be prevalent in the tailings.

The metalloporphyrins which have been in the higher concentrations are nickel and vanadium, reported at 11 ppm and 32 ppm, respectively³⁷. The presence of these compounds is indications of the reservoir maturity and provides insight into the upgrading and processability of this oils^{34,37,38}.

The metalloporphyrin structure is a derivative of the chlorophyll structure, where the oxovanadium complex (VO_2) or the nickel cation ion replaces the central metal complex, as described in Figure 2.3^{5,37,38,40}. The types of peripheral groups observed, depending on a variety of factors, such as type of crude, the age and crude fractionation process was performed. The peripheral groups have important effects on the electronic structures, as they increase conjugation, delocalizing the electrons, decreasing the energy required for absorption and causes bands at greater wavelengths.

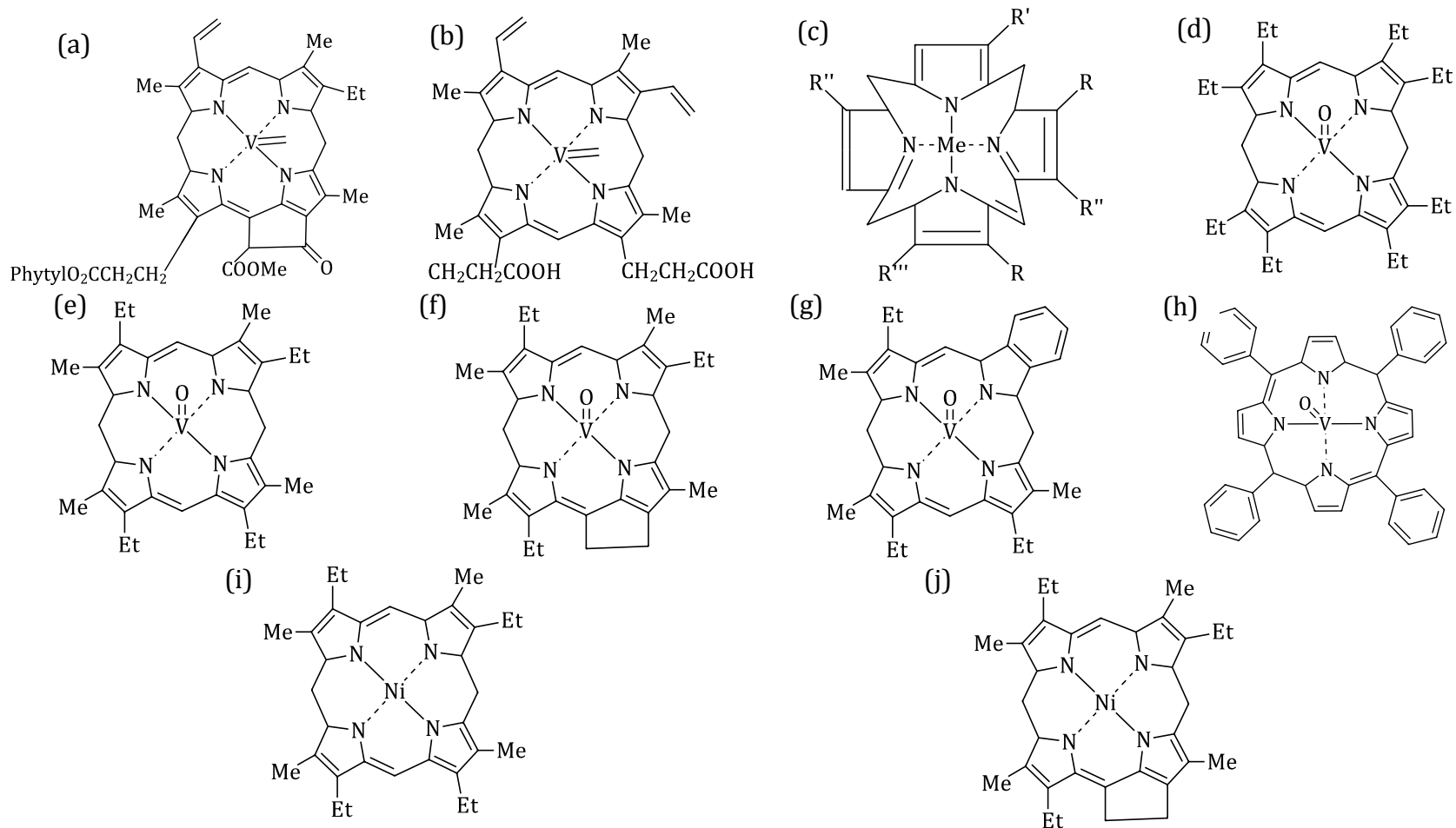


Figure 2.3. The chemical structures for the (a) chlorophyll precursor (b) heme precursor (c) general porphyrin structure (d) vanadyl octethylporphyrin (e) vanadyl etioporphyrin (f) vanadyl deoxyphyllerythroetioporphyrin (DPEP) (g) vanadyl benzoetioporphyrin (h) vanadyl mesotetraphenylporphyrin (i) nickel etioporphyrin (j) nickel deoxyphyllerythroetioporphyrin^{5,37,38,40}

2.4.1. History of studies performed on the centrifuged tailings solids

The characterization of organic solids can be performed in one of two methods: analysis of the solvents themselves or the extraction of the hydrocarbons from the surfaces of the clays.

Xu et al. studied asphaltene content through solvent extraction and gasification for the paraffinic froth treatment tailings²⁶. The hydrocarbons were extracted from the centrifuged solids using toluene, then by removing the toluene, a purified supernatant. The extraction efficiencies of the asphaltenes assessed by two main parameters: (1) amount of asphaltene recovered, and (2) aromaticity of the asphaltenes. Performing extractions at elevated temperatures 40 °C, 60 °C and 80 °C would increase the extraction efficiency, making it easier to characterize the solids. The secondary limitation is the focus on the naphtha treatment process FTT rather than the paraffinic froth treatment process.

Li et al.²⁵ investigated the solvent extraction conditions to comment on the extraction efficiency for individual parameters for the bitumen froth. The main extraction conditions investigated are solvent-to-oil ratio, temperature, stirring rate and contact time. The concentration of the bitumen extracted supernatant was then estimated by performing a mass balance and then fractionating the bitumen residue as per ASTM D4124. Temperature increased the extraction of the hydrocarbons in solution²⁵. Contact time also increases the total amount of hydrocarbons extracted, but is not specific to the type of hydrocarbon which could be extracted²⁵. On the other hand, the stirring rate and solvent to solid ratio had minimal impact in extraction efficiency²⁵. The optimal variables for contact time were times less than 1 hour, and temperatures below 95 °C. Any time or temperature higher than these criteria may reduce the recovered bitumen quality²⁵. The results from this study applicable primarily to the hydrophobic solvents; however, experiments observing extractions with a polar solvent (such as an alcohol) were not performed. The understanding of the extraction parameters from the different fractions of the raw bitumen are applicable to the tailings stream. The recovery of the hydrocarbons vary due to the composition of the hydrocarbons within the tailings stream. For the tailings stream of interest, the effect of manipulating parameters such as temperature, solvent and retention time. While there have been many studies that aim to address the presence of asphaltenes and metalloporphyrin structures

through combustion and gasification methods, an investigation which observes the presence of asphaltenes in the organic extracts and assessed using spectroscopic methods is an area requiring further research.

Investigations performed by Banda-Cruz et al., Alboudwarej et al., Yoon et al., and Dechaine et al. outlined the various spectroscopic techniques to analyse metalloporphyrins in the crude^{38,41-43}. The combination of spectroscopic methods, such as Ultraviolet-Visible spectrophotometry (UV-Vis), Electron Paramagnetic Resonance (EPR), proton Nuclear Magnetic Resonance (proton-NMR or H-NMR), and FTIR can analyze the trace metal ions present in the porphyrin structure. The characteristic porphyrin structures are responsible for absorption peaks in the ultraviolet spectra.

The solvent choice may alter the recovery of the metalloporphyrins as determined by Dechaine et al³⁸. Here, Dechaine et al., characterized the porphyrin content using a variety of solvents such as dimethyl sulfoxide (DMSO), dimethylformamide (DMF), methanol and pyridine³⁸. These studies utilize the fractionation of the gel permeation capillary tubes to extract the various asphaltenes. The solvent choice is crucial as it determines the extent to which the asphaltenes and the metalloporphyrin complexes dissolved in the organic solutions. Additionally, it may be possible that the organic compounds are adsorbed onto the solids in the FTT. Therefore, extraction parameters like solvent choice, temperature and contact time are vital to extracting these compounds.



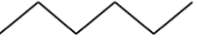
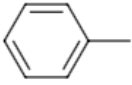
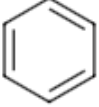
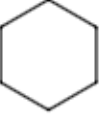
2.4.2. Solvent choices for the studies with centrifuged solids from the FTT

It should be noted that solvent choice is dependent on parameters such as polarity, the ability of the solvent to 'self-associate,' polar hydrogen bonding, aromaticity, cyclicity, boiling point and lastly, the safety aspect in performing these experiments²⁵. While 'good' solvents for solubilizing asphaltenes have a Hildebrand Solubility parameter range between 15.3 MPa^{1/2} to 23 MPa^{1/2} (further details summarized in Table 2.6), the criteria for solvent selection is not purely dependent on the numerical values of the parameters. The parameters are compared to the desired solubility classes for the bitumen froth. Due to the wide variety of

the compounds present in the oil sands froth, solvents which can dissolve both the aliphatic compounds and the polar compounds must be chosen.

Solvent choice dictates the fractions of the bituminous residue extracted, and the hydrocarbons still adsorbed on the clay surfaces. Once the supernatant are extracted, the methods for characterization for the supernatant are analysis of the liquids or analysis of the solid phase. Conducting these studies will allow us to better able to ascertain the relevant functional groups of the hydrocarbons which have migrated to the solvent phases. The comparison of various solvents and their inherent properties are summarized in Table 2.6.

Table 2.6. The solvent properties for various classes of hydrocarbons used to extract asphaltenes from the solids³³.

Solvent Name	Chemical structure	Boiling point (°C)	Polarity	Solubility parameters (cal ^{1/2} cm ^{-3/2})
n-Pentane		36.1	0.9	14.32
n-Heptane		98.4	1.2	15.34
n-Hexane		68	6.9	14.93
Toluene		110.6	9.9	18.20
Benzene		80.1	11.1	18.70
Cyclohexane		80.8	0.6	16.77

2.4.3. Analyzing the tailings solids post extractions

Adegoroye et al. characterized the organics coated on the solids, the metal ions, from tailings prepared in the lab⁴⁴. A 30:70 heptane and toluene (heptol) mixture was used to separate

the bitumen froth⁴⁴. The elemental composition showed that the solids in the bitumen froth were rich in sulphur, titanium and iron. It should be noted, that these solids used by Adegoroye et al., are rich in carbonates, sulphides and adsorbed hydrocarbons rather than the FTT samples which will be studied here⁴⁴.

The IR spectra from the Diffuse Reflectance Infrared Technique (DRIFT) analysis showed the presence of aliphatic hydrocarbons (methyl and methylene groups), ketones (aromatic and aliphatic), and carboxylic acids^{36,45}. While the DRIFT technique confirmed the presences using the solids in the crude samples, the observations which we might notice are going to have lower concentrations here. Another technical challenge is the sample preparation which is more challenging for various repeating runs. Therefore, this direction will be pursued in this investigation.

2.4.4. Analyzing the liquids post solvent extraction

Once the supernatant has been collected and filtered, the specific functional groups identified through a medium of spectroscopic techniques. As asphaltenes are large aggregates containing several functional groups, several spectroscopic tools may be used to analyse different aspects of the asphaltic structure. For instance, FTIR analysis of the supernatant will show peaks at the characteristic wavelengths, which are signatures of functional groups present. Studies conducted in literature demonstrate that there were strong peaks at 2924 cm^{-1} , 2855 cm^{-1} , 1458 cm^{-1} and 1376 cm^{-1} ⁴². These corresponded to the aliphatic hydrogen bonds for the $-\text{CH}_2$, and the $-\text{CH}_3$, C—H stretching, and the $-\text{CH}_2$ bonds for the methylene structures in bitumen⁴². There were also peaks noticed in the C—O, corresponding to the ether region, found at 3052 cm^{-1} for the aromatic rings, and at 3453 cm^{-1} , corresponding to the O—H and N—H stretching bonds⁴². Earlier, as FTIR is used to confirm the presence of the organic functional groups present, any information pertaining to the quantify or the structure of the backbone molecules cannot be ascertained. Therefore, FTIR spectroscopy are combined with other techniques such as UV visible, fluorescence spectrophotometry, Carbon NMR and Proton NMR to understand various properties of the porphyrins extracted.

Ultraviolet-Visible Spectroscopy (UV-Vis) for the bitumen crude revealed strong peaks for the vanadyl porphyrins at 410 nm and a weak peak or shoulder between 560 and 580 nm which is characteristic for the α band found in nickel porphyrins⁴². Following the observations by Dechaine et al., and D'Souza et al., any structural differences the peripheral groups for the metalloporphyrins resulted in the shift between 500 nm - 600 nm^{38,46}. The absorption bands for specific porphyrins, as well as any present peripheral compounds, may result in shifts of certain absorbances. Table 2.7, the effects of peripheral groups and their corresponding absorption bands are summarized in Table 2.8. The main difference between the tables are the solvents used. The main differentiating factor there the positions of the Soret bands for the variety of studies described are attributable to the type of spectrometer used, solvent used for extraction and the nature of the crude samples from which the metalloporphyrins were extracted.

Table 2.7. Soret bands for the vanadyl and nickel porphyrins from various sources^{5,38,47}.

Metalloporphyrin	Soret band (nm)	α band (nm)	β band (nm)	Ref.
Vanadyl Porphyrin	408 - 410	531	570	[5]
Nickel porphyrins	390 - 395	514	550	[5]
General metal porphyrins	410	N/A ^a	N/A ^a	[47]
Vanadyl etioporphyrin	406.6	570.7	532.8	[38]
Vanadyl octethylporphyrin	407.3	570.9	533.2	[38]
Vanadyl deoxophylloerythroetioporphyrin (DPEP)	410.5	573.0	533.3	[38]
Vanadyl benzoetioporphyrin	414	578.7	544.7	[38]

*All fractions showed a maximum absorption peak at 410 nm similar to Soret band.

^aDid not report the absorption band.

Table 2.8. Absorption spectra for the different peripheral groups in organic solutions from the UV-Visible Spectra^{46,48,49}.

Metalloporphyrin	Soret band (nm)	Organic solvent	Q bands (nm)				Ref.
			Q1	Q2	Q3	Q4	
Meso-tetraphenylporphyrin	417	N/A ^a	514	550	593	646	[48]
Meso-tetraphenylporphyrin	420	DCM	515	550	590	650	[49]
Nickel octylethylporphyrin	379	Benzonitrile	554	N/A ^a	740	838	[46]

^aDid not report the solvent used.

Results were typically combined with high resolution proton nuclear magnetic resonance (H-NMR) spectra⁴². The data from the H-NMR revealed the relative ratios of the hydrogens bonded to aliphatic, olefinic, naphthenic and aromatic hydrocarbons. The presence of surrounding protons affects the ability of the hydrogen atoms to resonate with the external magnetic field. The attached groups will be able to comment on the surrounding groups characteristics. The integrated areas under the peaks returns the relative numbers of the proton for the region the peaks occur.

By varying the solvent, temperature, and retention time, the hydrocarbons can vary. Performing a combination of these analyses as mentioned above, we will be able to understand the types of hydrocarbons present and comment on any changes observed between the different extraction conditions.

2.5. Hypotheses

A review of the relevant literature in the previous sections revealed areas for further research. These are the characterization research for the froth treatment tailings and a comparison between the various types of froth treatment tailings.

For the aqueous phase, while there is data outlining the presence of various acidic fractions and the methods for extractions, there is little comparing these fractions together in the

different froth treatment tailings. The extraction methods used for a majority of these studies are liquid-liquid extractions, for different solvent types and pH varying between 5.0 and 2.0 have been performed. However, the effect of temperature on the partitioning of these trace compounds has not been performed. As the bitumen froth has been studied extensively for the metallic porphyrin complexes, similar techniques for the identification of metalloporphyrins in NFT and PFT are yet to be conducted. It is expected that the waste stream from the froth treatment facility contain traces of asphaltenes and metalloporphyrins may be present in small concentrations. The comparison between the hydrocarbons extracted for the different tailings with different extraction conditions such as temperature and retention time are scarce. Solvent choices, extraction temperature and contact time dictate not only the amount but also the type of hydrocarbons extracted. An increase in temperature and contact time should increase the types of hydrocarbons extracted, while an aliphatic solvent will dissolve aliphatic hydrocarbons and aromatic solvents dissolve aromatic hydrocarbons better.

2.5.1. Hypothesis for liquid-liquid extractions

Temperature and pH affect the ability of the organic solvents to extract or partition hydrocarbons from the aqueous samples. A fair number of studies use dichloromethane as a solvent, and as solvents like chloroform have similar polarity and solubility parameters, an alternative to DCM was chosen to observe the extraction at 40 °C and 60 °C. The pH which will be measured is 3.0, 2.0 and 1.0. A decrease in the pH and increase in temperature should increase the extraction of the dissolved organic matter. The increase in temperature would increase the solubility of the carboxylic acids in the organic phases.

2.5.2. Hypothesis for solid phase extractions

As there are various classes of hydrocarbons in the tailings stream, a combination of polar and non-polar solvents like toluene and heptane will be able to extract different hydrocarbons and metalloporphyrins at different conditions. Since the extraction process often has two competing forces: liberation from the adsorbed clay surfaces and the

extraction of the hydrocarbons from the emulsion. This may be addressed by performing these extractions at a higher temperature, (ie, 40 °C and 60 °C). As the boiling point of DCM is at 34 °C, toluene would be a better solvent for the extraction at higher temperatures.

2.6. Proposed Methods

The proposed methods for the liquids and solids phase extractions are summarized in the following sections. Before performing these extractions, experiments will be performed using centrifugation, rotary evaporator and the thermogravimetric analysis to characterize the feedstock.

2.6.1. Methods for the liquid phase extractions

Chloroform is used to extract the AEO from the acidified filtered aqueous solutions for the paraffinic and the naphthenic froth treatment tailings. These extractions will be performed at room temperature, 40 °C and 60 °C and at different pH varying from 3.0, 2.0, and 1.0. These extracts and aqueous solutions will be collected. Once collected, contents in the chloroform extracts will be analyzed using FTIR spectroscopy to confirm the presence of any polar hydrocarbons.

2.6.2. Methods for the solid phase extractions

The asphaltenes from the solid phases will be extracted using an aromatic and an aliphatic hydrocarbon. The extractions will be performed at room temperature, 40 °C, 60 °C, 0.5 hour, 1 hour, 2 hours, 4 hours and 6 hours. These extracts will then be analyzed using UV-Visible spectra and low-resolution H-NMR to compare the aromaticity and the aliphaticity of the extracts for the conditions which have been studied.

3. Analytical Techniques

3.1. Reagents and Materials Used

For this study, samples provided by the industrial client for paraffinic and the naphthenic froth treatment tailings were used. The solvents used in this study are toluene, chloroform and heptane. The brand name, solvent purities are summarized in Table 3.1. Glassware and equipment which was in contact with the tailings solids were cleaned with toluene and air-dried. Acetone was used to clean all glassware and equipment, which the aqueous phase of the tailings. Acetone was used to clean the cells for the UV-Visible Spectroscopy and the Attenuated Total Reflection Fourier Transform Infrared spectroscopy. Both cells for the UV-visible spectroscopy and the Attenuated total Reflection Fourier Transform Infrared spectroscopy were air-dried before any measurements. The LECO Thermogravimetric Analyzer (TGA) crucibles were cleaned with distilled water and stored overnight in a furnace at 130 °C. Concentrated sulfuric acid was used to prepare standard solutions as a buffer for the pH meter and for reducing pH for the aqueous samples.

Table 3.1. Summary of the composition of the naphthenic froth treatment tailings, paraffinic froth treatment tailings, organic solvents and acid properties used in this study.

Naphthenic Froth Treatment Properties			
Component		Percentage (%) ^a	
Lighter hydrocarbons and water		33.5	
Heavier hydrocarbons		57.1	
Bituminous residue		1.9	
Mineral solids		7.6	
Paraffinic Froth Treatment Properties			
Component		Percentage (%) ^a	
Lighter hydrocarbons and water		75.4	
Heavier hydrocarbons		19.2	
Bituminous residue		0.5	
Mineral solids		3.5	
Solvent Properties			
Solvent	Brand	Purity (%) ^b	CAS Number ^c
Toluene	Fisher Chemical	99.9	108-88-3
Acetone	Fisher Chemical	≥ 99.5	67-64-1
Heptane	Sigma-Aldrich	≥ 99	142-82-5
Chloroform	Fisher Chemical	99	67-66-3
Hydrochloric Acid	Fisher Chemicals, J.T. Baker	36.5 – 38.0	7647-01-0
Acetic Acid, Glacial	Fisher Chemical	99.7	64-19-7
Chloroform – D	Sigma-Aldrich	99.8	865-49-6

a. The percentages reported are in weight percent.

b. The purity (on a mass basis) guaranteed by the supplier

c. CASRN. Chemical Abstracts Services Registry Number

A summary of the planned experiments to be performed for the NFT and PFT are described in Figure 3.1 and Figure 3.2.

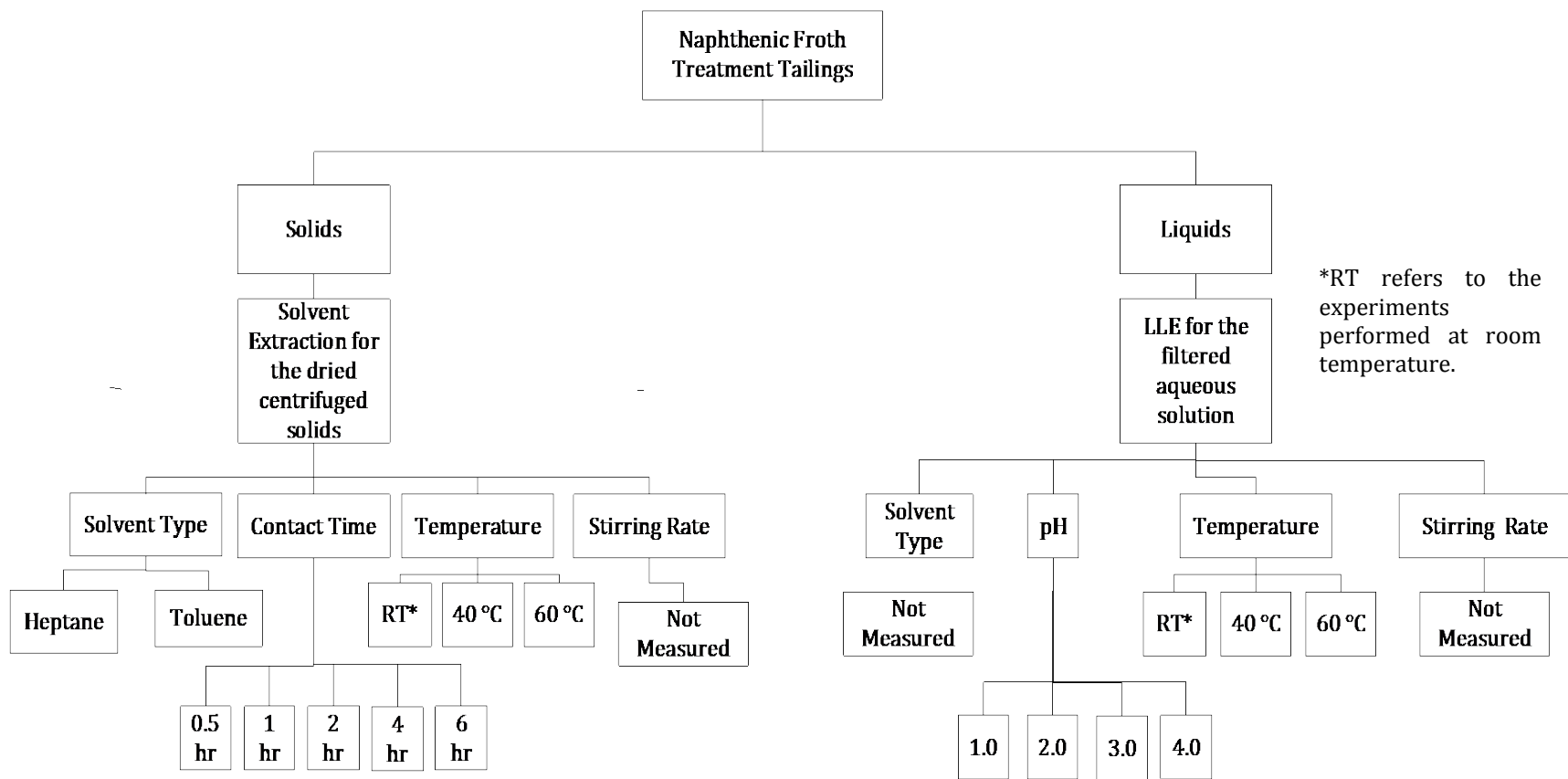


Figure 3.1. The scheduled experiments for the naphthenic froth treatment tailings.

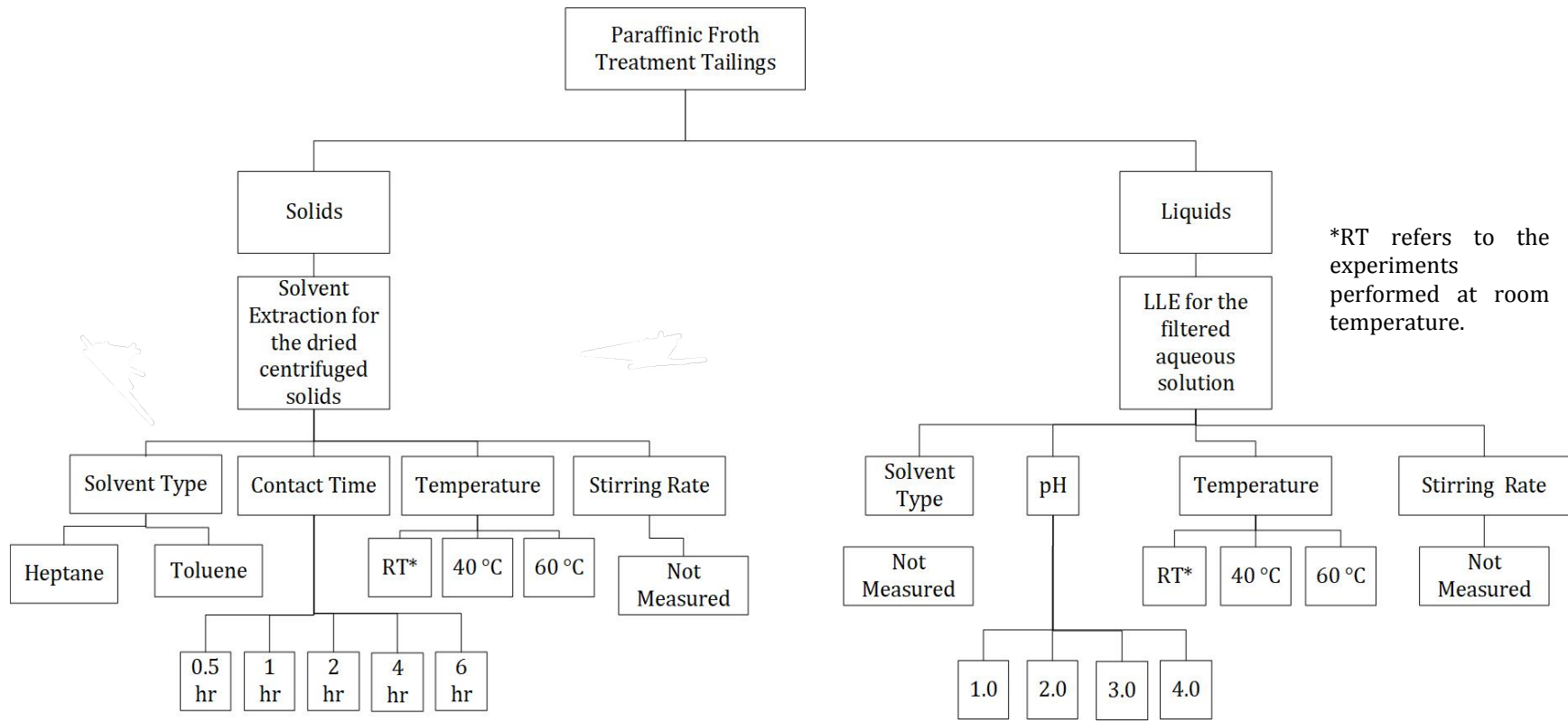


Figure 3.2. The scheduled experiments for the paraffinic froth treatment tailings.

3.2. Equipment and Procedures

3.2.1. Rotary Evaporator

The NFT and the PFT samples were thoroughly shaken and then placed in the Heindolph Rotary Evaporator. This rotary evaporator was operated at 700 mbar using a vacuum pump. Heating oil was used to uniformly heat the samples at 140 °C and 210 °C. The temperature was measured during the runs to ensure that the temperature of the heating oil used did not vary significantly. There were negligible differences between the runs for the temperature set point and the actual temperature measurement. 100 mL of tailings samples measured and recording using a graduated glass cylinder for volume and Mettler Toledo weighing scale for the weight in g.

The samples remained in the hot bath for approximately 1 hour at 140 °C. Then the distillate was collected. The sample weight was recorded again, and the rotary evaporator temperature was adjusted to 210 °C. To ensure that the oil temperature was constant throughout the experiment, a thermometer was used to measure the oil bath temperature twice during the time interval. First measurement was taken as the flask was lowered into the bath and second measurement was halfway through the experiment. Once the sample was done heating at 210 °C for 1 hour, the distillate was collected, and weight recorded.

3.2.2. Mass Balance for Froth Treatment Tailings and their centrifuged solids

The naphthenic and the paraffinic froth treatment tailings were prepared in triplicate for the LECO TGA runs. The triplicates were performed to minimize variability in the TGA profiles with the data obtained. The targeted weights for the tailings emulsion was between 4.50 g and 5.00 g. The samples and the ceramic crucibles were weighted using a Mettler Toledo XS105 Dual Range balance with 10 µg readability with a range of 0 to 105 g. The tailings samples were vigorously shaken for a minute and poured into a smaller beaker, stirred again and poured into the crucibles. This was done carefully to avoid getting any outside of crucibles. The crucibles were placed into the middle of the appropriate compartments carefully. Triplicates were measured to minimize the variability between the different

samples. Nitrogen was used for the evaporation step and the air was used for the combustion step. The components remaining after the combustion step are assumed to be ash from the combustion of asphaltenes and residual mineral solids. The initial masses of the empty crucibles, and with the samples were recorded before and after the TGA run was completed. The weight loss, the derivative of the weight loss and the temperature of the furnace was collected post run. This procedure was repeated for both the tailings. This was performed for the NFT, PFT and the solids after the centrifugation of the tailings to better understand the weight losses at different stages. The equipment and the multi-step heating method used is presented in Figure 3.3 and Table 3.2.



Figure 3.3. LECO Thermogravimetric Analyzer – TGA 701 Instrument

Table 3.2. Multi-step heating method used for the thermogravimetric experiments on the froth treatment tailings samples.

Step	Atmosphere	Start temperature (°C)	End temperature (°C)	Ramp rate (°C/min)	Hold time (min)	Total time (min)
Step 1	Nitrogen	25	80	5	5	16
Step 2		80	95	1	5	20
Step 3		95	100	1	5	10
Step 4		100	110	1	5	15
Step 5		110	165	5	5	16
Step 6		165	220	5	5	16
Step 7		220	275	5	5	16
Step 8		275	350	5	5	20
Ash 1	Oxygen	350	420	5	5	19
Ash 2		420	480	5	5	17
Ash 3		480	550	5	5	19
Ash 4		550	650	5	5	55

3.2.3. Centrifugation of the Froth Treatment Tailings

The separation of the tailings emulsion into the aqueous and the solids phases can be achieved via centrifugation. Centrifugation was chosen as a method for the separation of the solids from the liquids, whereby separation occurs based on the relative densities of the samples. The higher density material settles below while the lower density floats in aqueous phase. The Eppendorf Centrifuge 5430 with the Rotor F-35-6-30 was used. In this process, the gravitational forces and the centrifugation time are vital in ensuring proper separation of the materials. The speed and time for the centrifuge were, 7000 rotations per minute and half an hour, respectively. The samples were inserted in the 50 mL Corning Tubes with a conical bottom. The samples were centrifuged for different times, and the details of this can be found in Appendix A and the equipment is shown in Figure 3.4.



Figure 3.4. (left) The Eppendorf Centrifuge 5430 used in the centrifugation for the separation of the components of the froth treatment tailings, (right) rotor used alongside the centrifuge for the separation of the tailings.

For the centrifugation process, the tailings samples were shaken vigorously for 1 minutes and poured into a smaller beaker. The contents of the beaker were also thoroughly mixed before being poured into centrifuge tubes. Tubes placed diagonally across from each other were balanced within 0.50 grams. The weights of the centrifuge tube pre and post centrifugation were recorded. A schematic describing the following procedure is outlined in the Figure 3.5.

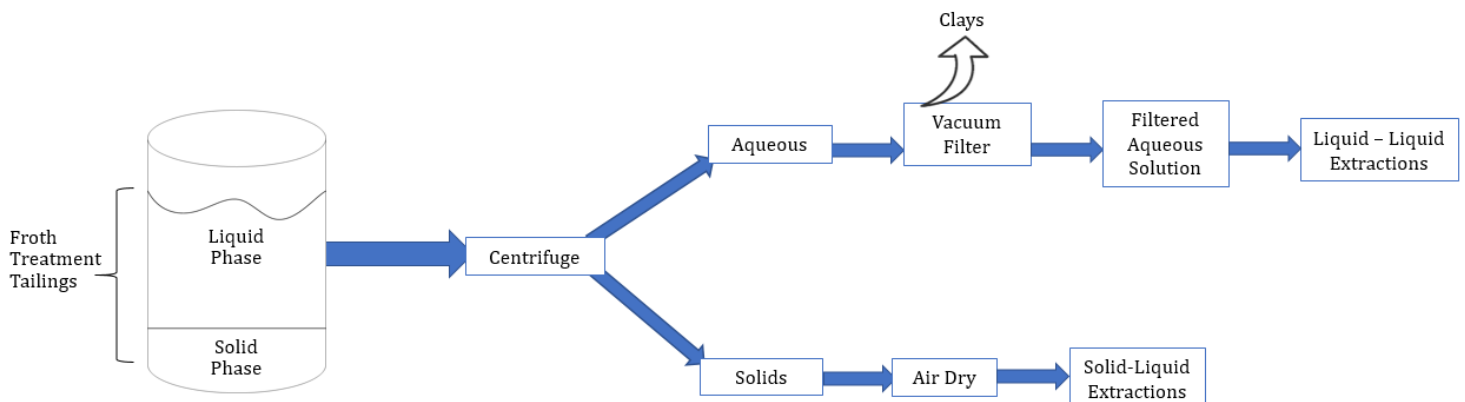


Figure 3.5. Detailed experimental schematic describing the separation of the two types of the froth treatment tailings leading to the solid-liquid and liquid-liquid extractions.

The composition of the aqueous and solids phase for the NFT and PFT are summarized in Table 3.3

Table 3.3. Compositional breakdown for the aqueous and the solids phases in the froth treatment tailings

Components	Aqueous phase ^a	Solids phase ^a
NFT	75.5%	24.5%
PFT	69.8%	30.2%

^aThe percentages reported are the weight percent.

The solids were collected and left in the fumehood to allow for evaporation of any residual liquids. The solids from different runs were homogenized to minimize the variability between the different days, and sample beakers. The solids were then used in the LECO TGA to for further analysis of the compositional breakdown.

The aqueous supernatant was collected and filter using the following set up as shown below in Figure 3.6. The filter paper used was the Millipore 0.45 μm filter paper of 47 mm diameter. The Millipore vacuum filtration unit was used, the cooling fluid temperature was set to 4 °C.

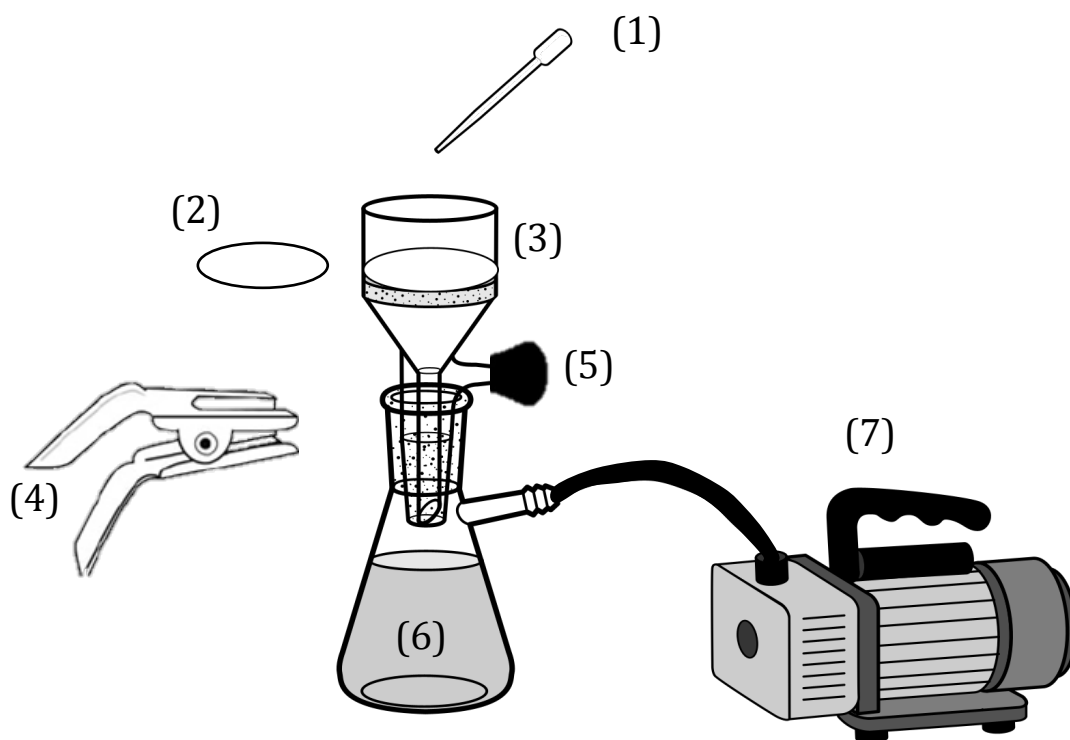


Figure 3.6. Vacuum filtration set-up with: (1) glass pipette to insert samples (2) Millipore 0.45 micron filter paper (3) Buchner funnel with glass sample holder (4) clamp used to hold the flask and the Buchner funnel together (5) stopper to close the side arm of the funnel (6) Erlenmeyer flask used to collect the filtrate (7) vacuum pump.

The filtered aqueous solution was collected in a glass jar and stored at room temperature. To ensure homogeneity, the filtrate from various runs were collected and stored together. Once collected, the procedures for the liquid-liquid extractions were performed.

3.2.4. Procedure used for liquid-liquid extractions

The liquid-liquid extractions were performed using vials and Oakton pH meter. Once the solution was acidified to the target pH, the aqueous and the organic phases were mixed. These extractions were performed over a hot plate and were constantly stirred at 150 rpm for half an hour before the solvent was added again for a second and third time. The samples were weighted using a Mettler Toledo XP1203S scale with maximum weighing capacity of 1210 g.

At higher temperatures and contact times, the samples were placed in a hot oil bath over a Fisher Scientific Isotemp hot plate, with the temperature probe inserted in the bath, without touching the glass of either the oil bath or the vials. When the stirring rate was maintained at 100 rpm per minute, the timer was started. For the higher temperatures, it was ensured that a blank sample was inserted inside the oil bath to ensure that it remained hot. The oil levels are to be maintained above the liquid levels and the jars lid was closed with a perforated lid to prevent excessive weight loss.

The top layer and bottom layers were collected using a 9-inch glass pipette and stored in different amber glass vials at room temperature. Once collected, these samples were ready for analysis using the ATR-FTIR. An experimental schematic is summarized in Figure 3.7.

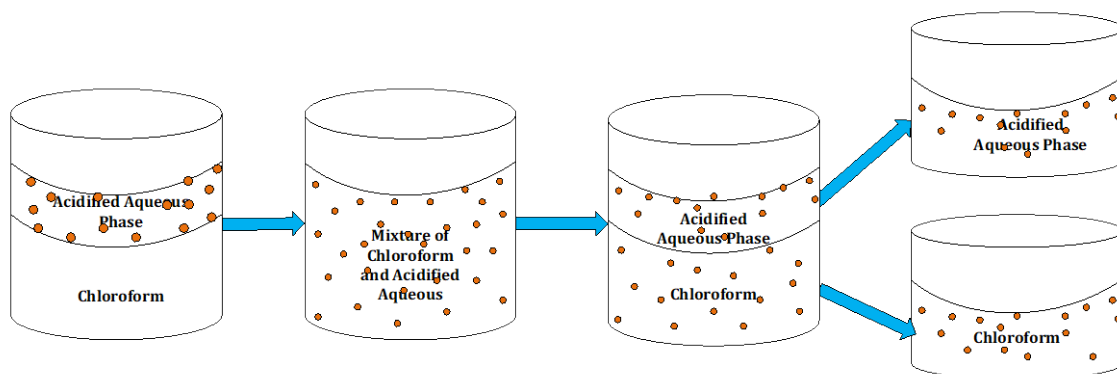


Figure 3.7. Detailed experimental schematic for the liquid-liquid extractions of the filtered aqueous naphthenic and paraffinic froth treatment tailings with chloroform at 20 °C, 40 °C and 60 °C, where the orange dots are representative of the polar hydrocarbons.

3.2.5. Procedure used for solid-liquid extractions

The solid phase extractions were performed on the hot plate while being constantly stirred at 200 rpm using magnetic stirrers. The weights were recorded with a Mettler Toledo PB3002S scale for the centrifuged solids, and the solvents added. The extractions were

performed as summarized in Figure 3.8 at 20 °C, 40 °C, 60 °C, 0.5 hour, 1 hour, 2 hours, 4 hours and 6 hours. Once the desired temperatures and stirring rates are achieved, the mixture stirred for the target times. Once done, the total weight of the jar, stirrers and emulsion was collected. The solvents were collected using a 9-inch glass pipette and filtered using a medium porosity glass filter to remove any of the entrained solids. These solvents were further analyzed spectroscopically. The solids were collected and stored overnight in a fume hood to remove any residual solvents prior to storage and not analyzed further.

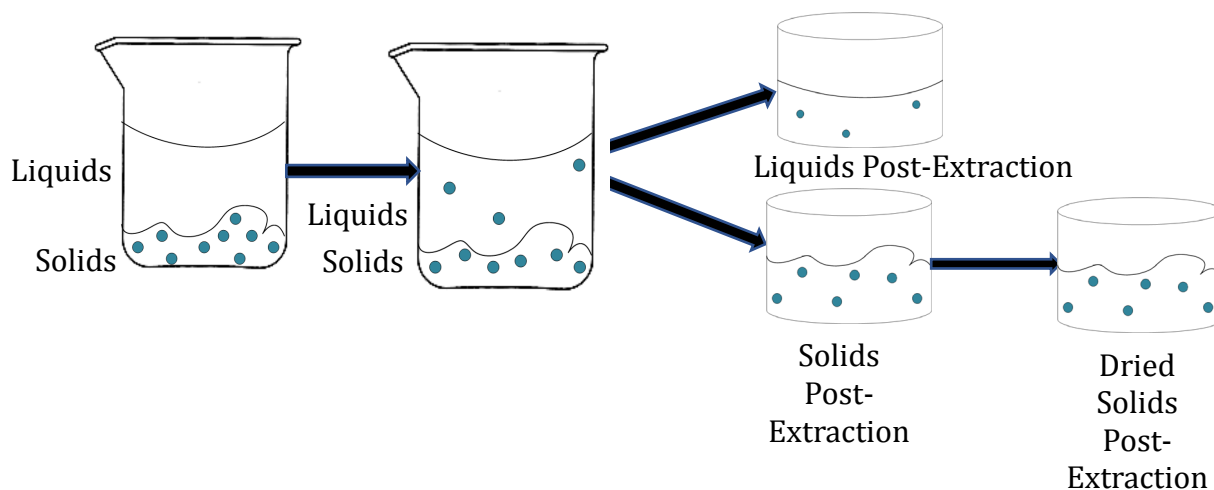


Figure 3.8. Detailed experimental schematic for the solid-liquid extractions of the filtered aqueous naphthenic and paraffinic froth treatment tailings emulsion with heptane and toluene, performed at different temperatures and contact times. Blue dots are representative of the asphaltene aggregates.

The solvent was added, once the desired temperature and stirring rate was achieved. The mixture was left to stir for half an hour. Once completed the mass loss was measured and the solids and liquids were collected separately. The solvents were now ready for analysis using the UV-Visible Spectrometry.

3.3. Analyses Methods

An Oakland PC700 benchtop meter was used to measure the pH of the samples prior to the liquid-liquid extractions. Before and after each use, the meter was buffered to ensure reliable readings. Between readings, the pH meter was soaked in distilled water and air dried to

prevent sample contamination. The pH of the NFT and the PFT tailings were 8.60 and 7.67, respectively.

The ABB MB3000 instrument with a MIRacle™ Reflection Attenuated Total Reflectance (ATR) Fourier Transform Infrared Spectrometry (FTIR) shown in Figure 3.9 was used to collect IR spectra of the samples post liquid-liquid extractions to characterize the hydrocarbons. The samples were analyzed on a diamond crystal plate and clamp. Prior to each measurement, a reference spectrum was collected to eliminate the background noise when collecting the spectra for the samples. The samples were analyzed at a resolution of 8 cm^{-1} , 100 scans, detector gain of 80.62 cm^{-1} , between 400 cm^{-1} and 4000 cm^{-1} , with all measurements being performed at room temperature. This was used to analyze the samples post liquid-liquid extractions. The samples were analyzed crystal glass plate using a 9-inch glass pipette. The crystal was cleaned with pure acetone and wiped with Kimwipes. The standard curves for chloroform, carboxylic acid, distilled water and acetone can be found in Appendix A. Any spectrum which required the baseline correction was amended using the spectral processing software.



Figure 3.9. ATR-FTIR used for the qualitative analysis of the chloroform extracts for various experimental conditions.

The UV Visible spectrophotometer as shown in Figure 3.10, was used as tool to determine the presence of the metal porphyrins in the hydrocarbons in the extracted solvents. The cuvettes were made of Spectrosil, had a rectangular shape and were 10 mm path length. The UV light source was 323 nm, and all measurements were performed at room temperature. The samples were analyzed between 185 nm to 800 nm, with a fast scan speed. The slit width was 2.0 nm and the sampling interval was 0.5 nm. Pure solvents were measured and then used as a reference sample. Any peaks corresponding to the neat solvents occur between 200 nm to 300 nm. In order to prevent the saturation of the detector, the samples were diluted with their respective pure solvents at various concentrations to prevent saturation of the detector. The samples were weighted using a Mettler Toledo XP1203S scale with maximum weighing capacity of 1210 g and were pipetted into small amber vials using 9-inch glass pipettes.



Figure 3.10. (left) The Shimadzu UV-2700 Spectrophotometer used for the qualitative analysis of the toluene and heptane analysis; (right) interior of the spectrophotometer, with the back position for the baseline cuvette (highlighted in blue) and for the sample (highlighted in green).

The Nanalysis 60 MHz NMReady – 60 Nuclear Magnetic Resonance (NMR) Spectrometer shown in Figure 3.11 was used to comment on the hydrogen environments for the toluene and heptane extracts from the solid liquid extractions. The spectral width collected was for 12 ppm and the number of scans were 32 with a full scan time period of 14 minutes. The equipment was calibrated with deuterated chloroform (Chloroform-D). The spectra were obtained for the pure extracts as well as diluted samples which were made to 0.1 mg of sample and 700 μ L of Chloroform-D. The samples were collected used the Norell NMR glass tubes and were analysed for a spectral width of 12 ppm, 32 scans per sample and average scan time of 25 seconds. The obtained spectral data was analyzed using the MestReNova software, and the areas were integrated for various regions (aliphatic, olefinic and aromatic). All spectra can be found in Appendix A.



Figure 3.11. (left) Nanalysis 60 MHz NMReady – 60 Nuclear Magnetic Resonance (NMR) Spectrometer, (right) heating area for the samples used. The temperature set point was 30 °C.

4. Results and Discussion

4.1. Compositional breakdown from TGA experiments

The compositional breakdown for the tailings emulsions from the TGA experiments are shown in Table 4.1, with thermograms in Figure 4.1. The lighter hydrocarbons and water are between 25 °C to 165 °C, while heavier hydrocarbons were evaporated between 165 °C and 350 °C. The mass loss during the combustion event are attributable to heavier asphaltenes³⁴. The thermal profiles in the nitrogen regime provides an estimation of the lighter and any heavier hydrocarbons which may be present. Any hydrocarbons combusted after 350 °C are assumed to be asphaltenes, while the weight loss events prior to 350 °C, are to the maltene fractions in crude oil. The thermograms for the NFT tailings showed evidence of multistep decomposition between 113 °C and 184 °C. Further thermogravimetric analysis coupled with infrared (FTIR) or mass spectroscopy (MS) characterizes any evaporated hydrocarbons in this regime. The TGA coupled with FTIR identifies the vibrational functional groups in the hydrocarbons, while mass spectroscopy identifies the individual hydrocarbons. Comparatively, between the NFT and the PFT, the percentage of the lighter and the heavier hydrocarbons are higher for the NFT, while the percentage of the heavier hydrocarbons are lower in the paraffinic froth treatment tailings. The percentage of asphaltenes is significantly lower for the PFT than the NFT. The amount of mineral solids is higher for the NFT than the PFT. The main differences between the NFT and the PFT are due to the type of froth treatment processes, the samples were obtained from. As a result, the residual crude in the naphthenic tailings streams is therefore lower. However, while paraffinic solvents have a demonstrated ability for greater precipitation of asphaltenes^{1,2,5,34}, the compositions of the asphaltic molecules in the PFT were much lower than the NFT.

Table 4.1. Composition of the naphthenic and the paraffinic froth treatment tailings from the thermogravimetric studies

Component	Temperature ranges (°C)	Naphthenic Froth Treatment Tailings (%)	Paraffinic Froth treatment tailings (%)
Lighter hydrocarbons and water	25 - 165	83.46	94.05
Heavier hydrocarbons	165 - 350	7.06	0.53
Asphaltene	350 - 650	1.91	1.94
Mineral solids	Residual solids	7.57	3.48

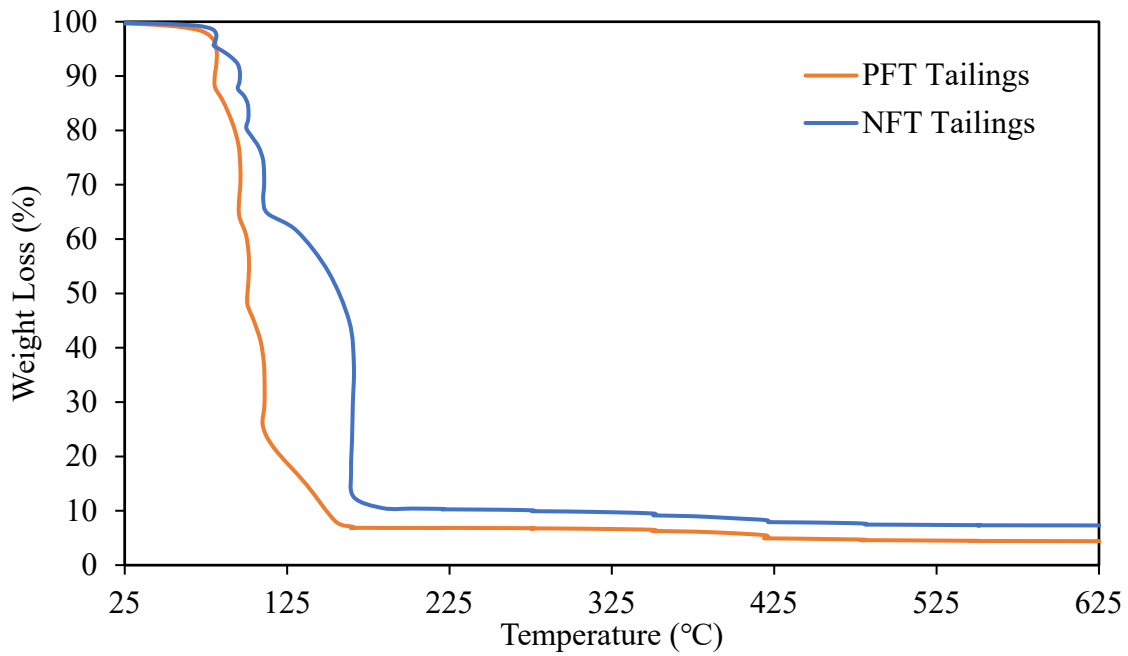


Figure 4.1. Thermogram for the tailings emulsion under nitrogen atmosphere up to 350 °C, followed by a combustion period under air environment from 350 °C to 650 °C.

As demonstrated in Figure 4.1, the thermogram between 350 °C and 635 °C demonstrated little change, therefore, the thermal profiles for the centrifuged solids in Figure 4.2 were analyzed to identify the maltenes or asphaltenes in the centrifuged solids. The compositional breakdown in the centrifuged tailings are summarized in Table 4.2. For the PFT there were higher concentrations of asphaltenes and lower concentrations of mineral solids. The concentrations of heavier hydrocarbons, lighter hydrocarbons and water were lower for the NFT solids. The second event for the NFT tailings showed some evidence of multistep decomposition. However, this was more pronounced for the NFT tailings in Figure 4.1 rather than Figure 4.2. As well, based on the curves, the NFT solids noticed larger weight losses, while the PFT solids showed minimal shifts between the events at 115 °C. For both the solids, the events between 350 °C – 420 °C and 420 °C – 480 °C showed rapid weight loss when compared to the combustion events after 480 °C. This is indicative that the asphaltic compounds which may be present are combusted between 350 °C and 420 °C as opposed to 480 °C to 650 °C.

Table 4.2. The composition of the centrifuged solids from the naphthenic and the paraffinic froth treatment tailings from the thermogravimetric studies

Component	Temperature ranges (°C)	Centrifuged solids from the Naphthenic Froth Treatment Tailings (%)	Centrifuged Solids from the Paraffinic Froth treatment tailings (%)
Lighter hydrocarbons and water	25 – 165	45.88	50.40
Heavier hydrocarbons	165 – 350	3.17	2.01
Asphaltenes	350 – 650	14.37	16.55
Mineral solids	Residual solids	36.58	31.04

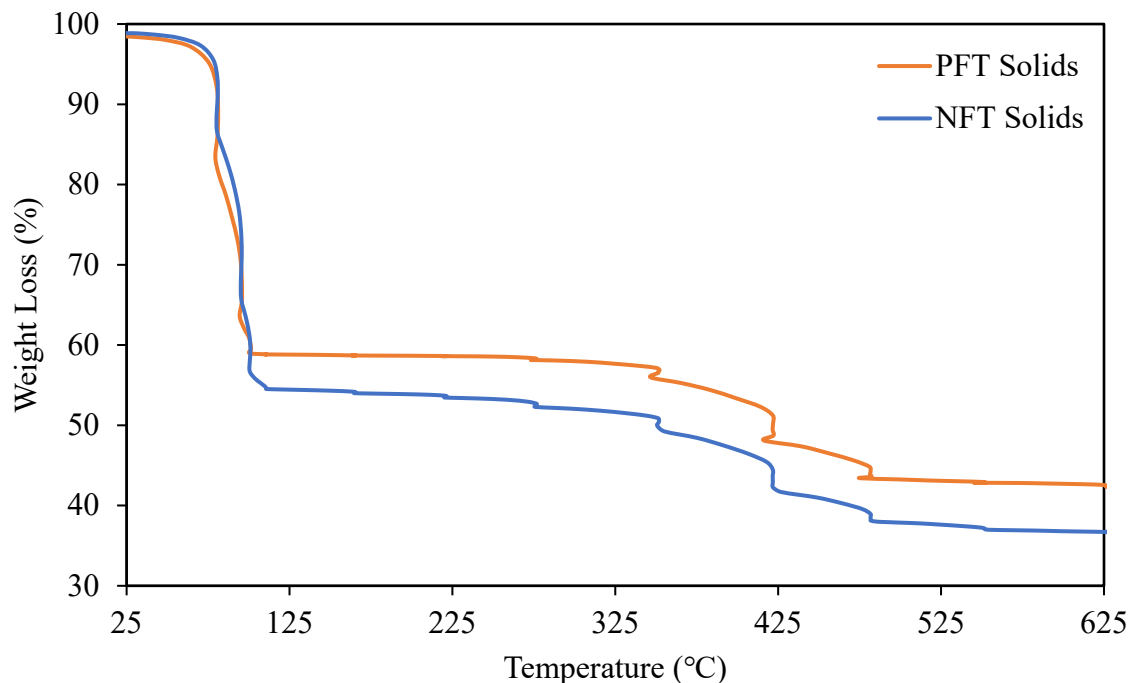
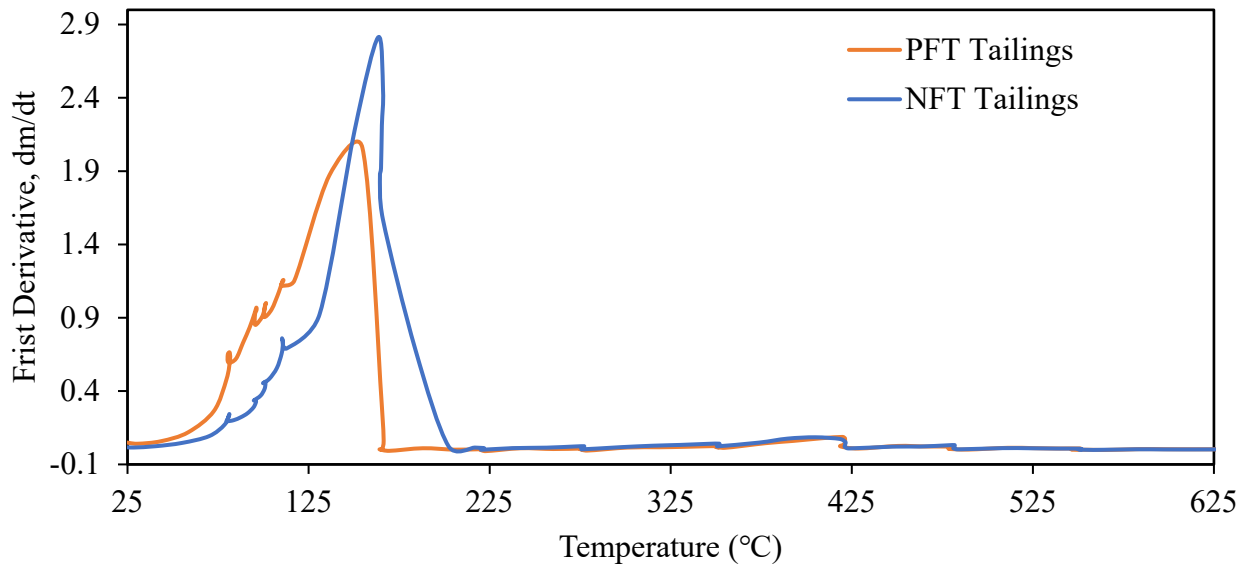
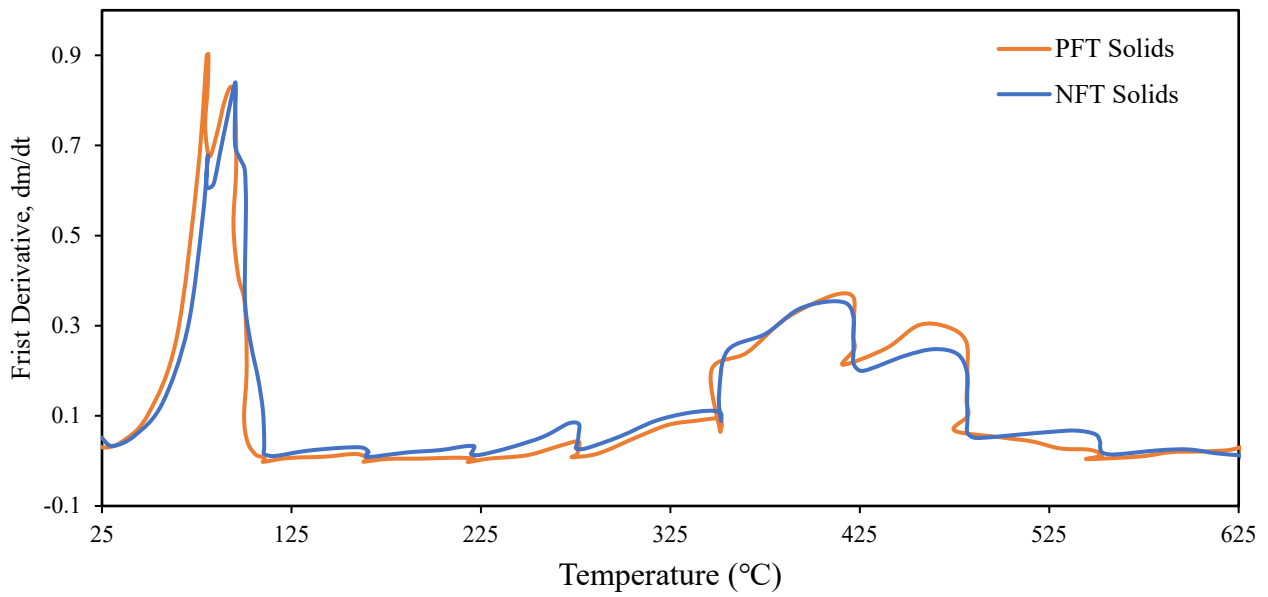


Figure 4.2. Thermogram for the tailings solids under nitrogen atmosphere upto 350 °C , followed by a combustion period under air environment from 350 °C to 650 °C.

The thermograms for the tailings and their respective centrifuged solids confirms the presence of the heavier hydrocarbons and asphaltic molecules. Figure 4.3 shows the derivative TGA curves with respect to temperature. As temperature increase, the derivative of the weight loss increases, meaning that mass loss increases until the derivative begins to decrease. The peak with the highest intensity for the NFT tailings rather than PFT tailings. The trends for the centrifuged solids, demonstrated similar trends where, there was little difference between the naphthenic and the paraffinic solids.



(a)



(b)

Figure 4.3. Derivative weight loss and temperature for: (a) PFT and NFT tailings emulsion from 25 $^{\circ}C$ to 650 $^{\circ}C$; (c) PFT and NFT solids.

The impact of centrifugation time and the composition of the solids and the aqueous phases for the naphthenic and the paraffinic froth treatment tailings are summarized in Table 4.3. The effects of centrifugation times were varied for 10 minutes, 20 minutes and 30 minutes. 30 minutes had the highest impact on the clarity for the aqueous phases for the paraffinic froth treatment tailings. Higher times were not pursued, as the effect on clarity was negligible. Additionally, the aqueous phases were vacuum filtered for the removal of fine clays and not pursued further. The speed for centrifugation was used as 7000 rpm. The relationship between the speed is the gravitational forces which act on the solids particles forcing them to settle at the higher speeds. The proportion of the solids from the PFT is higher than the NFT solids.

Table 4.3. Composition for the NFT and PFT emulsion after centrifugation

Tailings Emulsion	Aqueous phase ^a (%)	Solids phase ^a (%)
PFT	69.8	30.3
NFT	75.5	24.5

^aReported as weight percent.

4.2. Analysis for the aqueous phase for froth treatment tailings

The filtered liquids were acidified and analyzed using FTIR for validating that the hydrocarbons migrated into the organic phases. An increase in temperature should result in a large amount by mass to migrate into the organic phase, while a decrease in pH will have similar effects. A decrease in pH will allow more carboxylic acids to migrate, as it increases the solubility of the acidic fractions in the organic phases. The temperature increases the solubility of the acid into the hydrocarbon phases. The extractions were performed at pH 3.0, 2.0, 1.0 and temperatures of 20 °C, 40 °C and at 60 °C.

The spectra for the chloroform extracts shown in Figure 4.4 and Figure 4.5 for the naphthenic froth treatment tailings collected at different temperatures and pH. The peaks below 500 cm⁻¹ are the fingerprint regions several compounds and do not help in the identification of the hydrocarbons and are therefore not included in Figures 4.4 and Figure 4.5. While absolute

quantitative estimation of the concentration of the hydrocarbons in the extracts cannot be made using the ATR-FTIR, an estimation of the transmittance peaks are summarized in Table 4.4. The peaks which are observed are C—O bonds and the O—H stretching bonds for the carboxylic bonds. The carbonyl bonds showed strong peaks, as they were typically weak with broad bands and were not further considered. There were minimal changes between 3000 cm^{-1} to 3024 cm^{-1} . While the mass extracted increased with a decrease in pH, there was little change in O—H peaks in the spectra. However, there were slight increase in the O—H peaks. While the spectra itself showed small differences in the intensities, the relative intensities as described in Table 4.4 showed an increase in the C—O bonds rather than the O—H bond.

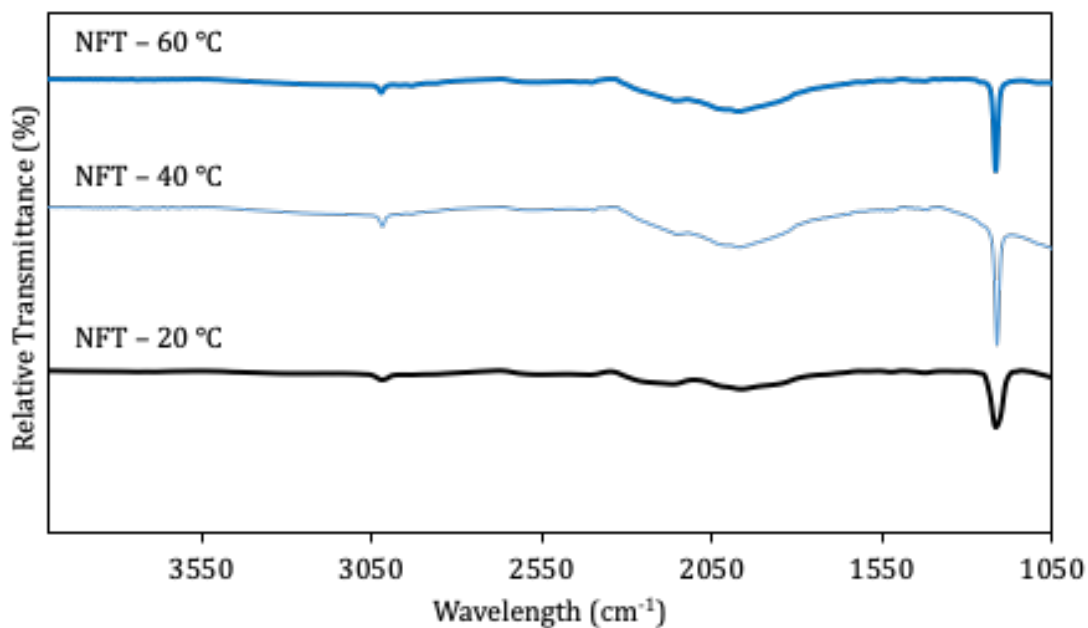


Figure 4.4. Relative transmittance for the chloroform extracts from NFT collected at differing temperature: (a) $T = 20\text{ }^{\circ}\text{C}$, (b) $T = 40\text{ }^{\circ}\text{C}$ and, (c) $T = 60\text{ }^{\circ}\text{C}$.

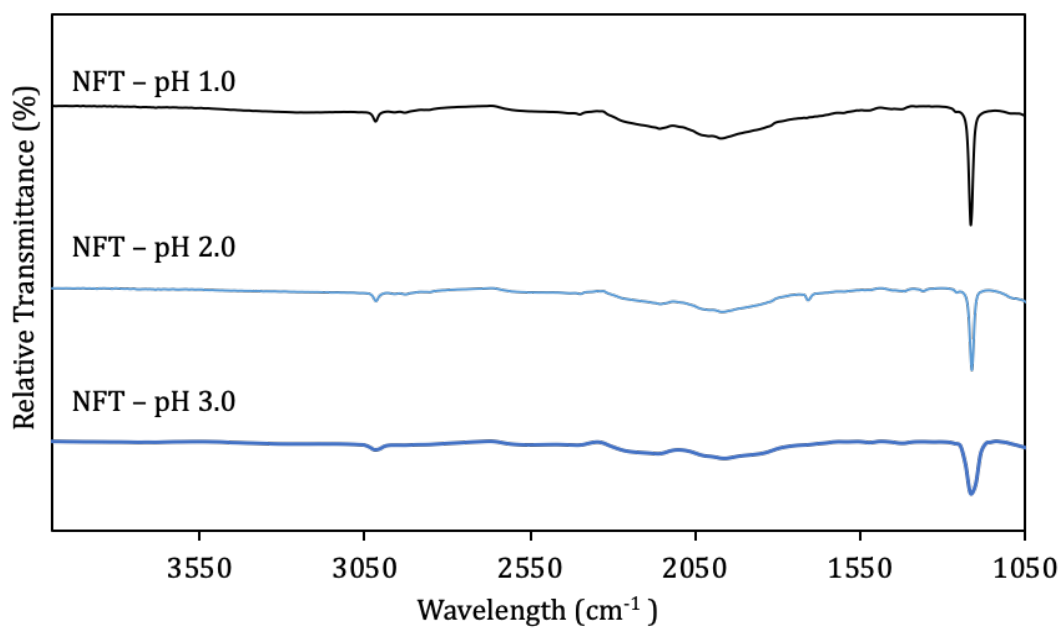


Figure 4.5. Relative transmittance for the chloroform extracts from NFT collected at differing pH: (a) pH = 3.0 (b) pH = 2.0 and (c) pH = 1.0.

Table 4.4. Relative intensities for the chloroform extracts obtained at different pH and temperature for the naphthenic froth treatment tailings.

Wavelength ranges (cm-1)	Functional groups	Experimental conditions ^c				
		3.0 ^a	2.0 ^a	1.0 ^a	40 °C ^b	60 °C ^b
1215	C—O	15	23	28	23	26
3000 -3024	O - H	2	9	4	3	3

^a Experiments performed at room temperature and the corresponding pH

^b Experiments performed at pH 3.0 and corresponding temperature

^c The percentages were the height of the peak to the baseline

Figures 4.6 and 4.7 shows the infrared spectra for PFT for decreasing pH and increasing temperature. As the temperature increases, C—O intensity decreases. As the pH decreases, O—H intensity increases. Therefore, temperature had little impact on the concentrations of the solutes transferred to the solutions. As the pH decreases, both the intensity of O—H and C—O bonds decreased. Based on experimental setup, the extractions performed at decreasing pH had little to no impact on the hydrocarbons transferred to solution. The relative quantitative measurements are summarized in Table 4.5. While the mass fraction extracted increased, the intensities of the peaks observed in Table 4.5. follows different trends. This may be attributable to two reasons: (1) the experimental setup of the extractions was not able to facilitate all the hydrocarbons to migrate in the extractions performed and (2) the relative change in concentrations were low to begin with. By using preconcentrating methods to analyse the infrared spectra, the concentrations might be high enough for the extraction to proceed. Once the extractions through these methods are conducted, the samples may be better analyzed using the ATR-FTIR.

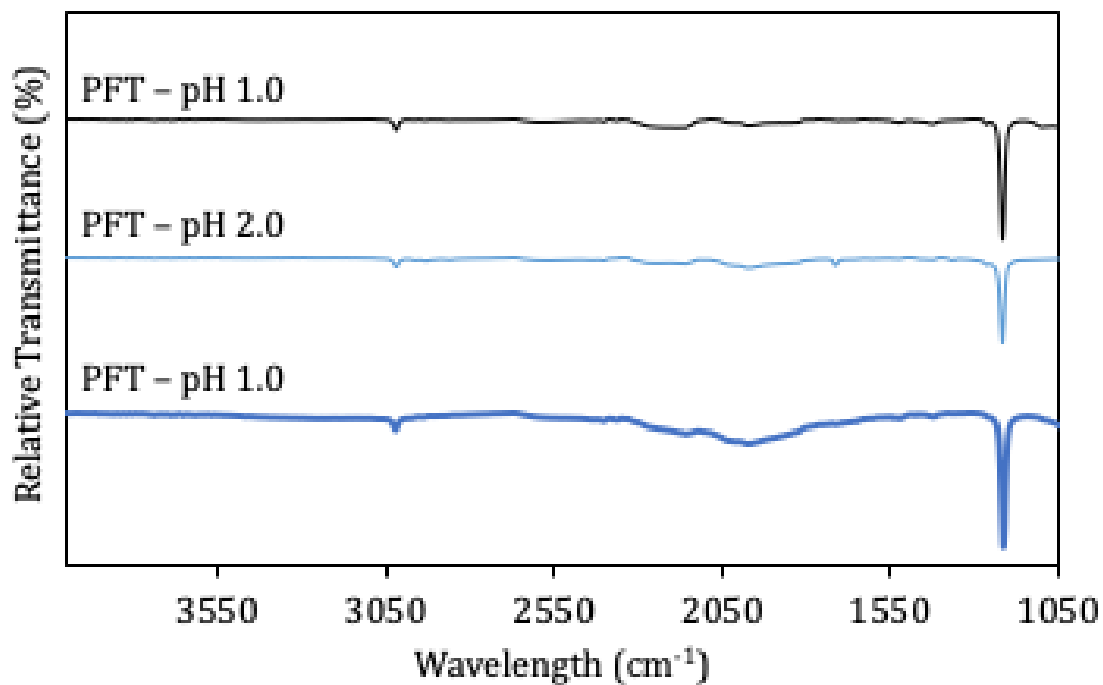


Figure 4.6. Relative transmittance for the chloroform extracts from PFT collected at: (a) pH = 1.0 (b) pH = 2.0 and (c) pH = 3.0

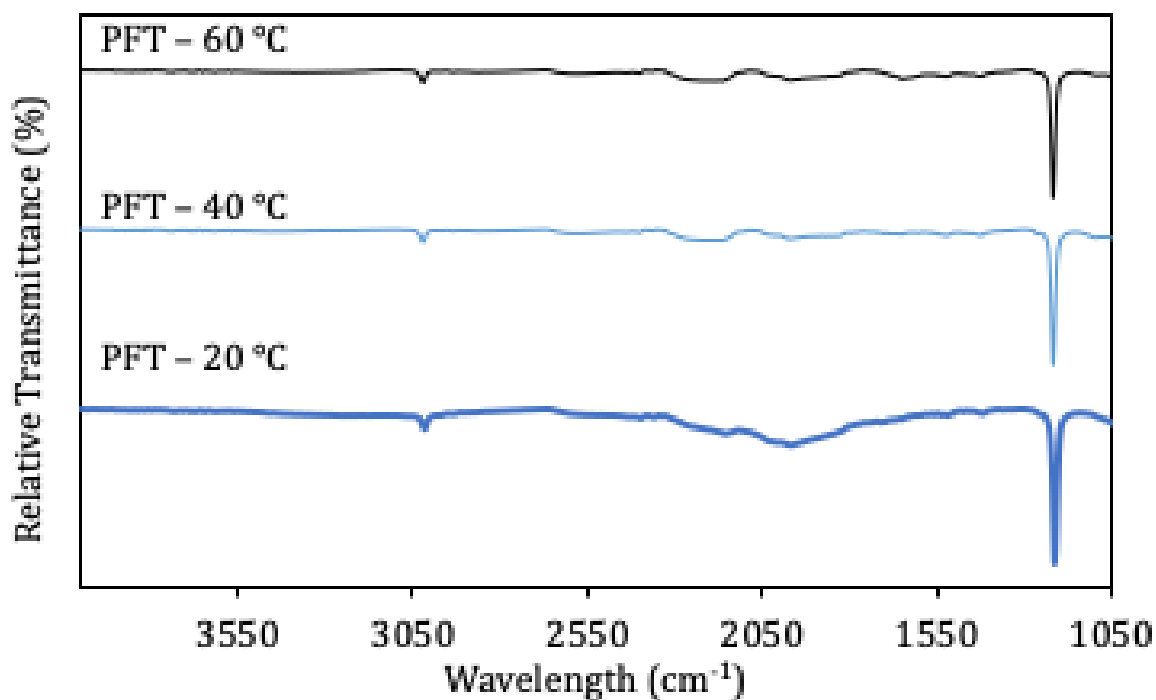


Figure 4.7. Relative transmittance for the chloroform extracts from PFT collected at: (a) 20 °C, (b) 40 °C, (c) 60°C

Table 4.5. Relative intensities for the chloroform extracts obtained at different pH and temperature for the paraffinic froth treatment tailings.

Wavelength ranges (cm ⁻¹)	Functional Groups	Experimental Conditions				
		3.0 ^a	2.0 ^a	1.0 ^a	40 °C ^b	60 °C ^b
1215	C – O	43	27	38	37	28
3000 - 3024	O – H	4	2	3	1	3

^a Experiments performed at room temperature and the corresponding pH

^b Experiments performed at pH 3.0 and corresponding temperature

^c The percentages were the height of the peak to the baseline

From Table 4.5 and 4.6 compares the relative amounts for the naphthenic and the paraffinic froth treatment tailings. As the pH decreased for the naphthenic froth treatment tailings, the intensities for the 1215 cm⁻¹ peak increased for the naphthenic froth treatment tailings and decreased for the paraffinic froth treatment tailings until it increased back again for pH 1.0. The 3000 cm⁻¹ – 3024 cm⁻¹ peak increases for naphthenic froth treatment tailings the intensity decreases for the paraffinic froth treatment tailings. As the temperature increases, the 1215 cm⁻¹ bond increases for the naphthenic froth treatment tailings and decreases for the paraffinic froth treatment tailings.

Contrary to the observations mentioned by Kislik, there was little increase in the 3000 cm⁻¹ peak for a change in temperature¹⁸. Alternative experimental procedures such as a reflux set-up, or a closed batch reactor might be used to perform the extractions¹⁸. This minimizes mass loss during the experiment and due to the increase in extraction of the desired hydrocarbons. These methods may be advantageous as the aqueous and organic samples both may be collected and analyzed further. Here, the temperature drives the evaporation of the chloroform, instead of the migration of these compounds between different phases. Doing so, we might be able to better understand the composition of the extracts obtained at 60 °C. Experiments should also be performed at smaller temperature intervals so that a trend between 40 °C and 70 °C might be observed. As seen above, there are small trend between the intensity of FTIR peaks with pH or temperature. By performing these extractions at even more elevated temperatures and using a quantitative tool such as a transmission FTIR with

a fixed path length, will enabling to comment of the concentration of the types of species able to migrate from a spectroscopic point of view.

4.3. Analysis of extracted centrifuged tailings solids

The solids portion of the froth treatment tailings shown to have bituminous residue from Section 4.1. Once the hydrocarbons are extracted at room temperature, 40 °C, 60 °C, 1 hour, 2 hours, 4 hours and 6 hours, these extracts collected are analyzed using UV Visible spectroscopy and low-resolution proton NMR. The hypothesis is that as the temperature increases, the ability of the solvent to extract hydrocarbons increases as the energy barrier required to dissolve the hydrocarbons decreases and the solubilities increases. As retention time increases, the solvent will have longer contact time with any hydrocarbons, facilitating the transfer into the organic phase. This is largely due to the different solubilities of the solutes in the solvents. The presence of asphaltenes will be confirmed by the peaks at 260 nm, 350 nm and 410 nm which corresponds to benzenes, naphthenes and the Soret bands from the metalloporphyrins, respectively. The ultraviolet spectrum was obtained for all extraction runs and solvents used.

4.3.1. Solid liquid extractions for the centrifuged solids from NFT

As demonstrated in Figure 4.8(a) absorbances decreases with increasing temperature. As the temperature was increased, the absorbances decreased, as driving forces are insufficient to promote migration of asphaltic compounds into the solvent phase. The regions, where the absorbances lie between 8-10 were not considered as the signals are saturated. As the temperature is increased from room temperature to 40 °C, the curve shifts upwards, while the transition from 40 °C to 60 °C pushes the spectrum down. Here, for the extracts obtained at 60 °C, the evaporation of the toluene takes precedence over the migration of hydrocarbons into the solvent phase. The peaks below wavelength of 400 nm are saturated for the toluene extract collected at 20 °C. There are small peaks at 362 nm, and 385 nm which are not porphyrins peaks, therefore a comparison between benzenes and naphthenic compounds should be considered. As postulated by literature, a distinct Soret band was observed at 410 nm for the toluene extract obtained room temperature, while the extracts collected at 40 °C and 60 °C showed shoulders, demonstrating that there is a potential for sharper and more distinct peaks for the Soret band. However, when concentrations were incrementally

increased to get distinct peaks, the detector was saturated. Figure 4.8(b) demonstrated the presence of certain absorption peaks between 500 nm and 600 nm; however, a significant number of these peaks saturated the detector, consequently not used for further analysis. The saturated peaks may be indicative of double bonded peripheral groups for the porphyrin structures.

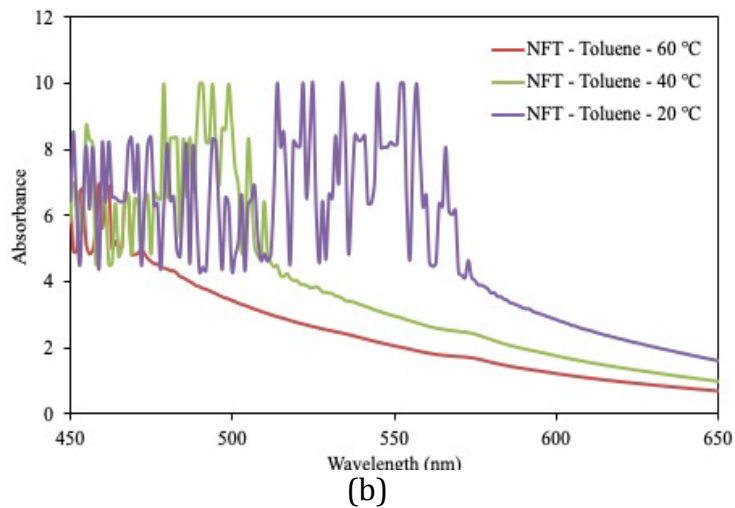
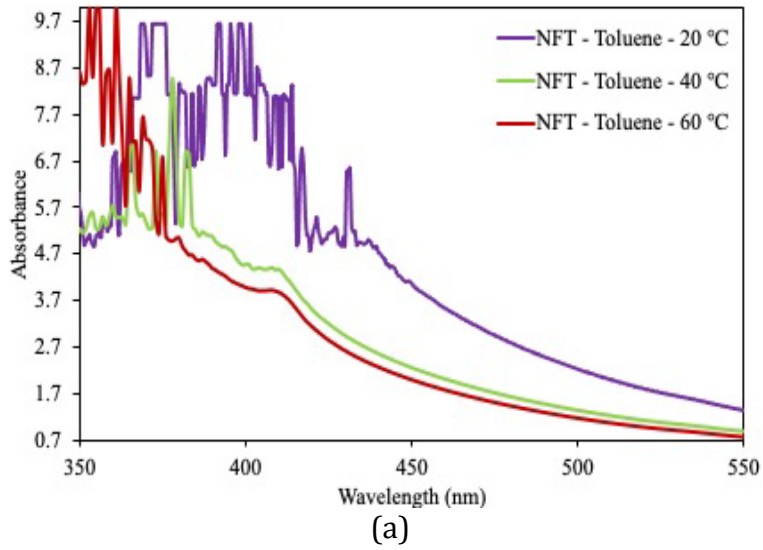


Figure 4.8. UV Visible spectra for the toluene extracts of the NFT centrifuged solids (a) the spectra obtained at 7% dilution with pure toluene and (b) the spectra obtained at 30% dilution with pure toluene.

The effect of increasing contact time on the hydrocarbons extracted using toluene were observed as well. Therefore, the solvent has a greater residence time for the compounds to reach chemical equilibrium and should increase in greater concentrations of the asphaltenes suspended in solution. As demonstrated in Figure 4.9(a), at 6 hours, there was a Soret band at 410 nm. There were bands observed at 409 nm and 413 nm for 0.5 hours, 4 hours and at 405 nm and 408 nm for 2 hours. The absorbance peaks associated with the Soret bands for 1 hour were observed at 403 nm, 408 nm and 412 nm. In terms of relative concentrations, the curves were shifted upwards indicative of increasing concentrations in the following order: 0.5 hour > 2 hours > 1 hour > 4 hours > 6 hours, which was not expected. Figure 4.9(b) demonstrates absorption peaks for the peripheral carbon atoms in the toluene extracts from the NFT collected at different times. As aforementioned, the detector is saturated for absorbances above 8. There was a shift upwards which is characteristic of increasing concentrations. The order of increasing concentrations to decreasing concentrations are: 0.5 hour > 2 hours > 1 hour > 4 hours > 6 hours. The regions of peaks observed for all spectra are between 570 nm and 575 nm. This is indicative of the etioporphyrin peripheral group as shown in Table 2.8 and Table 2.9. This shows as a peak at 0.5 hour and a 'shoulder' or the remaining contact times. This means that there are enough concentrations of the sample to create an indication of a curve but not enough to create distinct peaks. The other peaks observed at 0.5 hour are at 564 nm, 567 nm, and at 569 nm. The peaks at 567 nm and 569 nm may be indicative of the α band in the octethylprophyrin or the etioporphyrin groups. The slight shift may be attributable to the nature of the samples or the spectrophotometer used. The bands at 548 nm and 550 nm were observed at 2 hours are indicative for the nickel porphyrins or band for the meso-tetraphenyl porphyrin as shown in Table 2.8 and Table 2.9. Also, the band at 530 nm indicative of the α band for the vanadyl porphyrins were observed. At a value of 4 hours for contact time, a weak peak at 530 nm, indicative of the vanadyl porphyrins were observed.

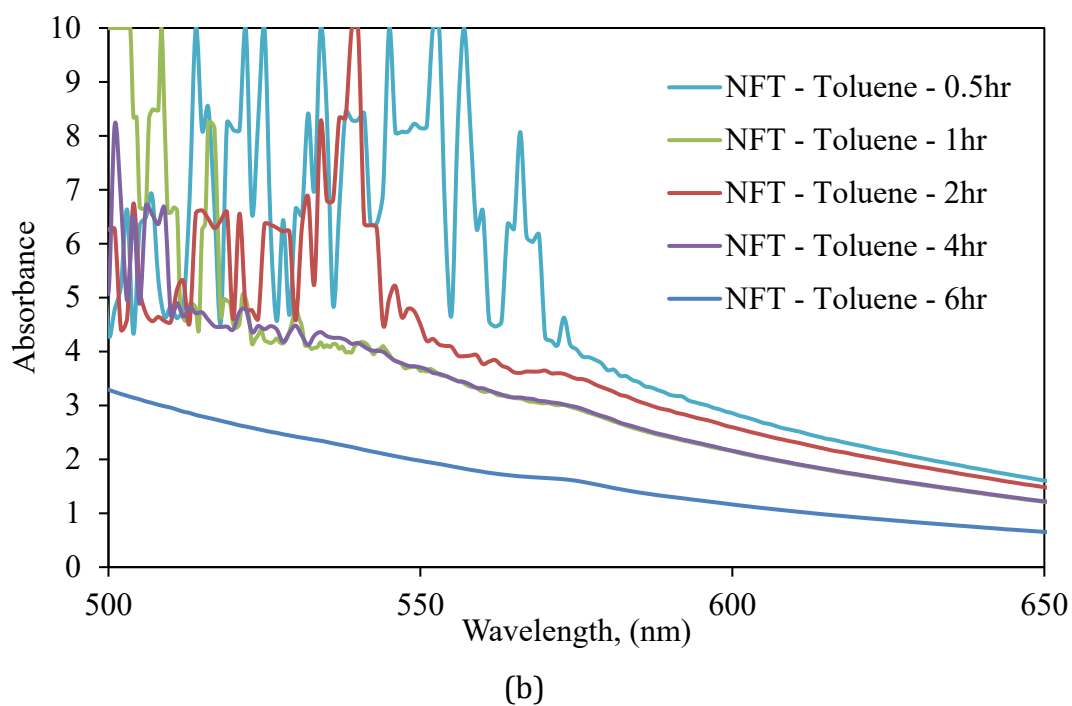
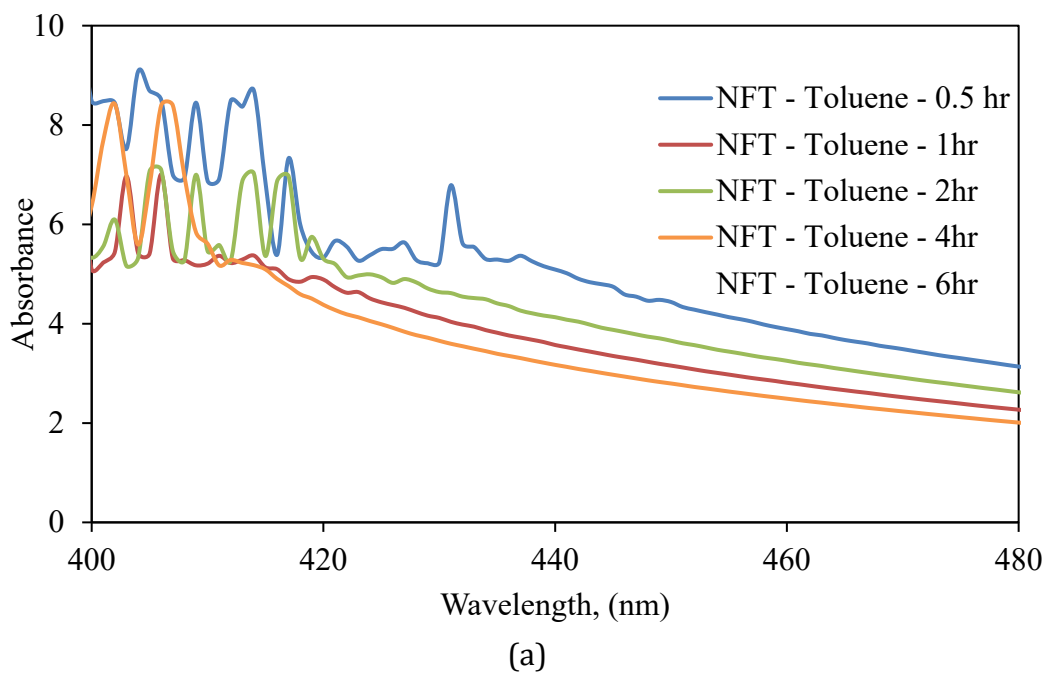
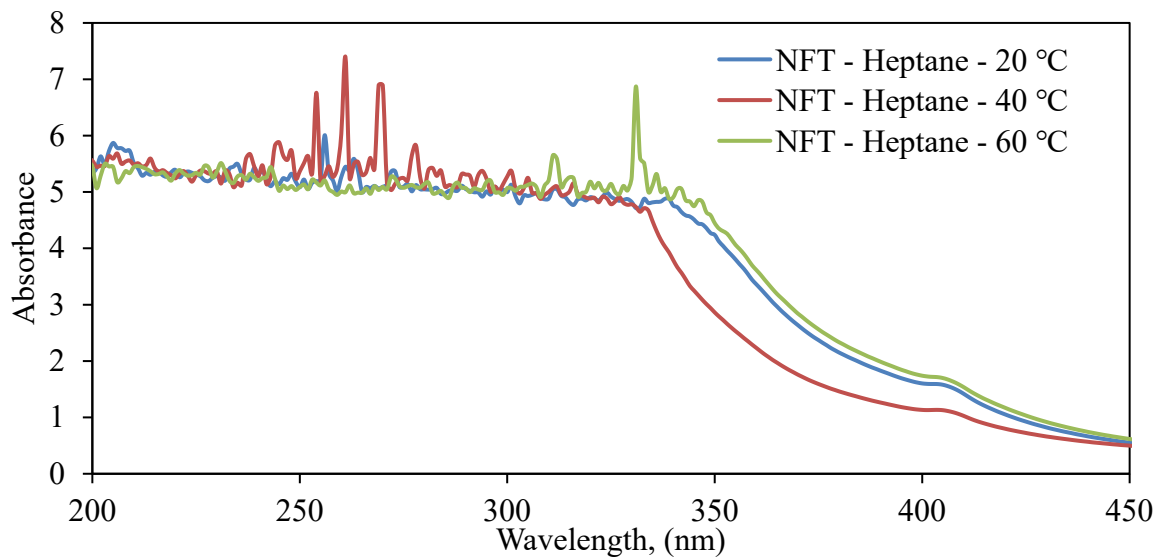
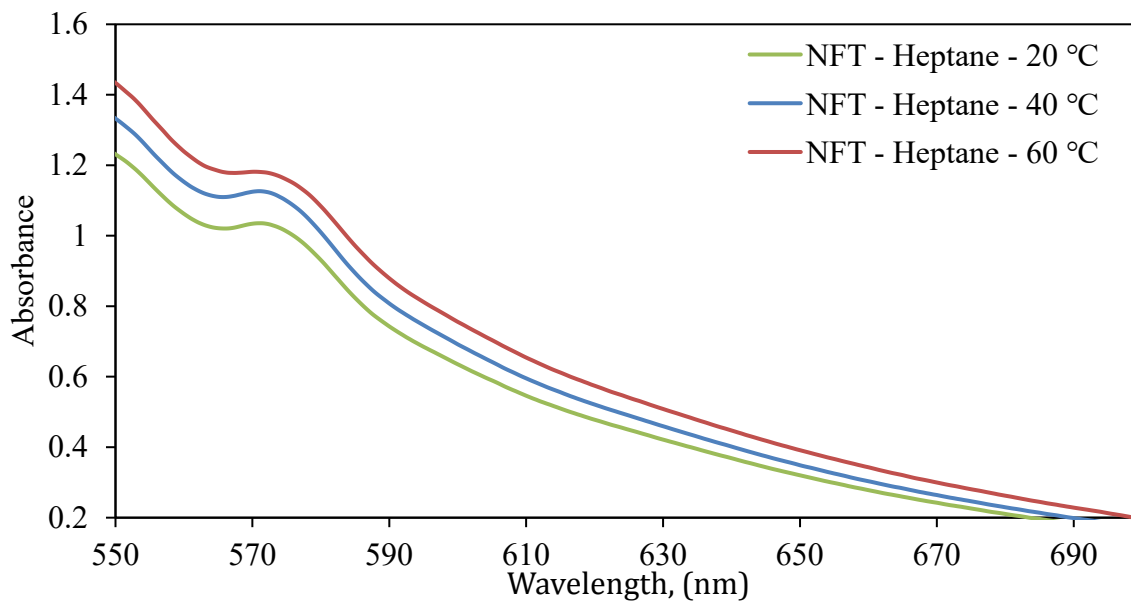


Figure 4.9. UV Visible spectra for the toluene extracts for increasing contact time (a) the spectra obtained at 7% dilution with pure toluene and (b) the spectra obtained at 30% dilution with pure toluene.

Figure 4.10 shows the absorption bands for the extractions performed with heptane at different temperatures. As expected, the shoulder at 410 nm are indicative of metalloporphyrins. In terms of relative concentrations, the curves were shifted upwards indicative of increasing concentrations in the following order: 60 °C > 20 °C > 40 °C. Rather than the original hypothesis where the increase in temperature should result in an increase in extraction of porphyrinic compounds, this trend is not observed. For the trends demonstrated in Figure 4.10(b), the absorption shoulders were also present at 570 nm – 600 nm. This may be indicative of the α band in the vanadyl porphyrin. In decreasing order of 60 °C > 40 °C > 20 °C. These are the pure spectra for the heptane extracts without further dilution. The absorbances for Figure 4.3(b) and 4.3(a) was significantly lower than 3. Perhaps pre-concentrating samples prior to analysis between 500 nm and 600 nm should be performed. As the solubility for the polar and aromatic compounds in the heptane solvent is significantly low, rather than performing the extractions as described in Chapter 3, the experiments might be performed in soxhlet extractor. The repeated addition of the solvent to the solids, might increase the transfer of the asphaltic compounds from one phase to another. Another alternative might be to perform the extractions using a reactor. By using a completely enclosed reactor, and a solvent like DCM, which has a known capability to extract at different temperatures, greater concentrations might be observed the subsequent UV-Visible spectral analysis.



(a)



(b)

Figure 4.10. UV Visible spectra for the heptane extracts for increasing temperature (a) the spectra obtained at 7% dilution with pure toluene and (b) the spectra obtained at 30% dilution with pure heptane

Figure 4.11(a) and Figure 4.11(b) shows the absorption bands for the extractions performed with heptane at different times. In decreasing order of concentrations, the extractions conditions are: 6 hours > 4 hours > 2 hours > 0.5 hour > 1 hour. In all spectra, there were shoulders between 405 nm to 410 nm for the Soret bands. The wavelengths between 500 nm to 600 nm are indicative of the effects which occur due to the peripheral groups in certain porphyrin structures. There were shoulders observed for all conditions except 1 hour. The order of increasing concentrations was similar for these spectra. The peak between 570 nm to 575 nm were indicative of the α band for the vanadyl porphyrins. For Figures 4.11(a) and Figure 4.11(b), the absorbances ranged from 1.5 – 4.9 and 0.7 – 2.1, respectively. These absorbances were lower than the optimal ranges for the spectrophotometer and need to be pre-concentrated with samples of metalloporphyrins. Alternatively, spiking the samples with these solutions might lead to a shift in absorbance to between 3 to 8. Furthermore, if the extractions were performed using a soxhlet extractor, higher concentrations for quantitative analyses may be performed for these samples.

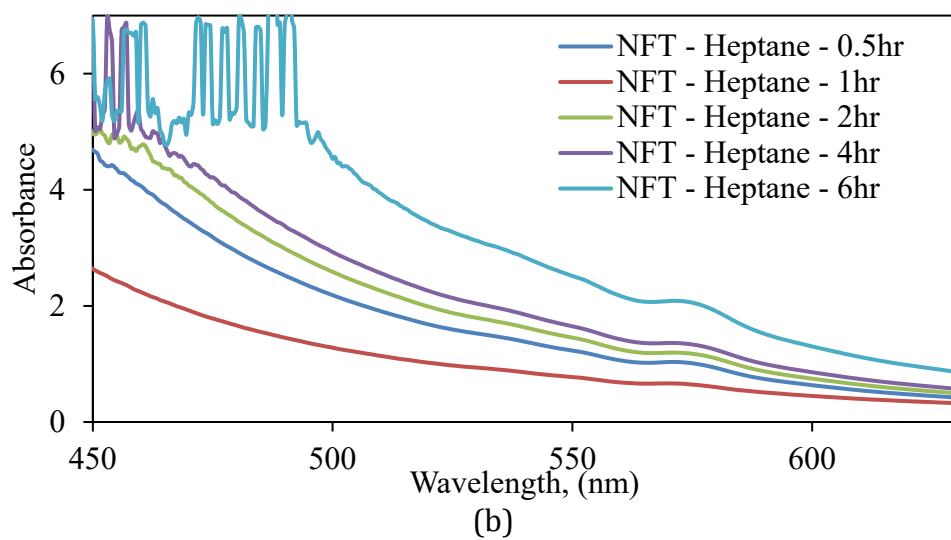
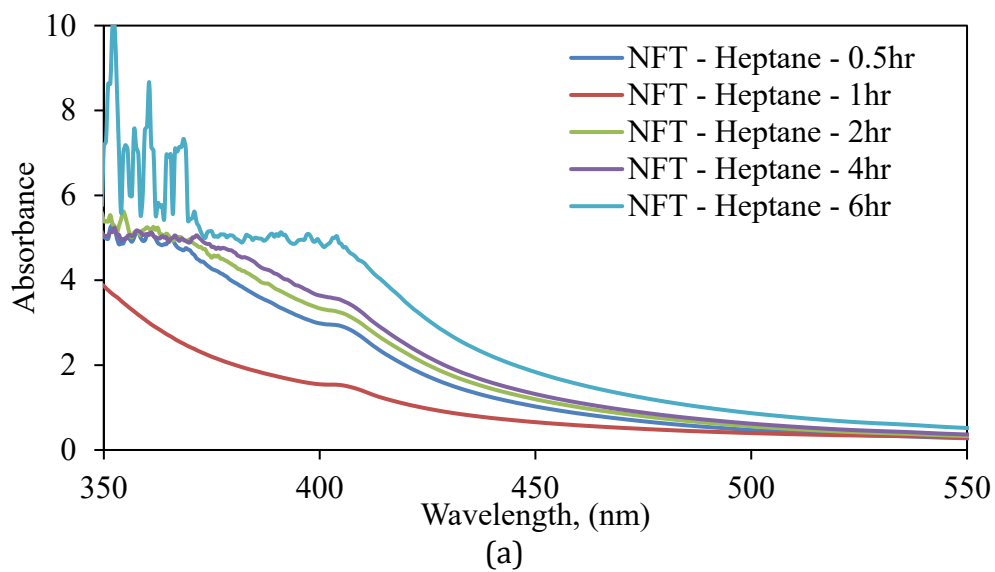


Figure 4.11. UV-Visible spectra for the heptane extracts for increasing contact time (a) the spectra were obtained at 7% dilution with pure toluene and (b) the spectra obtained from undiluted samples

4.3.2. Solid liquid extractions for the centrifuged solids from PFT

Figure 4.12(a) and Figure 4.12(b) summarize the UV spectra for the different toluene extracts collected at 20 °C, 40 °C and 60 °C. The Soret band was observed at 412 nm at all temperatures. The spectra for 40 °C was saturated, however the remaining curves show the indications of a peak at 413 nm. The order of decreasing concentrations is 40 °C > 60 °C > 20 °C. The Figure 4.12(b) summarized the shoulder for peaks at 575 nm. The order of decreasing concentrations was similar for all. In Figure 4.12(a), the absorbances of the peaks were observed between 2.8 and 10.0, with absorbances over 8 not being considered, as the detectors were likely saturated in this regime. While the spectra for 40 °C and 60 °C were within the optimal ranges, the peaks obtained for the 40 °C spectra cannot be used for any quantitative analysis as the detector for the spectrophotometer was saturated. In order to prevent the saturation at 40 °C, it may be remedied by replacing the detector, using narrower cuvettes, dilution of the samples with two orders of magnitude or using a spectrophotometer with a finer sensitivity for any measurements.

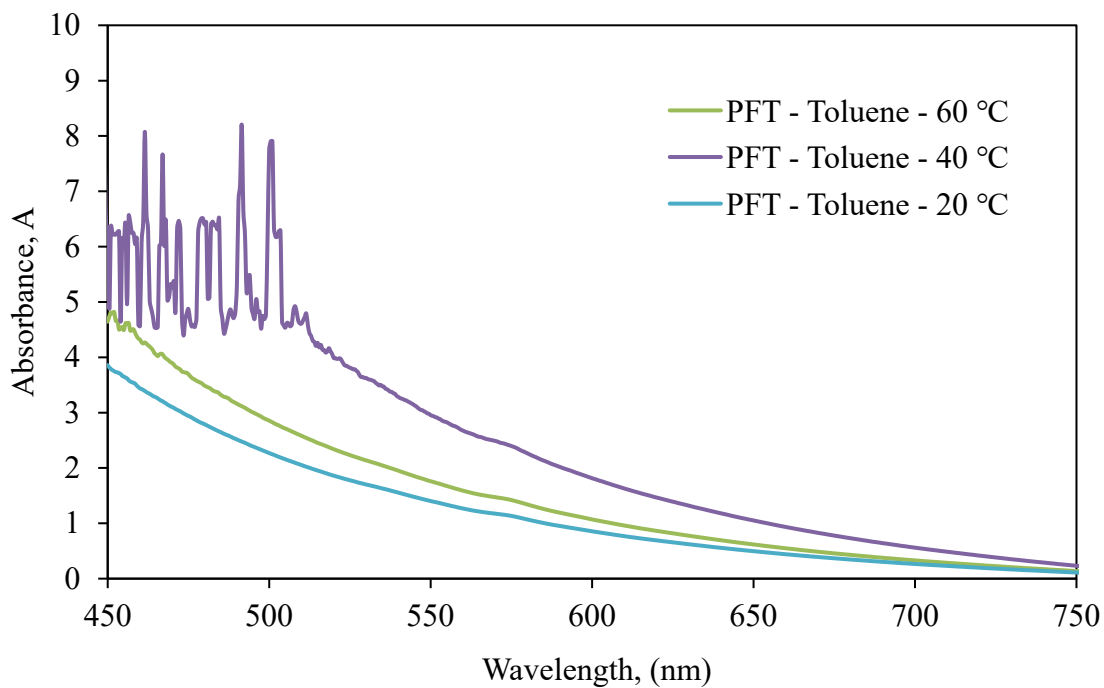
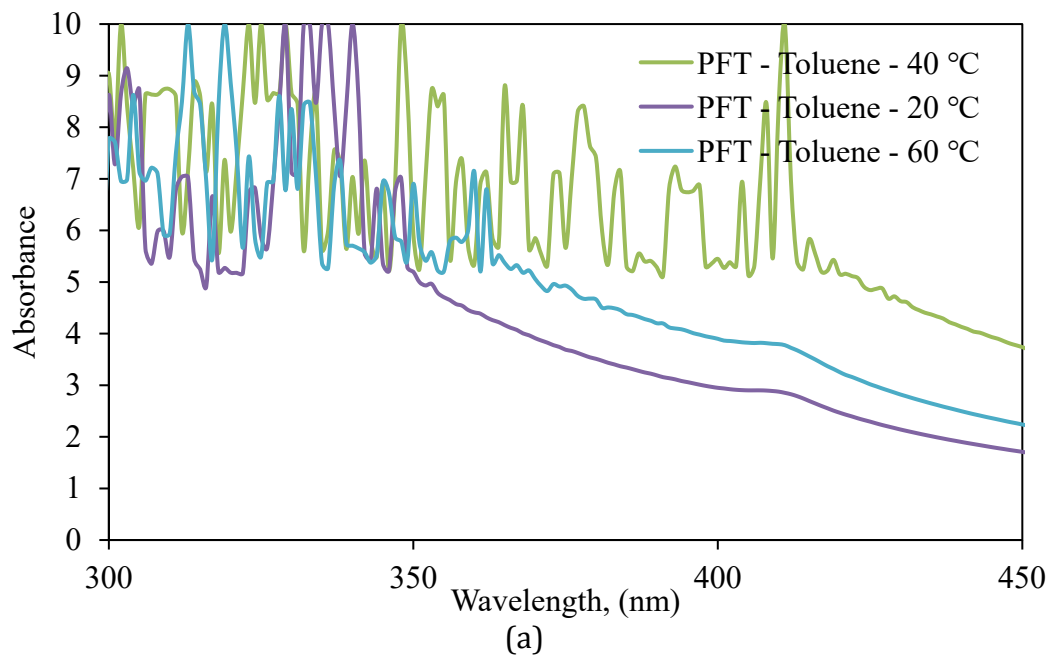


Figure 4.12. UV-Visible spectra for the toluene extracts for increasing temperature (a) the spectra obtained at 7% dilution with pure toluene and (b) the spectra obtained at 30% dilution with pure toluene

Figure 4.13(a) and 4.13(b) summarizes the trends for the toluene extracts from the PFT solids collected at different times. There were no significant peaks corresponding to the Soret bands. The order of decreasing concentrations is 1 hour > 6 hours > 2 hours > 4 hours > 0.5 hour. The spectra between 475 nm and 700 nm showed little change in the trends for the signature peaks of etioporphyrins or octethylporphyrins. The spectra obtained at 4 hours showed indications of the peak at 500 nm which was indicative of the peripheral groups. Since the concentrations of the asphaltenes are rather low as indicated by the absorbances for accurate quantitative analysis. Methods for preconcentration, may be applied here in order to ascertain the optimal extracts to gain a better quantitative understanding of the metalloporphyrins and aromatic compounds in the solids.

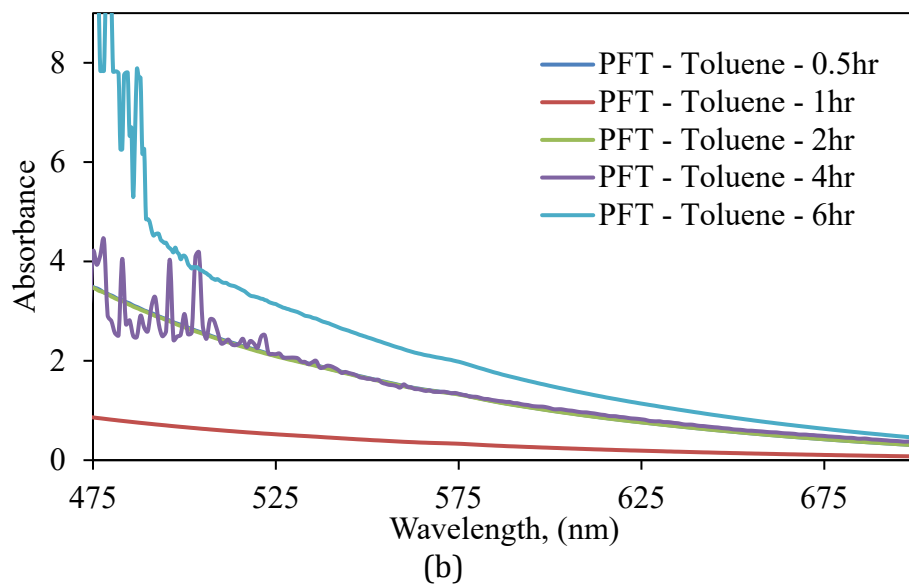
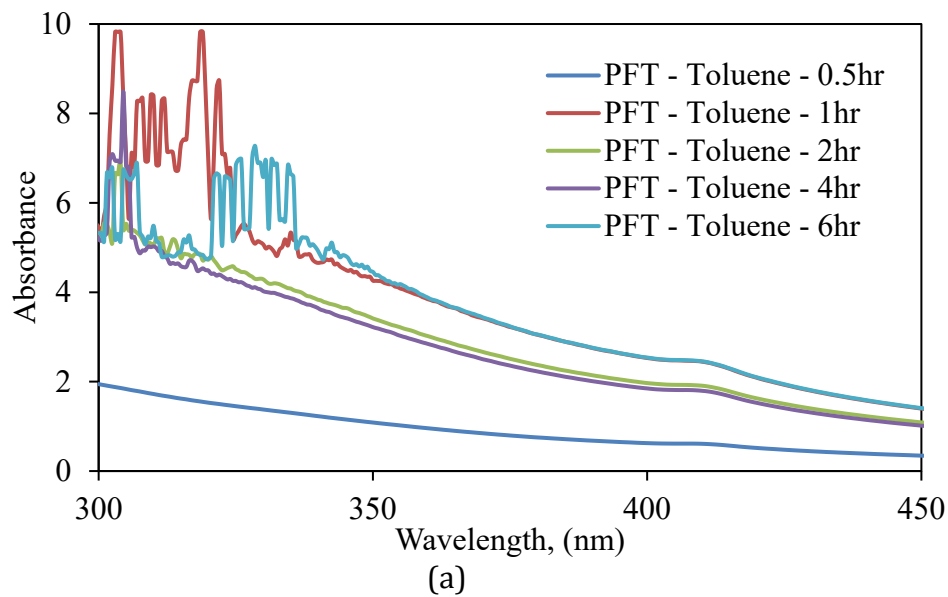


Figure 4.13. UV Visible spectra for the toluene extracts for increasing temperature (a) with 1% dilution and (b) the spectra obtained at 10% dilution with pure toluene

Figure 4.14(a) and Figure 4.14(b) summarizes the trends for the heptane extracts from the PFT solids collected at different temperatures. There were no significant peaks corresponding to the Soret bands. The spectra between 475 nm and 700 nm showed little change in the trends for the signature peaks. The spectra at 60 °C showed the highest peak for the absorption peak at 575 nm. These are indicative of the peripheral groups of the metalloporphyrins such as etioporphyrins and octethylporphyrins. The other spectra between 550 nm and 600 nm however shows slight shoulders indicating the potential for a peak if concentrations were increased. However, as the spectra in Figure 4.14(b) were obtained without dilutions, the samples may need further preconcentration in order to increase the intensity of any peaks. However, the trend is in decreasing concentrations from 60 °C > 40 °C > 20 °C.

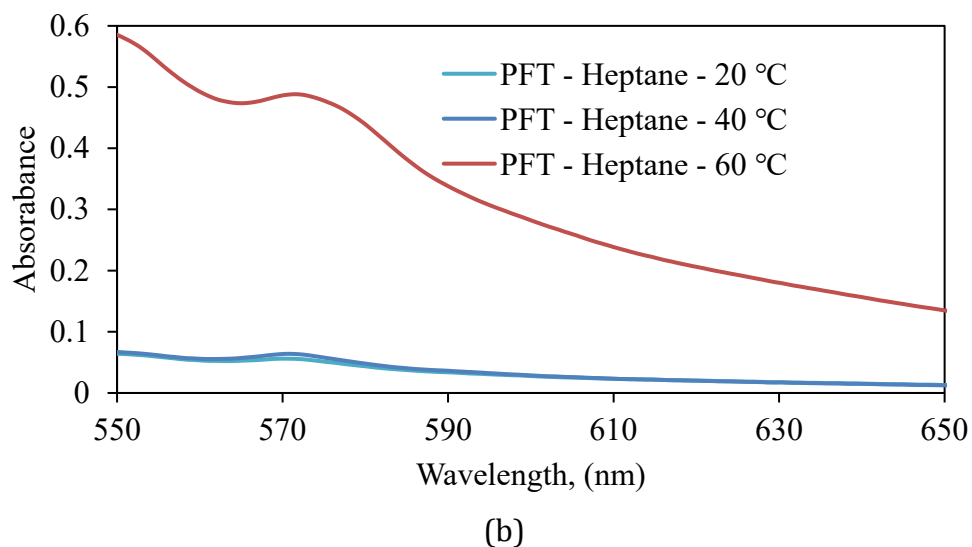
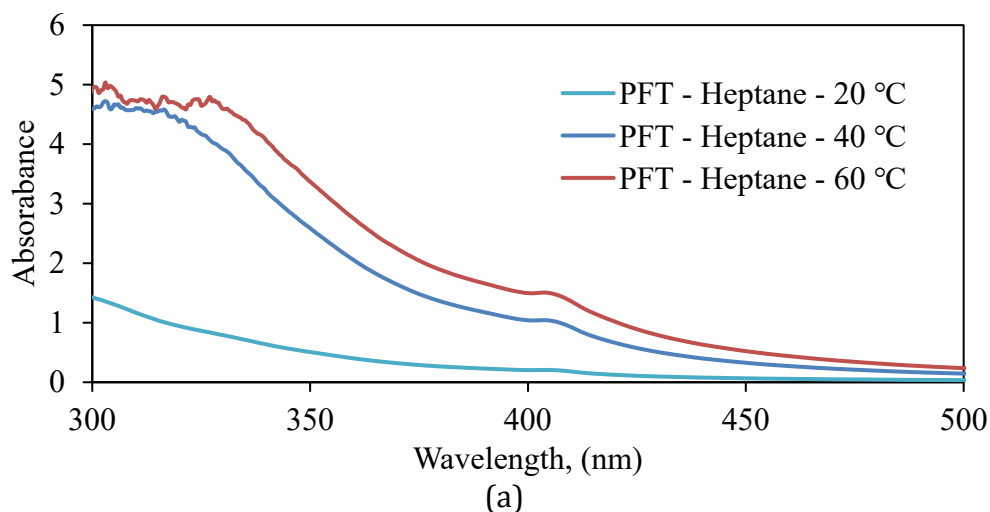


Figure 4.14. UV-Visible spectra for the heptane extracts for increasing temperatures (a) with 20% dilution (b) the spectra obtained without dilution.

Figure 4.15(a) and 4.15(b) are the UV-Visible spectra obtained at different times for the heptane extracts collected at different times. The order of decreasing concentrations based on the spectra obtained are 4 hours > 6 hours > 2 hours > 1 hour > 0.5 hour. However, all peaks did not show distinct peaks for the Soret bands at 410 nm. However, weak peaks for 4 hours, 6 hours and 2 hours were observed. Any spectra obtained at 1 hour and 0.5 hour showed indications of shoulders for the Soret bands. However, any distinct peaks as such were not measured. The regions between 500 and 600 nm showed indications of weak

shoulders being measured. This shows indication of the etioporphyrin peripheral groups or the octethyl peripheral groups.

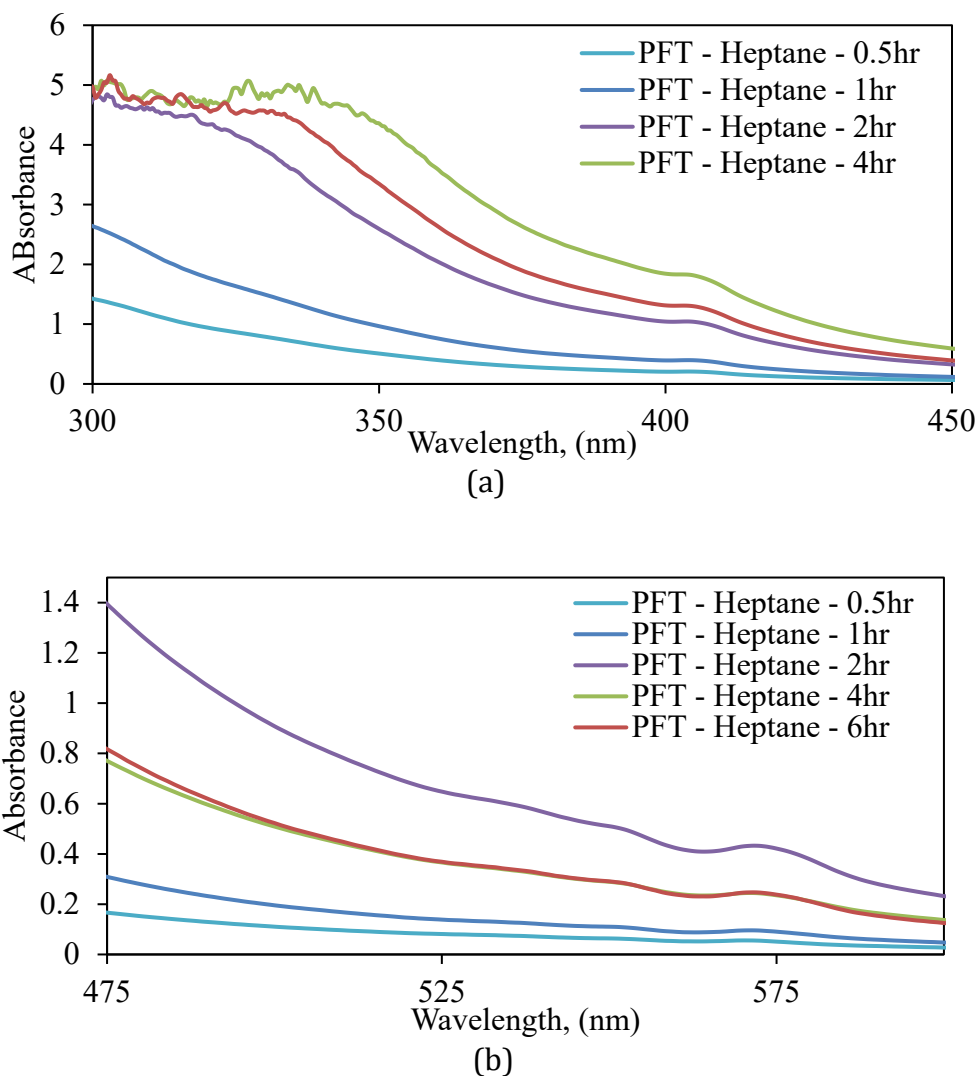


Figure 4.15. UV-Visible spectra for heptane extracts with increasing time (a) 20% dilution with pure heptane and (b) the spectra obtained without dilution.

4.4. H-NMR studies for the froth treatment tailings

Figure 4.16(a), 4.16(b), 4.16(c) and 4.16(d), summarizes the low-resolution NMR spectra for pure samples obtained at different temperatures and contact times for heptane and toluene. These may be indicative of the hydrogens bonded to the aliphatic and the aromatic carbons. The main areas of abundance are shown to be for the aromatic regions and the aliphatic

regions. It should be noted that while the chemical shift for deuterated chloroform is reported at 7.26, but was lower than expected for all the contact times and the temperatures. The cluster of peaks observed for the pure spectra may be indicative of the multiples or spin-spin coupling effects. However, such an understanding may not be understood without performing further high-resolution studies on the spectra. Figure 4.16(a) showed clusters of lower abundance for the regions 7.5 ppm to 8.0 ppm. Figure 4.16(b) on the other hand, documented similar clusters, however the abundances were greater in intensity than the increase in temperature in the aliphatic regime. The indication of several peaks near each other may be indicative of the hydrogen environment surrounding the nucleus. Further analysis with a high resolution might yield results which may provide more insight regarding the nature of these peaks and their significance. Figure 4.16(d) showed similar aliphatic peaks however, with lower abundances, while Figure 4.16(d) showed wider peaks in the aliphatic regimes.

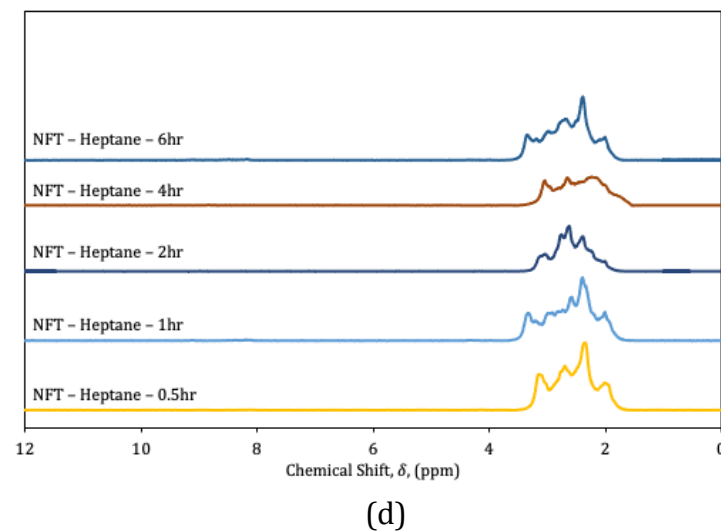
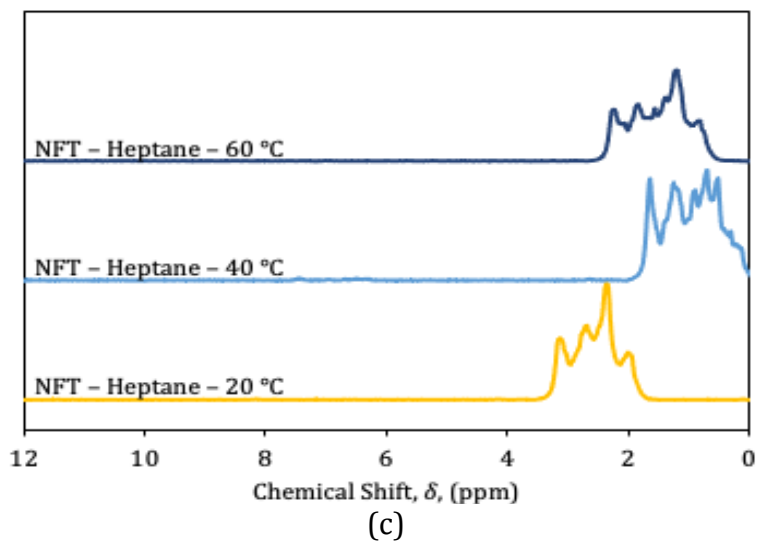
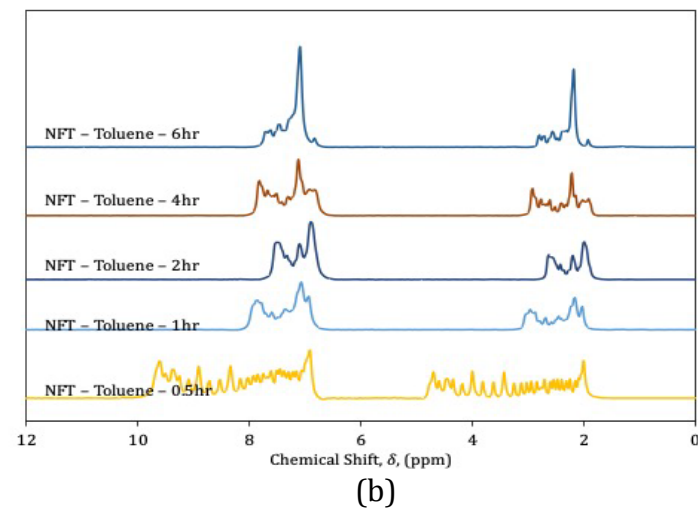
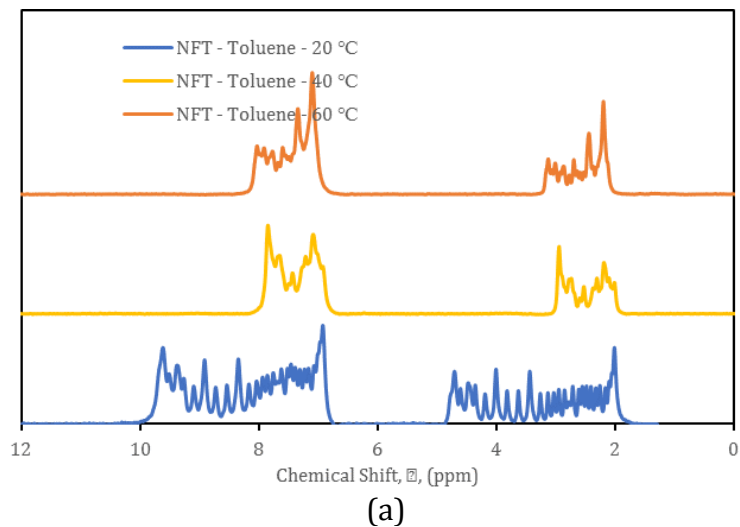


Figure 4.16. Low resolution H-NMR spectra for (a) NFT toluene extract for increasing temperatures, (b) NFT toluene extract for increasing contact times, (c) NFT heptane extract for increase temperatures, (d) NFT heptane extract for increasing contact times.

Figure 4.17(a), 4.17(b), 4.17(c) and 4.17(d) summarizes the low resolution NMR spectra for pure samples obtained at different temperatures and contact times for heptane and toluene for centrifuged solids from the paraffinic froth treatment tailings. However, these are indicative of the hydrogens bonded to aliphatic and aromatic carbons. The chemical shift for chloroform-D is reported at 7.26 ppm as shown in Appendix A, the chloroform peak was lower than expected for PFT - Toluene - 60°C. It should be noted that the spectra measured for heptane at different contact times and temperatures were consistently shifted downfield. However, such an understanding may not be understood without performing further high-resolution studies on the spectra. Figure 4.17(a), and 4.17(b) showed downfield shifts of the chloroform at approximately 6 ppm rather than 7.26 ppm showed clusters of lower abundance for the regions 7.5 to 8.0 ppm. Figure 4.17(c) and Figure 4.17 (d) showed the downfield shifts as well. This may be remedied by adding tetramethylsilane (TMS) was not manually added (as an internal standard) to samples. Figure 4.17(a) exhibited sections of peaks in the aromatic regimes. Figure 4.17(c) and Figure 4.17(d) had large clusters in aliphatic regions. This may be indicative of a greater concentration of the aliphatic carbons. While for this analysis, only the integrated peaks were considered, the presence of broad clusters may be indicative of effects due to the surrounding organic matter. If further analysis is performed, the details of the peaks and any coupling effects should be analyzed. The indication of several peaks near each other may be indicative of the hydrogen environment surrounding the nucleus. Further analysis with a high resolution might shed more light to the significance of the clusters.

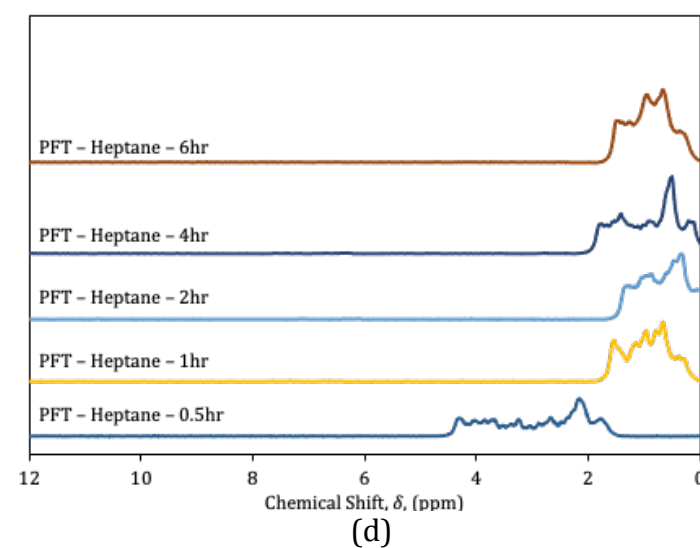
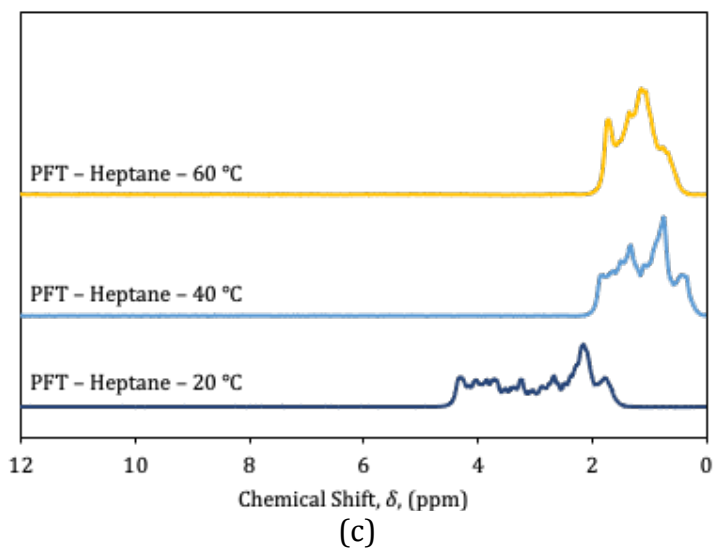
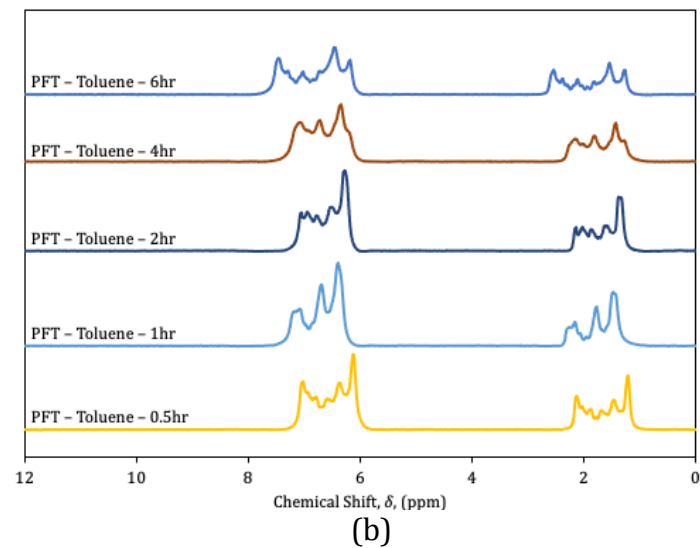
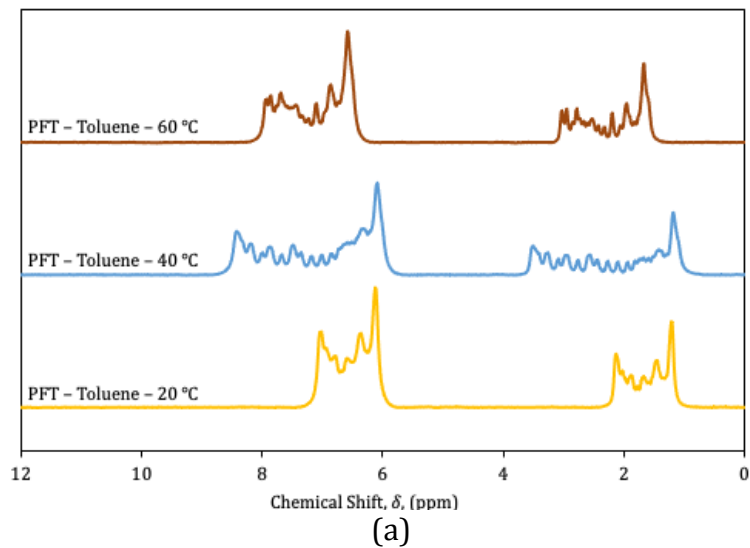


Figure 4.17. Low resolution H-NMR spectra for (a) PFT toluene extract for increasing temperatures, (b) PFT toluene extract for increasing contact times, (c) PFT heptane extract for increase temperatures, (d) PFT heptane extract for increasing contact times.

Figure 4.18 summarizes the comparison between the hydrogens bonded to aromatic carbons to the hydrogens bonded to the aliphatic carbons (Aro/Aliphatic ratio) for the toluene extracts obtained at different temperatures. These ratios were obtained using the pure samples for the naphthenic and the paraffinic solvents. It should be noted at 20 °C, the Aro/Aliphatic ratio for PFT was negligible. Both the H-NMR spectra for the toluene and the heptane extracts from the naphthenic and the paraffinic solids indicates that as the temperature increases, the ratio of aromatic hydrogens are increasing. However, there ratio for the paraffinic solids are consistently lower than the naphthenic solids. It could be inferred that the amount of the aromatic hydrogens extracted from the NFT were significantly higher than the PFT.

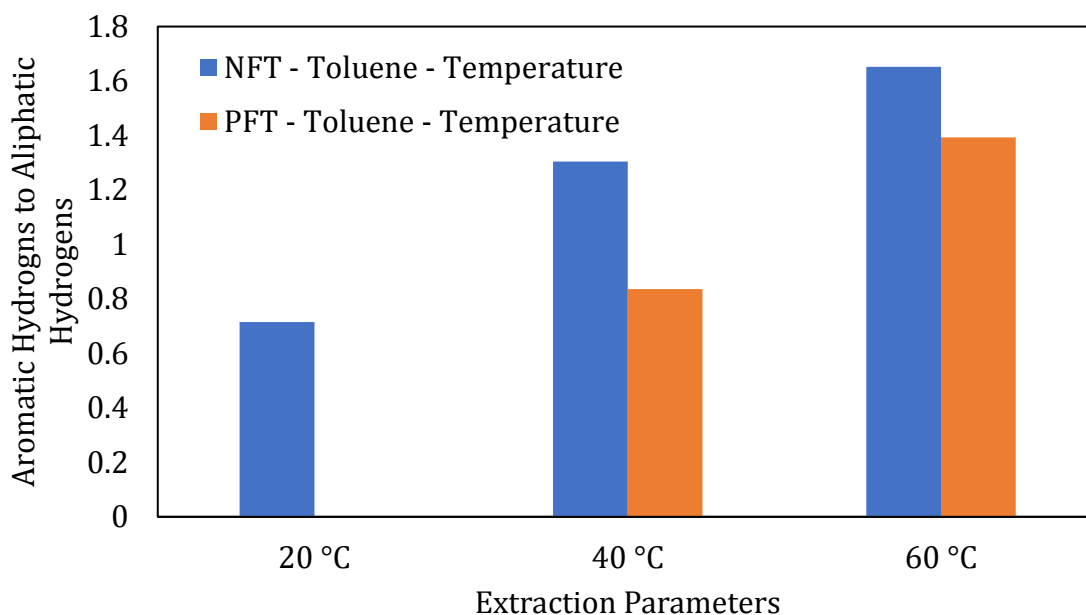


Figure 4.18. Aromatic-to-aliphatic ratios for the toluene extracts collected with increasing temperatures.

Figure 4.19 summarizes the comparison between the hydrogens bonded to aromatic carbons to the hydrogens bonded to the aliphatic carbons (Aro/Aliphatic ratio) for the toluene extracts obtained with increasing contact times. These ratios were obtained using the pure samples for the naphthenic and the paraffinic solvents. It should be noted at 0.5 hour, the Aro/Aliphatic ratio for the solids from the NFT and PFT were negligible. For the extraction times from 1 hour to 6 hours, the trends for the solids from PFT were relatively constant, with the lowest

ratio obtained at 2 hours. The highest Aro/Ali ratios which were obtained for the extractions at 1 hour and 6 hour.

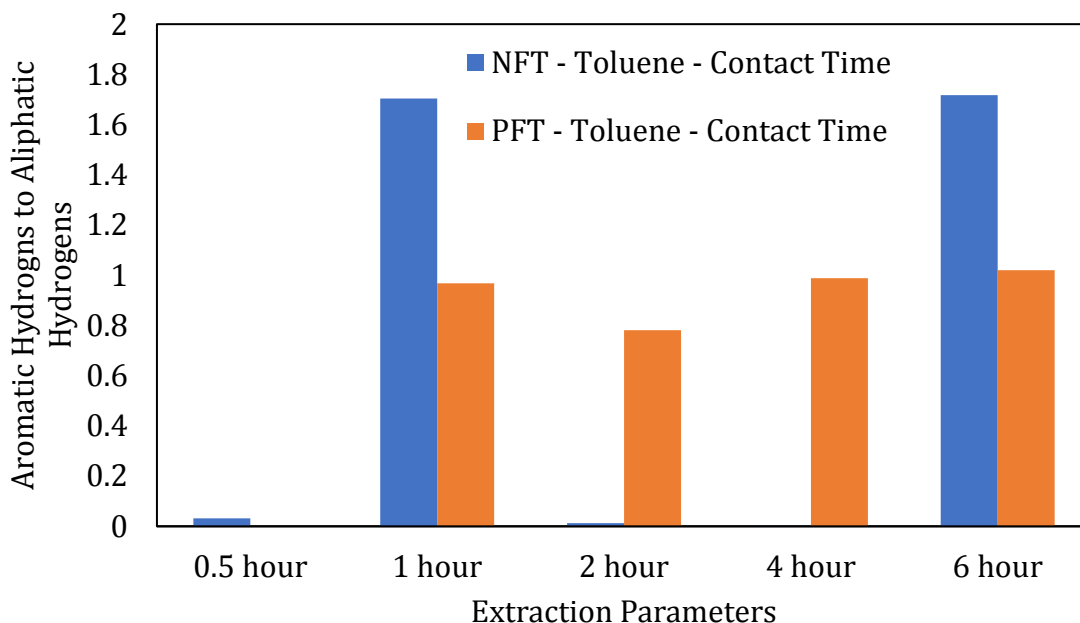


Figure 4.19. Aromatic-to-aliphatic ratio for the toluene extracts collected with increasing contact times.

Figure 4.20 shows the trends between the increasing Aro/Ali ratio for the heptane extracts for NFT and PFT with increasing temperature. The ratio decreased for increasing temperatures for NFT and increased for increasing temperature for PFT. Comparatively for the Figures 5.11 and 5.12 the Aro/Ali ratios are significantly lower for the heptane extracts than the toluene extracts. This could be indicative that using heptane for the extraction of aromatic hydrocarbons was not effective.

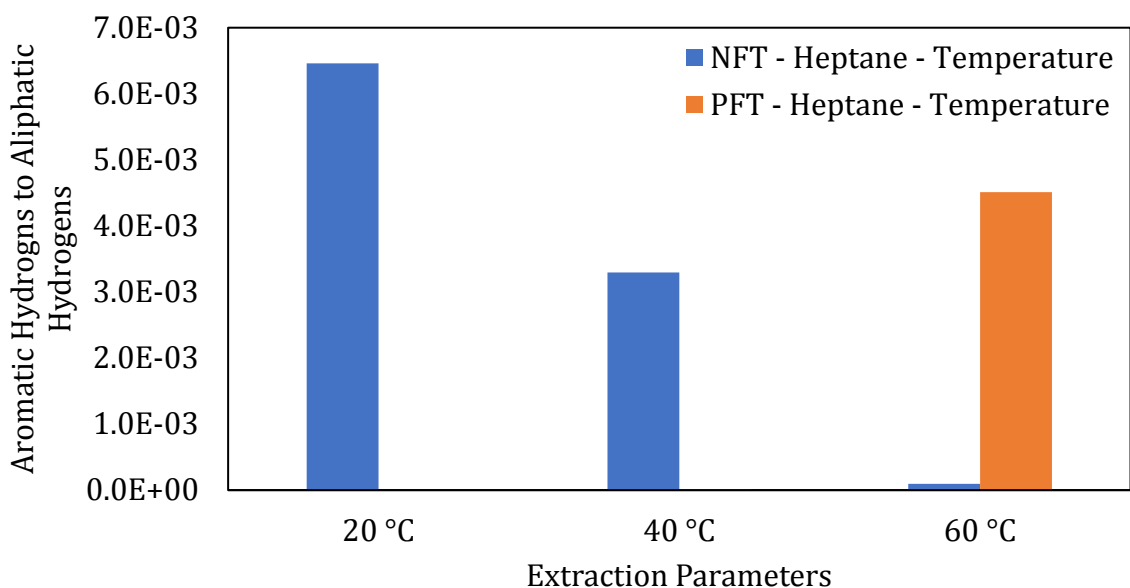


Figure 4.20. Aromatic-to-aliphatic ratio for the heptane extracts collected at increasing temperatures.

Figure 4.21 summarizes the comparison between the hydrogens bonded to aromatic carbons to the hydrogens bonded to the aliphatic carbons (Aro/Al_i ratio) for the heptane extracts obtained at different contact times. These ratios were obtained using the pure samples for the naphthenic and the paraffinic solvents. It should be noted that Aro/Al_i ratio for PFT were significantly lower than the negligible. Both the H-NMR spectra for the toluene and the heptane extracts from the naphthenic and the paraffinic solids indicates that as the contact time increases, the ratio of aromatic hydrogens are decreasing excluding the data point for 2 hours. However, there ratio for the paraffinic solids are consistently lower than the naphthenic solids. It could be inferred that the amount of the aromatic hydrogens extracted from the NFT were significantly higher than the PFT.

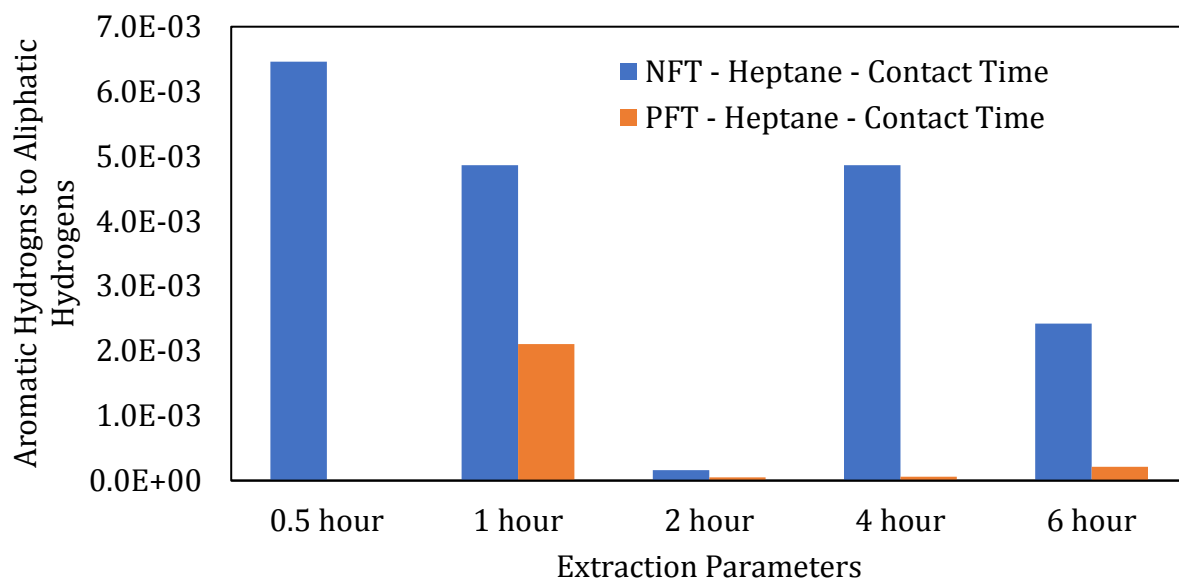


Figure 4.21. Aromatic-to-aliphatic ratio for the heptane extracts collected at increasing contact times.

The solid liquid extractions need to be performed in order to analyze the presence of metalloporphyrin compounds present in the compounds, the analysis confirmed the presence of metal porphyrins, however, the absorbances measured for a few runs were lower than the optimal range. This could be indicative that using the current experimental method the concentrations of the metalloporphyrins observed were lower in the sample. Perhaps the use of a Soxhlet extractor, or a reflux set up might provide a greater yield for certain experimental runs, potentially increasing the absorbances of the samples to the optimal ranges required. The next step would be to extract asphaltenes and more specifically metal porphyrins from the bitumen and creating a calibration curve. With the combination of the greater concentrations in the sample and the calibration curve, an accurate quantitative understanding of the trends in the extraction mechanism as well as the concentrations might be understood. This addresses the extractions of asphaltene compounds. The next step would be to analyze the samples using a high-resolution NMR. The clusters present in the NMR spectra might be better understood. Additionally, if the analyses were

combined with an FTIR, an understanding of the key functional groups could be better understood.

5. Summary and Conclusions

The thermogravimetric analyses provided an indication for various components based on the boiling points for the naphthenic and paraffinic froth treatment tailings. Asphaltene content are greater in the PFT than NFT. The combustion regimes from 350 °C and 625 °C showed the weight loss for the asphaltenes for the tailings and their centrifuged solids. Comparatively, the NFT solids were found to have higher amounts of hydrocarbons combusted between 350 °C to 420 °C, than the event between 420 °C and 635 °C. The NFT and PFT emulsions were centrifuged to separate the aqueous and solids phase. Relatively, the NFT was composed of 75.5% liquids and 24.5% solids, and 69.7 % liquids and 30.2% solids.

For the aqueous phases, there were O—H and C—O peaks observed using ATR-FTIR. As the pH decreases, there was no trend with the O—H peaks for the PFT extracts, while the extracts showed a decrease in O—H and increase in C—O bonds. An increase in temperature (except for 60 °C), aided in evaporation of the chloroform rather than promoting the migration from the aqueous phase to the organic phase. This trend was observed in both the NFT and the PFT extracts. While the mass extracted, there was an increase in the O—H and the C—O bonds. For the PFT extracts, there was an increase in C—O and increase in O—H. The maximum recovery from the aqueous phase of NFT was 19 % for extraction at 20 °C and pH 1.0 and 60 °C and pH 3.0. For the PFT, the maximum recovery hydrocarbons from the aqueous phase was 23.2% at 20 C and pH 2.0.

Centrifuged solids from the naphthenic and the paraffinic tailings, were extracted with heptane and toluene. The peaks between 400 nm and 500 nm were observed for electronic absorption peaks for nickel or vanadium porphyrins. An increase in the contact times for the toluene extracts demonstrated the following order of the absorbances where 0.5 hour > 2 hours > 1 hours > 4 hours > 6 hours for the toluene NFT extracts. The presence of Soret bands characteristic of the nickel and vanadium porphyrins were observed for all extracts, in varying intensities. An increase in temperature in the NFT extracts, decreased the intensity of the curves, meaning that the concentrations of the hydrocarbons decreased. The

absorbances between the 500 nm and 600 nm are evident of the octethyl peripheral group or the etioporhyrin peripheral groups. These peaks or shoulders were observed in all spectra but were excluding those obtained for the PFT extractions with toluene at increasing temperatures and increasing contact time. The extracts obtained from the NMR indicated several peaks within the aromatic and the aliphatic regions. The extracts obtained for increasing temperatures for the NFT or PFT had increasing aromatic hydrogen to aliphatic hydrogen ratios, while with the increasing contact times, the highest ratios were observed for the toluene extracts of the NFT and PFT at 1 hour and 6 hours. It should be noted that the H-NMR spectra revealed the presence of some spectra yielded certain peaks in the aliphatic and the aromatic regions, with negligible amounts of olefinic peaks.

6. Recommendations for Future Work

There are several areas of improvement or room for studies which need to be performed. To begin with, the thermogravimetric studies performed to analyze the feedstock exhibited multistep decomposition for the naphthenic froth treatment process. TGA coupled with mass spectroscopy or infrared spectroscopy would reveal the nature of the hydrocarbons evaporated from the emulsion. Performing a coupled thermal and spectroscopic methods would be interesting as it might provide a better understanding to the classes of compounds evaporating in that regime. TGA analyses with the centrifuged solids, showed different amounts of solids combusting between the different regimes. The different zones of combustion might yield a better understanding to the nature of the hydrocarbons. As well, it would be interesting to see what results a TGA-FTIR study reveals, with relation to the types of the functional groups evaporating at different temperature regimes.

The liquid-liquid extractions confirmed the presence of small amounts of hydrocarbons migrating between the different phases. While the mass extracted showed increased extraction, peaks of similar magnitude were not described in the FTIR spectra obtained. The chloroform extracts could be analysed with a transmittance FTIR. As the path length is fixed, a calibration curve for the C—O bond, C—C aromatic wag peaks can be constructed. While performing the spectral analysis using a quantitative analysis, the peaks between the wavelengths 1600 cm^{-1} and 2400 cm^{-1} , need to be deconvoluted. Doing so, we may be able to construct a calibration curve for the C = O bond more commonly used for quantification of carboxylic acids. Using a calibration curve, once the relative concentrations are estimated, analysis using an FTIR with a fixed path length must be performed. These experiments would provide insight regarding the molecular weights of the compounds containing the aromatic and the carboxylic rings.

Once the presence of carboxylic acids are confirmed using these extracts, a comparison between different solvents and the feedstock should be performed. While a previous understanding regarding the solubility parameters drove the decision to choose chloroform

other solvent with better properties such as an ether, or an alcohol might give certain differences in the compounds to be analyzed.

The solid-liquid extractions need to be performed in order to analyze the presence of metallic porphyrin compounds present in the compounds, the analysis confirmed the presence of metal porphyrins, however, the absorbances measured for a few runs were lower than the optimal range. This inhibited any sort of quantitative analysis to be performed. This could be indicative that using the current experimental set up the concentrations of the metal porphyrins observed were lower in the sample. Perhaps the use of a Soxhlet extractor might provide a greater yield for certain experimental runs, potentially increasing the absorbances of the samples to the optimal ranges required. The next step would be to extract asphaltenes and more specifically metal porphyrins from bitumen and creating a calibration curve. With the combination of the greater concentrations in the sample and the calibration curve, an accurate quantitative understanding of the trends in the extraction mechanism as well as the concentrations might be understood. This address the asphaltic portion of the compounds extracted. The next step would be to analyze the samples using a high-resolution NMR. By doing so, the analysis from section 4.4 would be more precise.

Bibliography

- (1) Masliyah, J. H.; Czarnecki, J. A.; Xu, Z. *Handbook on Theory and Practice of Bitumen Recovery from Athabasca Oil Sands: Volume 2. Industrial Practice*; 2013.
- (2) Masliyah, J. H.; Xu, Z.; Czarnecki, J. A. *Handbook on Theory and Practice of Bitumen Recovery from Athabasca Oil Sands: Volume 1. Theoretical Basis*; Kingsley Knowledge Pub: Cochrane, 2011.
- (3) Lin, F.; Stoyanov, S. R.; Xu, Y. Recent Advances in Nonaqueous Extraction of Bitumen from Mineable Oil Sands: A Review. *Org. Process Res. Dev.* **2017**, *21* (4), 492–510. <https://doi.org/10.1021/acs.oprd.6b00357>.
- (4) Hein, F. J. Heavy Oil and Oil (Tar) Sands in North America: An Overview & Summary of Contributions. *Nat. Resour. Res.* **2006**, *15* (2), 67–84. <https://doi.org/10.1007/s11053-006-9016-3>.
- (5) Strauz, O. P.; Lown, E. M. *The Chemistry of Alberta Oil Sands, Bitumens, and Heavy Oils*, First.; Alberta Energy Research Institute: Calgary, 2003.
- (6) Allen, E. W. Process Water Treatment in Canada's Oil Sands Industry: II. A Review of Emerging Technologies. *J. Environ. Eng. Sci.* **2008**, *7* (5), 499–524. <https://doi.org/10.1139/S08-020>.
- (7) Berkowitz, N.; Speight, J. G. The Oil Sands of Alberta. *Fuel* **1975**, *54* (3), 138–149. [https://doi.org/10.1016/0016-2361\(75\)90001-0](https://doi.org/10.1016/0016-2361(75)90001-0).
- (8) Rao, F.; Liu, Q. Froth Treatment in Athabasca Oil Sands Bitumen Recovery Process: A Review. *Energy and Fuels* **2013**, *27* (12), 7199–7207. <https://doi.org/10.1021/ef4016697>.
- (9) Masliyah, J.; Zhou, Z. J.; Xu, Z.; Czarnecki, J.; Hamza, H. Understanding Water-Based Bitumen Extraction from Athabasca Oil Sands. *Can. J. Chem. Eng.* **2008**. <https://doi.org/10.1002/cjce.5450820403>.
- (10) Allen, E. W. Process Water Treatment in Canada's Oil Sands Industry: I. Target Pollutants and Treatment Objectives. *J. Environ. Eng. Sci.* **2008**, *7* (2), 123–138. <https://doi.org/10.1139/S07-038>.
- (11) Xu, Z.; Masliyah, J. Bitumen Production from Canadian Oil Sands Deposits. In *AIChE Annual Meeting, Conference Proceedings*; 2007.
- (12) Small, C. C.; Cho, S.; Hashisho, Z.; Ulrich, A. C. Emissions from Oil Sands Tailings Ponds: Review of Tailings Pond Parameters and Emission Estimates. *Journal of Petroleum Science and Engineering*. 2015. <https://doi.org/10.1016/j.petrol.2014.11.020>.
- (13) BGC Engineering Inc. Oil Sands Tailings Technology Review. *Oil Sands Res. Inf. Netw.* **2010**. [https://doi.org/OSRIN Report No. TR-1](https://doi.org/OSRIN%20Report%20No.%20TR-1).
- (14) Pudasainee, D.; Khan, M.; Gupta, R. *Advanced Processing of Froth Treatment Tailings - Proof of Principle*; Edmonton, 2020.
- (15) Mahaffey, A.; Dubé, M. Review of the Composition and Toxicity of Oil Sands Process-Affected Water. *Environ. Rev.* **2017**, *25* (1), 97–114. <https://doi.org/10.1139/er-2015-0060>.
- (16) Masliyah, J.; Zhou, Z. J.; Xu, Z.; Czarnecki, J.; Hamza, H. Understanding Water-Based Bitumen Extraction. *Can. J. Chem. Eng.* **2004**, *82* (August), 628–654.
- (17) Li, C.; Fu, L.; Stafford, J.; Belosevic, M.; El-din, M. G. The Toxicity of Oil Sands Process-Affected Water (OSPW): A Critical Review. *Sci. Total Environ.* **2017**, *602*, 1785–

1802. <https://doi.org/10.1016/j.scitotenv.2017.06.024>.
- (18) Kislik, V. S. *Solvent Extraction: Classical and Novel Approaches*, First.; Jerusalem, 2013.
- (19) Mózo, B. S. *Solvent Extraction Principles and Practice*, Second Edi.; Rydberg, J., Cox, M., Musikas, C., Choppin, G. R., Eds.; Taylor & Francis, 2017; Vol. 53.
<https://doi.org/10.1017/CBO9781107415324.004>.
- (20) Clemente, J. S.; Fedorak, P. M. A Review of the Occurrence, Analyses, Toxicity, and Biodegradation of Naphthenic Acids. *Chemosphere*. July 2005, pp 585–600.
<https://doi.org/10.1016/j.chemosphere.2005.02.065>.
- (21) Yépez, O. On the Chemical Reaction between Carboxylic Acids and Iron, Including the Special Case of Naphthenic Acid. *Fuel* **2007**, *86* (7–8), 1162–1168.
<https://doi.org/10.1016/j.fuel.2006.10.003>.
- (22) Yépez, O. Influence of Different Sulfur Compounds on Corrosion Due to Naphthenic Acid. *Fuel* **2005**, *84* (1), 97–104. <https://doi.org/10.1016/j.fuel.2004.08.003>.
- (23) Alvisi, P. P.; Lins, V. F. C. An Overview of Naphthenic Acid Corrosion in a Vacuum Distillation Plant. *Eng. Fail. Anal.* **2011**, *18* (5), 1403–1406.
<https://doi.org/10.1016/j.engfailanal.2011.03.019>.
- (24) Slavcheva, E.; Shone, B.; Turnbull, A. Review of Naphthenic Acid Corrosion in Oil Refining. *Br. Corros. J.* **1999**, *34* (2), 125–131.
<https://doi.org/10.1179/000705999101500761>.
- (25) Li, X.; He, L.; Wu, G.; Sun, W.; Li, H.; Sui, H. Operational Parameters, Evaluation Methods, and Fundamental Mechanisms: Aspects of Nonaqueous Extraction of Bitumen from Oil Sands. In *Energy and Fuels*; 2012.
<https://doi.org/10.1021/ef300337q>.
- (26) Xu, Y.; Wu, J.; Dabros, T.; Rahimi, P.; Kan, J. Investigation on Alternative Disposal Methods for Froth Treatment Tailings-Part 2, Recovery of Asphaltenes. *Can. J. Chem. Eng.* **2013**, *91* (8), 1358–1364. <https://doi.org/10.1002/cjce.21822>.
- (27) Zhao, B.; Currie, R.; Mian, H. Catalogue of Analytical Methods for Naphthenic Acids Related to Oil Sands Operations. *Oil Sand Res. Inf. Netw.* **2012**, 65.
- (28) Headley, J. V.; Peru, K. M.; Fahlman, B.; Colodey, A.; McMartin, D. W. Selective Solvent Extraction and Characterization of the Acid Extractable Fraction of Athabasca Oils Sands Process Waters by Orbitrap Mass Spectrometry. *Int. J. Mass Spectrom.* **2013**, 345–347, 104–108. <https://doi.org/10.1016/j.ijms.2012.08.023>.
- (29) Rogers, V. V.; Liber, K.; MacKinnon, M. D. Isolation and Characterization of Naphthenic Acids from Athabasca Oil Sands Tailings Pond Water. *Chemosphere* **2002**, *48* (5), 519–527. [https://doi.org/10.1016/S0045-6535\(02\)00133-9](https://doi.org/10.1016/S0045-6535(02)00133-9).
- (30) Bowman, D. T.; Slater, G. F.; Warren, L. A.; McCarry, B. E. Identification of Individual Thiophene-, Indane-, Tetralin-, Cyclohexane-, and Adamantane-Type Carboxylic Acids in Composite Tailings Pore Water from Alberta Oil Sands. *Rapid Commun. Mass Spectrom.* **2014**. <https://doi.org/10.1002/rcm.6996>.
- (31) Celsie, A.; Parnis, J. M.; Mackay, D. Impact of Temperature, PH, and Salinity Changes on the Physico-Chemical Properties of Model Naphthenic Acids. *Chemosphere* **2016**, *146*, 40–50. <https://doi.org/10.1016/j.chemosphere.2015.11.122>.
- (32) Huang, R.; McPhedran, K. N.; Sun, N.; Chelme-Ayala, P.; Gamal El-Din, M. Investigation of the Impact of Organic Solvent Type and Solution PH on the Extraction Efficiency of Naphthenic Acids from Oil Sands Process-Affected Water. *Chemosphere* **2016**, *146*, 472–477. <https://doi.org/10.1016/j.chemosphere.2015.12.054>.

- (33) Smallwood, I. M. Handbook of Organic Solvent Properties. *Handb. Org. Solvent Prop.* **2012**, 1–306. <https://doi.org/10.1016/C2009-0-23646-4>.
- (34) Gray, M. R. *Upgrading Oilsands Bitumen and Heavy Oil*; Pica Pica Press: Edmonton, 2015.
- (35) Jivraj, M. N.; MacKinnon, M.; Fung, B. Naphthenic Acid Extraction and Quantitative Analysis with FT-IR Spectroscopy. *Synchrude Anal. Methods Man.* **1995**, 12.
- (36) Stuart, B. *Infrared Spectroscopy: Fundamentals and Applications*; John Wiley and Sons Ltd, 2004.
- (37) Filby, R. H. Origin and Nature of Trace Element Species in Crude Oils, Bitumens and Kerogens: Implications for Correlation and Other Geochemical Studies. *Geofluids Orig. Migr. Evol. fluids Sediment. basins* **1994**, No. 78, 203–219.
- (38) Dechaine, G. P.; Gray, M. R. Chemistry and Association of Vanadium Compounds in Heavy Oil and Bitumen, and Implications for Their Selective Removal. *Energy and Fuels* **2010**, 24 (5), 2795–2808. <https://doi.org/10.1021/ef100173j>.
- (39) Degens, E. T. *Biogeochemistry of Stable Isotopes*; 1969. <https://doi.org/10.1038/227634c0>.
- (40) Ali, M. F.; Abbas, S. A Review of Methods for the Demetallization of Residual Fuel Oils. *Fuel Process. Technol.* **2006**, 87 (7), 573–584. <https://doi.org/10.1016/j.fuproc.2006.03.001>.
- (41) Banda-Cruz, E. E.; Padrón-Ortega, S. I.; Gallardo-Rivas, N. V.; Rivera-Armenta, J. L.; Páramo-García, U.; Zavala, N. P. D.; Mendoza-Martínez, A. M. Crude Oil UV Spectroscopy and Light Scattering Characterization. *Pet. Sci. Technol.* **2016**, 34 (8), 732–738. <https://doi.org/10.1080/10916466.2016.1161646>.
- (42) Yoon, S.; Bhatt, S. D.; Lee, W.; Lee, H. Y.; Jeong, S. Y.; Baeg, J. O.; Lee, C. W. Separation and Characterization of Bitumen from Athabasca Oil Sand. *Korean J. Chem. Eng.* **2009**, 26 (1), 64–71. <https://doi.org/10.1007/s11814-009-0011-3>.
- (43) Alboudwarej, H.; Jakher, R. K.; Svrcek, W. Y.; Yarranton, H. W. Spectrophotometric Measurement of Asphaltene Concentration. *Pet. Sci. Technol.* **2004**, 22 (5–6), 647–664. <https://doi.org/10.1081/LFT-120034206>.
- (44) Adegoroye, A.; Wang, L.; Omotoso, O.; Xu, Z.; Masliyah, J. Characterization of Organic-Coated Solids Isolated from Different Oil Sands. *Can. J. Chem. Eng.* **2010**, 88 (3), 462–470. <https://doi.org/10.1002/cjce.20294>.
- (45) Clemente, J. S.; Fedorak, P. M. A Review of the Occurrence, Analyses, Toxicity, and Biodegradation of Naphthenic Acids. *Chemosphere.* 2005. <https://doi.org/10.1016/j.chemosphere.2005.02.065>.
- (46) D'Souza, F.; Boulas, P.; Aukauloo, A. M.; Guillard, R.; Kisters, M.; Vogel, E.; Kadish, K. M. Electrochemical, UV/Visible, and EPR Characterization of Metalloporphycenes Containing First-Row Transition Metals. *J. Phys. Chem.* **1994**, 98 (46), 11885–11891. <https://doi.org/10.1021/j100097a014>.
- (47) Zhao, X.; Liu, Y.; Xu, C.; Yan, Y.; Zhang, Y.; Zhang, Q.; Zhao, S.; Chung, K.; Gray, M. R.; Shi, Q. Separation and Characterization of Vanadyl Porphyrins in Venezuela Orinoco Heavy Crude Oil. *Energy and Fuels* **2013**, 27 (6), 2874–2882. <https://doi.org/10.1021/ef400161p>.
- (48) Lan, M.; Zhao, H.; Yuan, H.; Jiang, C.; Zuo, S.; Jiang, Y. Absorption and EPR Spectra of Some Porphyrins and Metalloporphyrins. *Dye. Pigment.* **2007**, 74 (2), 357–362. <https://doi.org/10.1016/j.dyepig.2006.02.018>.

- (49) Zheng, W.; Shan, N.; Yu, L.; Wang, X. UV-Visible, Fluorescence and EPR Properties of Porphyrins and Metalloporphyrins. *Dye. Pigment.* **2008**, *77* (1), 153–157.
<https://doi.org/10.1016/j.dyepig.2007.04.007>.

Appendix A

A.1. Mass Balance using the TGA for FTT tailings

The whole tailings for the NRU and the TSRU were measured in the TGA. Once a breakdown for the major components were obtained, the tailings samples were then centrifuged in order to estimate breakdown for these major components in the solids phase. The solids were then put into a TGA for the weight losses at difference temperatures. The following multi-step heating procedure was used to determine the relative amounts of solids present in the samples. Table 1 describes the multi-step heating method used for the TGA experiments for the centrifuged solids and the tailings itself. The method used for the multi-step heating method is summarized as follows in Table A.1.

Table A. 1. The multistep heating method used for the TGA experiments for the naphthenic and paraffinic froth treatment tailings and their centrifuged solids.

Step	Atmosphere	Start temperature (°C)	End temperature (°C)	Ramp rate (°C/min)	Hold time (min)	Total time (min)
Step 1	Nitrogen	25	80	5	5	16
Step 2		80	95	1	5	20
Step 3		95	100	1	5	10
Step 4		100	110	1	5	15
Step 5		110	165	5	5	16
Step 6		165	220	5	5	16
Step 7		220	275	5	5	16
Step 8		275	350	5	5	20
Ash 1	Oxygen	350	420	5	5	19
Ash 2		420	480	5	5	17
Ash 3		480	550	5	5	19
Ash 4		550	650	5	5	55

A.1.2. TGA experiments for the naphthenic froth treatment tailings

Table A. 2. Initial and final masses for the naphthenic froth treatment tailings

Sample name	Initial mass (g)	Final mass (g)
NFT-1	4.4973	0.3594
NFT-2	4.3567	0.3541
NFT-3	4.5433	0.2926

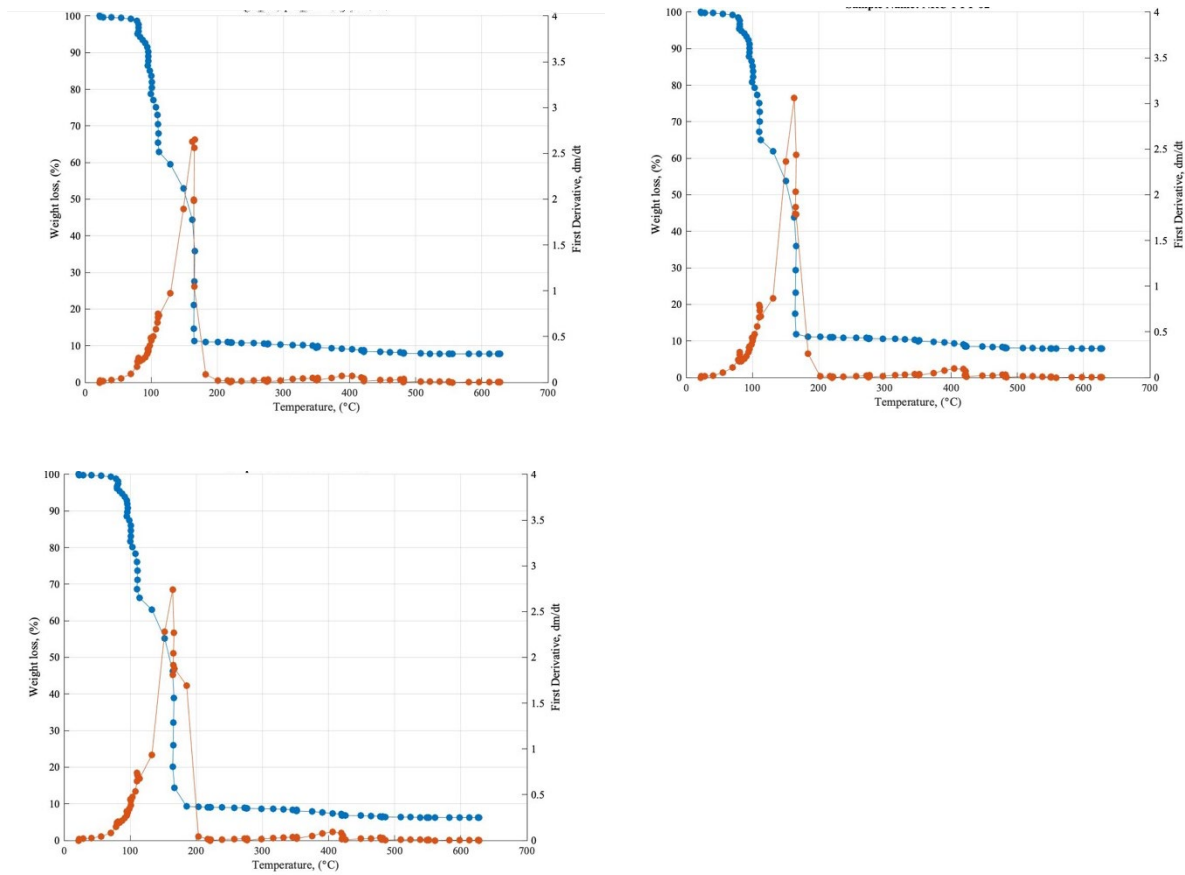


Figure A. 1. The weight loss and the first derivatives for the naphthenic froth treatment tailings emulsion.

Table A. 3. Summary of the weight loss for the naphthenic froth treatment tailings emulsion and the average weight loss for the triplicates.

Temperature		Heating rate (°C/min)	NFT - 1 (%)	NFT - 2 (%)	NFT - 3 (%)	Average weight loss (%)	Average weight loss (g)
Start (°C)	End (°C)						
25	80	5	4.07	3.94	3.25	3.75	0.168
80	95	1	9.42	8.26	7.53	8.40	0.375
95	100	1	7.73	6.95	6.93	7.20	0.322
100	110	1	15.91	13.54	13.02	14.16	0.632
110	165	5	51.55	49.80	48.48	49.94	2.230
165	220	5	0.51	6.53	11.14	6.06	0.271
220	275	5	0.42	0.25	0.31	0.33	0.015
275	350	5	0.88	0.58	0.57	0.68	0.030
350	420	5	1.12	1.46	1.21	1.26	0.056
420	480	5	0.50	0.49	0.41	0.47	0.021
480	550	5	0.12	0.18	0.12	0.14	0.006
550	650	5	0.05	0.03	0.04	0.04	0.002
Total weight loss			92.01	91.87	93.56		

Table A. 4. Complete mass balance for the naphthenic froth treatment tailings

Component	Weight percent (%)
Lighter hydrocarbons and water (25 °C and 165 °C)	83.46
Heavy hydrocarbons (165 °C and 350 °C)	7.06
Bitumen residue	1.91
Mineral solids	7.57
Total	100.00

A.1.3. TGA Experiments for the Centrifuged Solids from NFT

The above method was used to determine the rough weight losses within each temperature differential for the NRU and the TSRU tailings as well as the centrifuged solids.

Table A. 5. The sample names along with the initial and final masses for the TGA experiments using the centrifuged NFT solids.

Sample name	Initial mass (g)	Final mass (g)
NFT Solids - 1	4.2356	1.6492
NFT Solids - 2	4.6222	1.7129
NFT Solids - 3	4.7949	1.7777

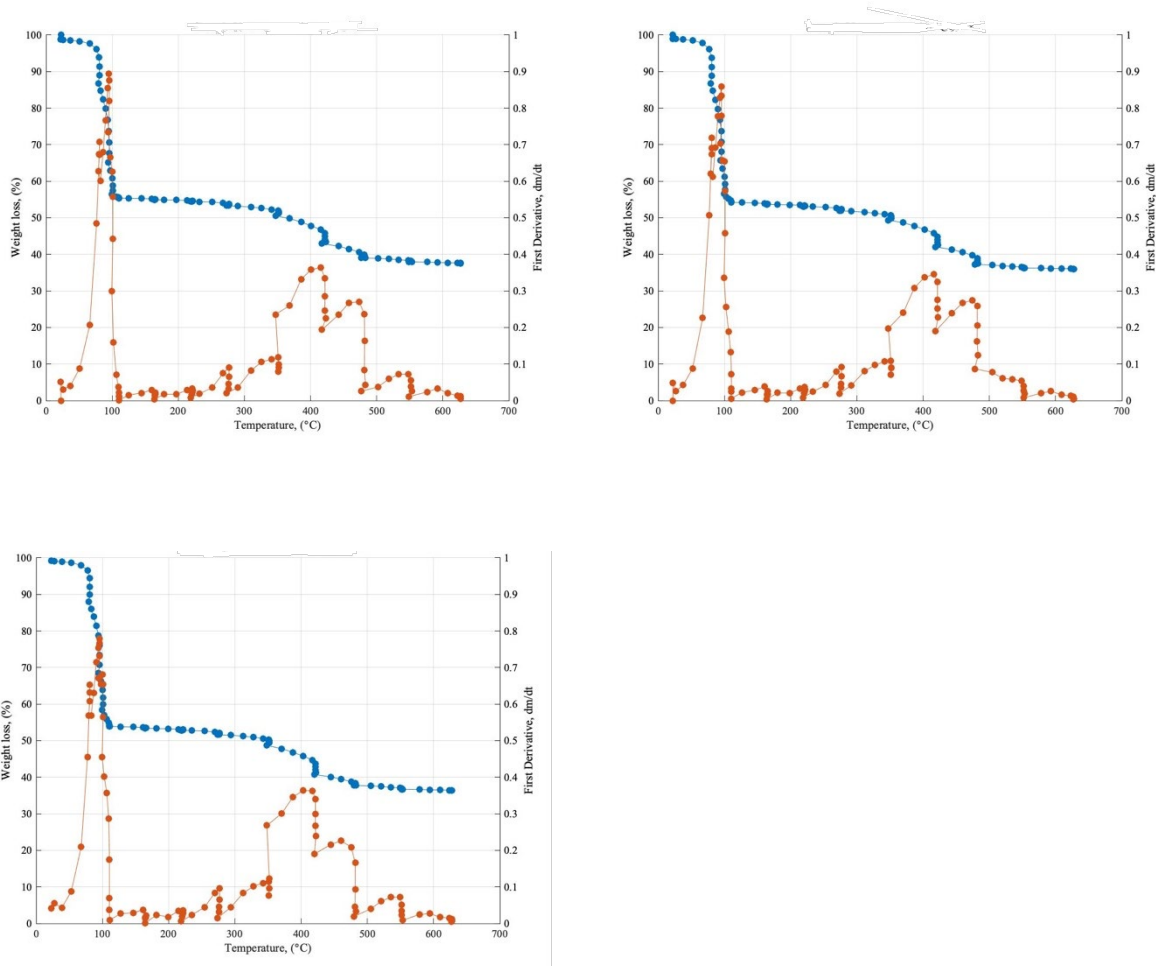


Figure A. 2. The weight loss and the first derivative for the centrifuged solids from the naphthenic froth treatment tailings (performed in triplicate)

Table A. 6. Summary of the weight loss for the centrifuged solids from the naphthenic froth treatment tailings.

Temperature		Heating rate (°C/ min)	NFT - Solids - 1 (%)	NFT - Solids - 2 (%)	NFT - Solids - 3 (%)	Average weight loss (%)	Average weight loss (g)
Start (°C)	End (°C)						
25	80	5	6.16	6.18	5.60	5.98	0.272
80	95	1	20.19	20.10	18.35	19.55	0.890
95	100	1	14.75	12.56	12.11	13.14	0.598
100	110	1	3.41	6.70	9.62	6.58	0.299
110	165	5	0.43	0.66	0.78	0.62	0.028
165	220	5	0.47	0.50	0.48	0.49	0.022
220	275	5	0.79	0.95	0.97	0.90	0.041
275	350	5	1.81	1.76	1.79	1.79	0.081
350	420	5	6.21	5.78	6.57	6.19	0.282
420	480	5	5.83	5.92	5.68	5.81	0.264
480	550	5	1.77	2.51	1.41	1.90	0.086
550	650	5	0.53	0.41	0.48	0.47	0.022
Total Weight Loss			62.37	64.03	63.85		

Table A. 7. Mass balance for the centrifuged solids from the naphthenic froth treatment tailings

Component	Weight percent (%)
Lighter hydrocarbons and water (25 °C and 165 °C)	45.88
Heavy hydrocarbons (165 °C and 350 °C)	3.17
Bitumen residue	14.37
Mineral solids	36.58
Total	100.00

A.1.4. TGA experiments for the PFT

Table A. 8. The sample names, along with the initial and final masses for the TGA experiments using the paraffinic froth treatment tailings.

Sample name	Initial mass (g)	Final mass (g)
PFT-1	4.4973	0.2730
PFT-2	4.3567	0.1960
PFT-3	4.5433	0.1675

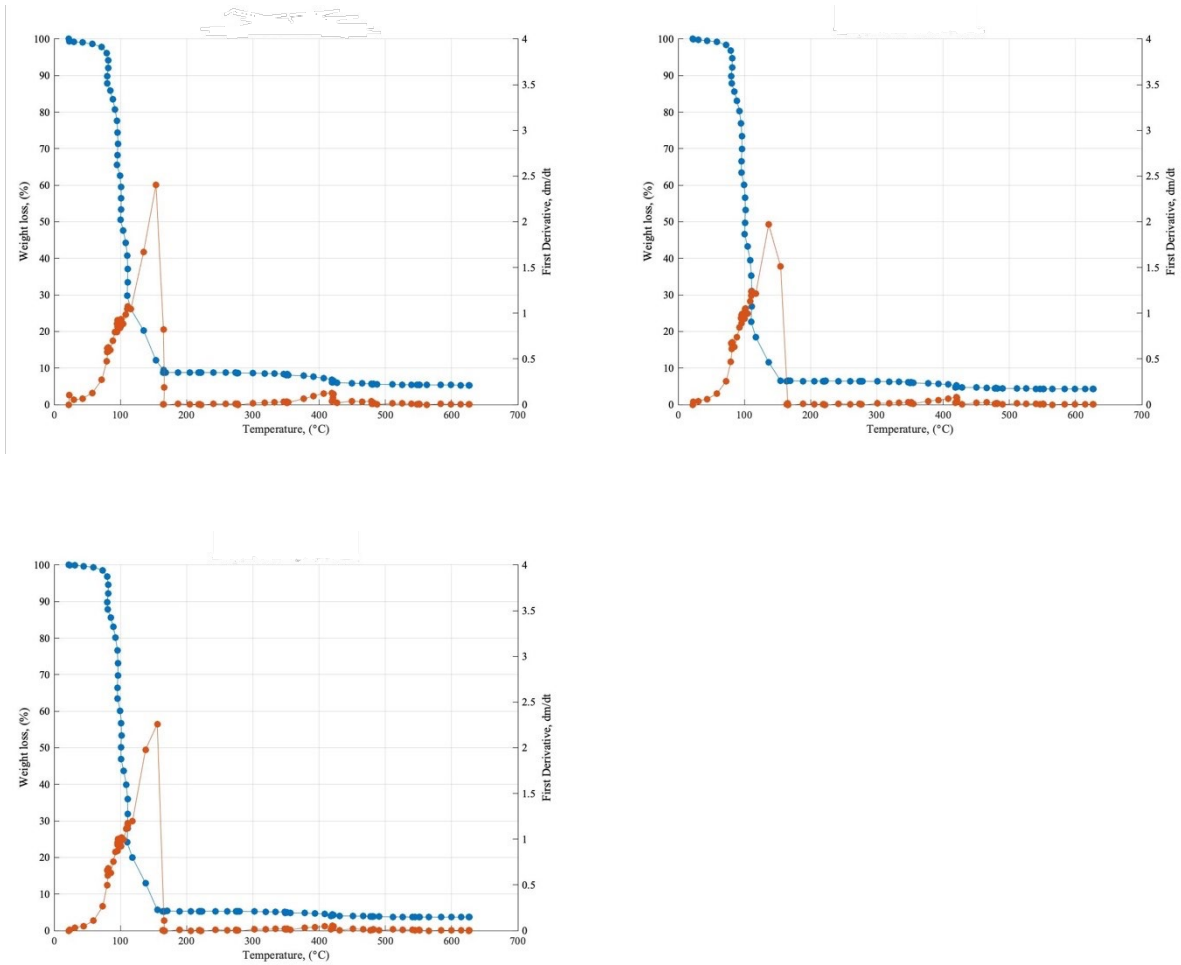


Figure A. 3. The weight loss and the first derivative for the paraffinic froth treatment tailings emulsion, performed in triplicate.

Table A. 9. The summary of the weight loss for the paraffinic froth treatment tailings.

Temperature		Heating rate (°C/ min)	PFT - 1 (%)	PFT - 2 (%)	PFT - 3 (%)	Average weight loss (%)	Average weight loss (g)
Start (°C)	End (°C)						
25	80	5	10.14	10.11	10.12	10.13	0.452
80	95	1	24.29	26.42	26.45	25.72	1.149
95	100	1	8.72	16.88	16.46	14.02	0.626
100	110	1	29.80	23.91	22.84	25.52	1.140
110	165	5	20.97	16.22	18.81	18.67	0.834
165	220	5	0.03	0.02	0.02	0.02	0.001
220	275	5	0.12	0.07	0.07	0.09	0.004
275	350	5	0.54	0.43	0.30	0.42	0.019
350	420	5	1.95	1.17	0.86	1.33	0.059
420	480	5	0.61	0.35	0.25	0.40	0.018
480	550	5	0.16	0.13	0.14	0.15	0.007
550	650	5	0.10	0.06	0.03	0.06	0.003
Total weight loss			97.44	95.78	96.35		

Table A. 10. Mass balance for the centrifuged solids for the paraffinic froth treatment tailings

Component	Weight percent (%)
Lighter hydrocarbons and water (25 °C and 165 °C)	94.05
Heavy hydrocarbons (165 °C and 350 °C)	0.53
Bitumen residue	0.49
Mineral solids	3.48
Total	98.54

A.1.5. TGA Experiments for the centrifuged solids from the PFT

Table A. 11. The sample names with the initial and final masses for the centrifuged solids from the paraffinic froth treatment tailings

Sample name	Initial mass (g)	Final mass (g)
PFT – Solids – 1	4.5134	1.3620
PFT – Solids – 2	4.3772	1.3967
PFT – Solids – 3	5.6868	3.3355

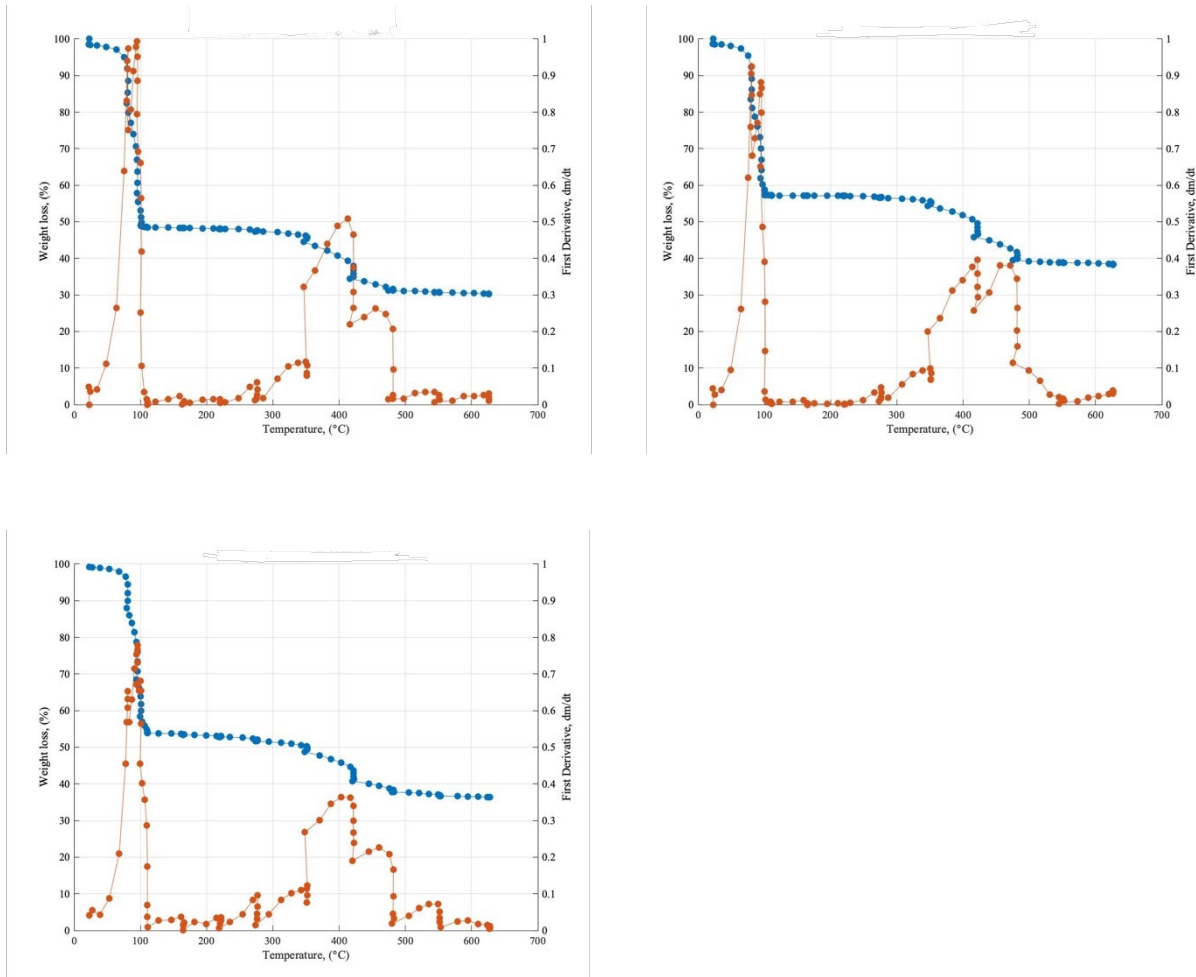


Figure A. 4. Thermograms for the centrifuged solids from the paraffinic froth treatment tailings performed in triplicate.

Table A. 12. Weight loss for the individual and average for the centrifuged solids from the paraffinic froth treatment tailings performed in triplicates.

Temperature		Heating rate (°C/ min)	PFT -	PFT -	PFT -	Average weight loss (%)	Average weight loss (g)
Start (°C)	End (°C)		Solids - 1 (%)	Solids - 2 (%)	Solids - 3 (%)		
25	80	5	17.63	13.86	17.55	15.75	0.700
80	95	1	24.55	22.37	11.46	23.46	1.043
95	100	1	8.75	12.09	0.19	10.42	0.463
100	110	1	0.52	0.70	0.03	0.61	0.027
110	165	5	0.20	0.11	0.08	0.15	0.007
165	220	5	0.19	0.03	0.02	0.11	0.005
220	275	5	0.44	0.29	0.26	0.36	0.016
275	350	5	1.83	1.25	1.10	1.54	0.068
350	420	5	7.95	6.01	4.80	6.98	0.310
420	480	5	6.32	7.86	3.33	7.09	0.315
480	550	5	0.86	2.79	2.07	1.83	0.081
550	650	5	0.58	0.73	0.47	0.65	0.029
Total Weight Loss			69.82	68.09	41.35		

Table A. 13. Mass balance for the centrifuged solids from the paraffinic froth treatment tailings

Component	Weight percent (%)
Lighter hydrocarbons and water (25 °C and 165 °C)	50.40
Heavy hydrocarbons (165 °C and 350 °C)	2.01
Bitumen residue	4.14
Mineral solids	31.04
Total	77.17

A.2. Summary of the centrifugation experiments

Since the driving factor in the successful centrifugation relies on two parameters: speed and time. The speed used was 7000 rpm and the times were varied from 15 minutes, 20 minutes and 30 minutes, at which points pictures of samples were taken to demonstrate the effect of the time for centrifugation. These were performed for the naphthenic and the paraffinic froth treatment tailings.

As seen above there can be three main zones in the tubes. The time chosen was 30 minutes as it resulted in the supernatant with the greatest clarity. The centrifugation time beyond 30 minutes was not pursued as it had negligible impacts on the aqueous filtrate. Additionally, as the collected aqueous filtrate would be filtered using the vacuum filtrate apparatus, it was unnecessary to increase the centrifugation time.

The sample summary of the centrifugation experiments for the naphthenic and paraffinic froth treatment tailings are shown in Table A14.

Table A. 14. Mass balance for the naphthenic froth treatment tailings and the paraffinic froth treatment tailings before and after the centrifugation experiments.

Naphthenic Froth Treatment Tailings						
Tubes Position	Emulsion (mL)	Emulsion (g)	Solid phase (g)	Aqueous phase (g)	Mass loss (g)	Mass loss (%)
1,2	96	99.94	16.28	66.93	16.73	16.74%
3,4	94	101.26	12.62	81.5	7.14	7.05%
4,5	91	95.67	12.16	75.81	7.7	8.05%
Paraffinic Froth Treatment Tailings						
Tubes Position	Emulsion (mL)	Emulsion (g)	Solid phase (g)	Aqueous phase (g)	Mass loss (g)	Mass loss (%)
1,2	88	90.96	15.67	70.12	5.17	5.68%
3,4	87	96.01	19.1	73.13	3.78	3.94%
4,5	93	95.92	38.55	54.12	3.25	3.39%

A.3. IR spectra for the various samples

The spectra from the FTIR for the standards for acetic acid, chloroform, distilled water and acetone are shown in Figure A5 and Figure A6.

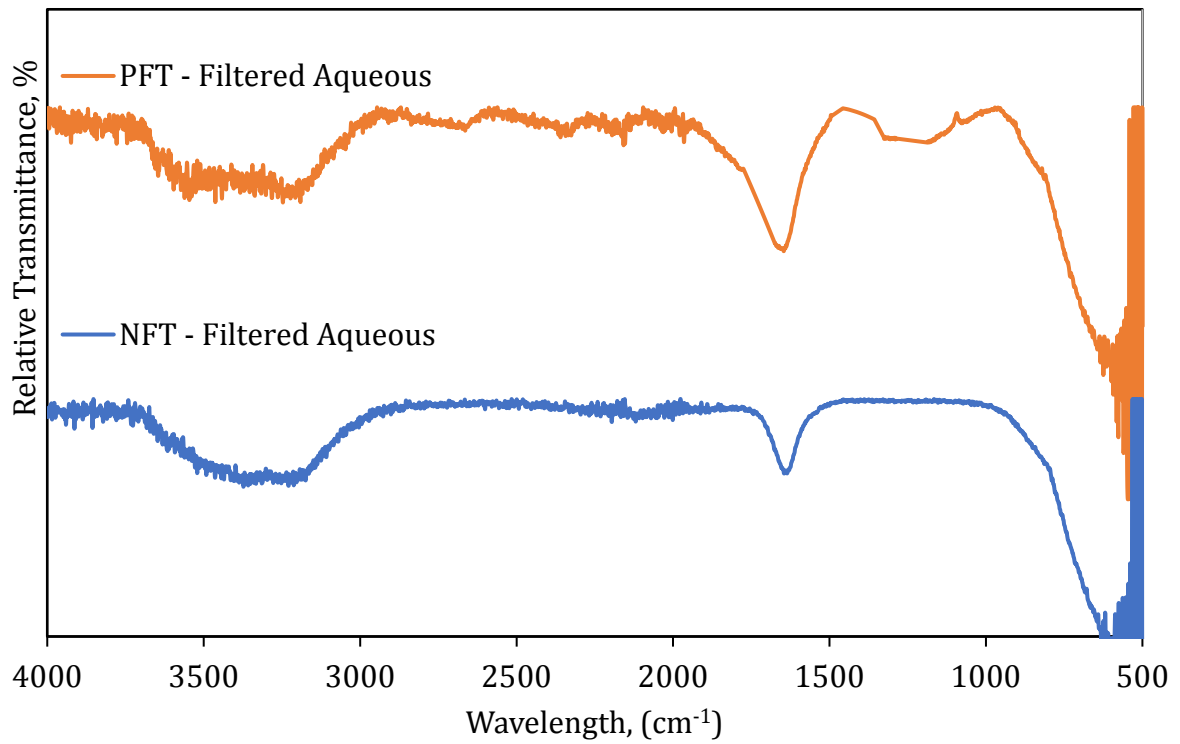


Figure A. 5. Infrared spectra for the comparison for the paraffinic and the naphthenic froth treatment tailings

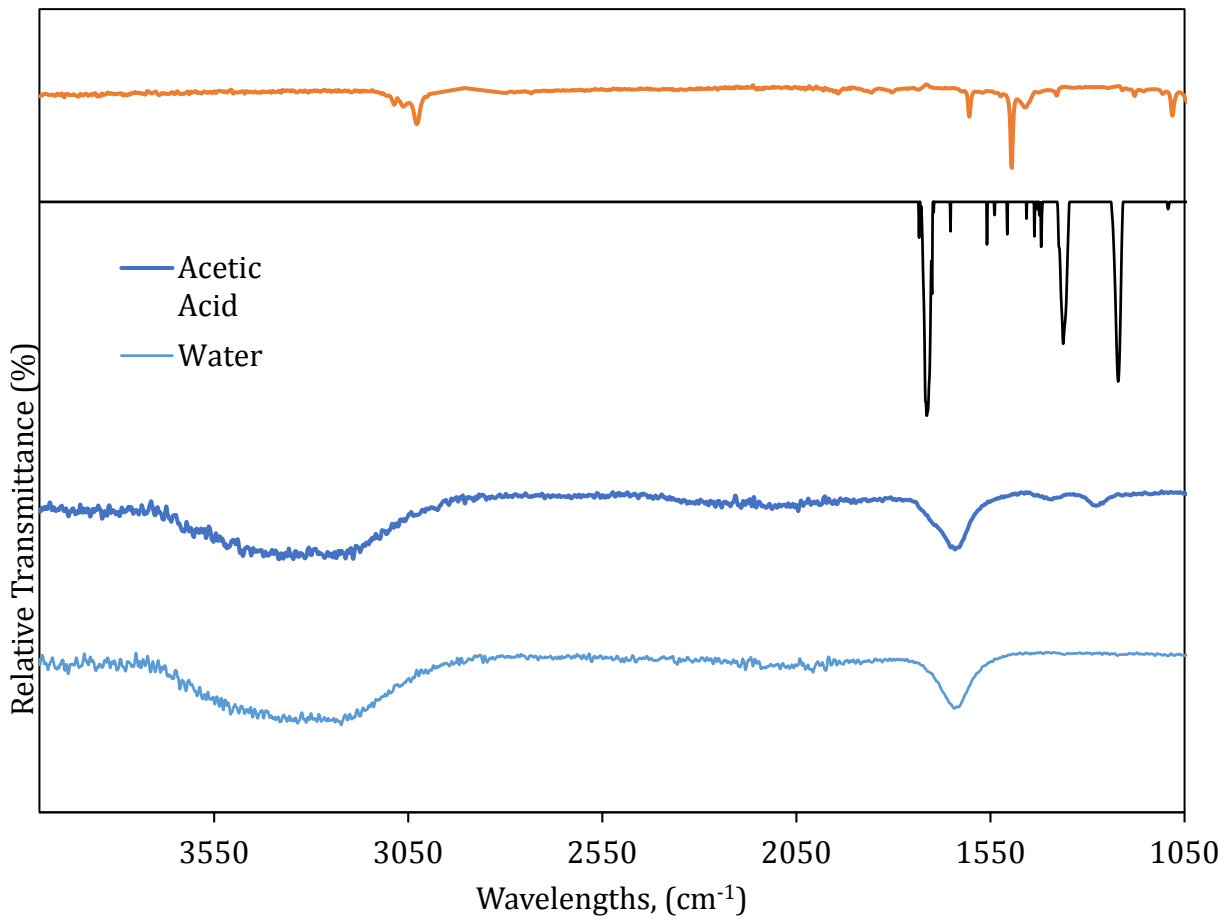


Figure A. 6. IR spectra for the standard solutions for pure toluene, chloroform, distilled water and acetic acid.

A.4. Diluted NMR spectra for the toluene and the heptane extracts

The samples were prepared with 0.1 mg of sample and 700 μ L of chloroform-D was added. The samples temperatures were raised to 30 C prior to any analysis. The low-resolution NMR spectra performed for the following materials is summarized as follows in Figure A7 to Figure A14.

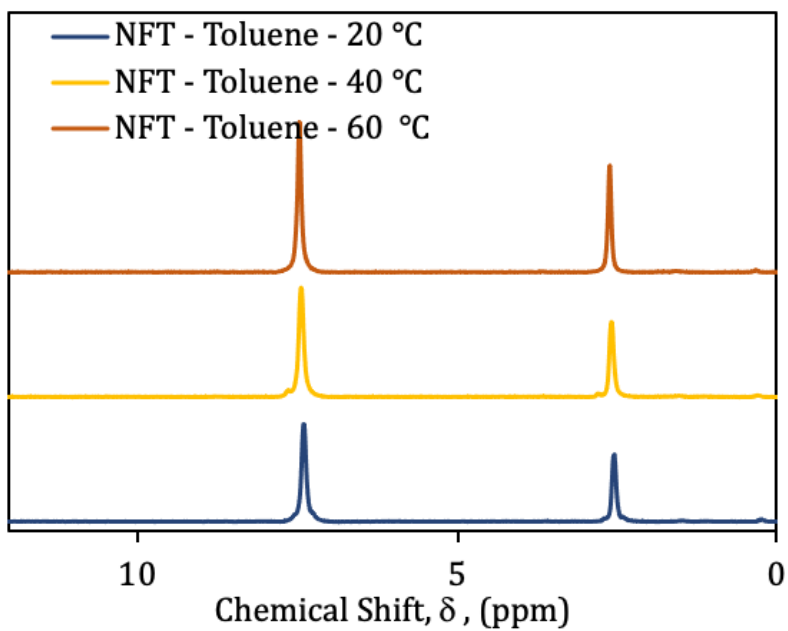


Figure A. 7. NMR spectra with NFT toluene at different temperatures.

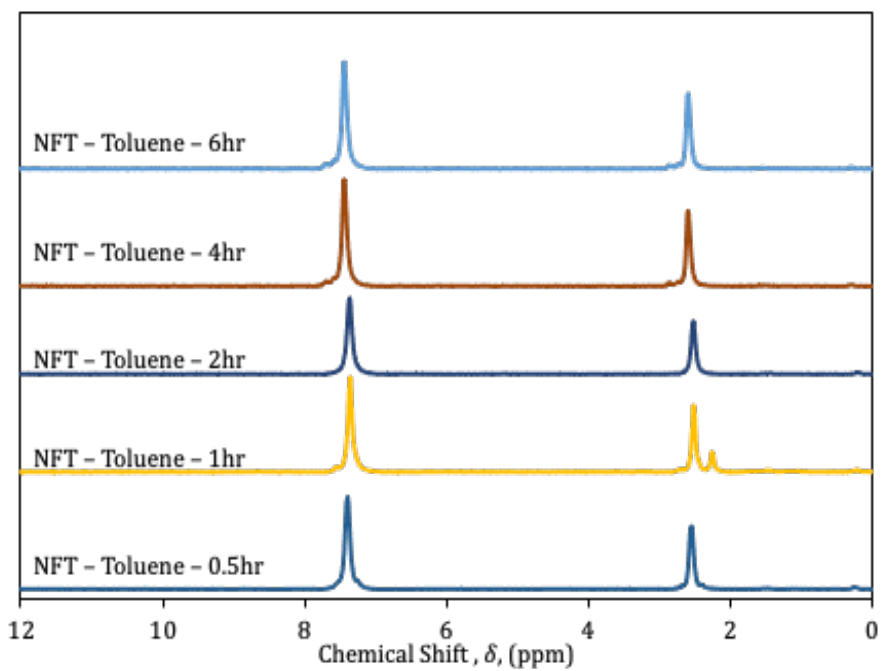


Figure A. 8. NMR spectra for the NFT toluene extracts at different contact times

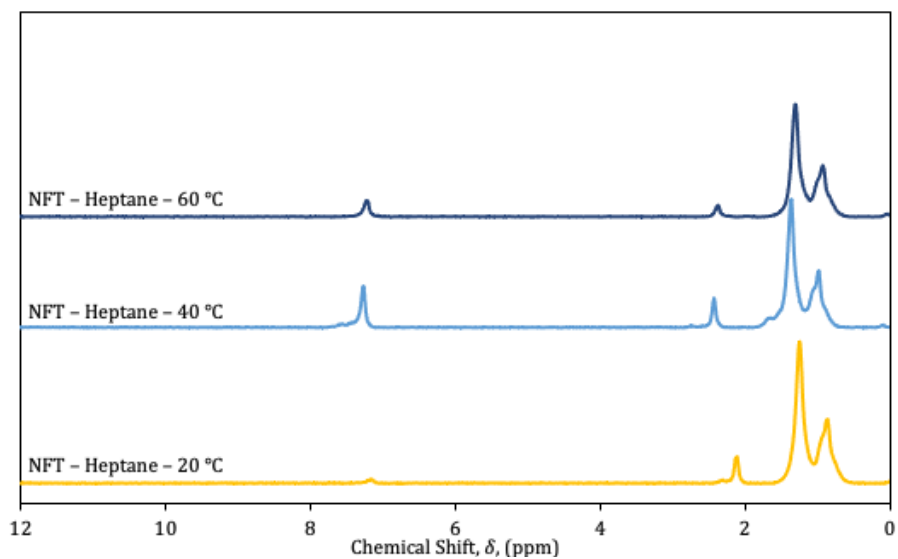


Figure A. 9. NMR spectra for the NFT heptane extracts at different temperatures

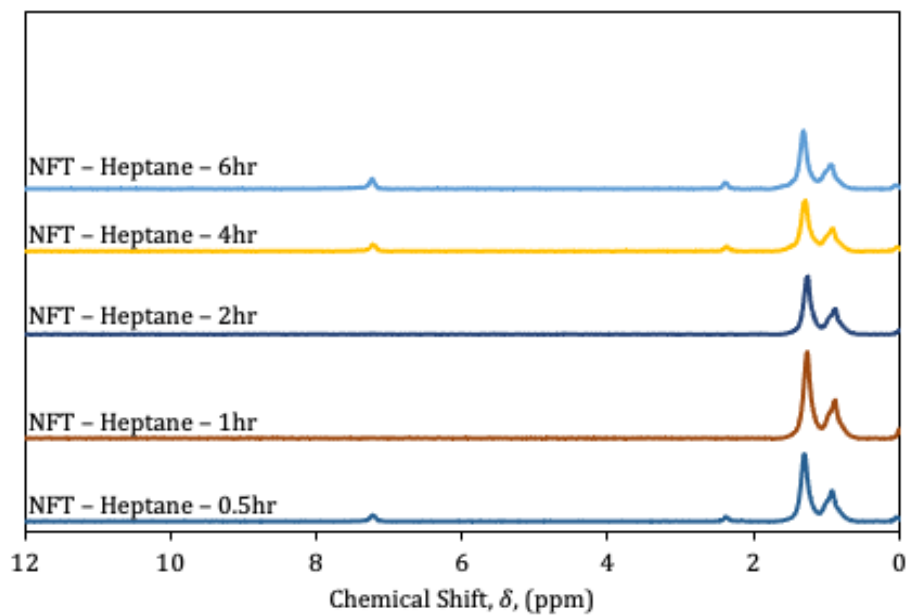


Figure A. 10. NMR spectra for NFT heptane extracts collected at different contact times

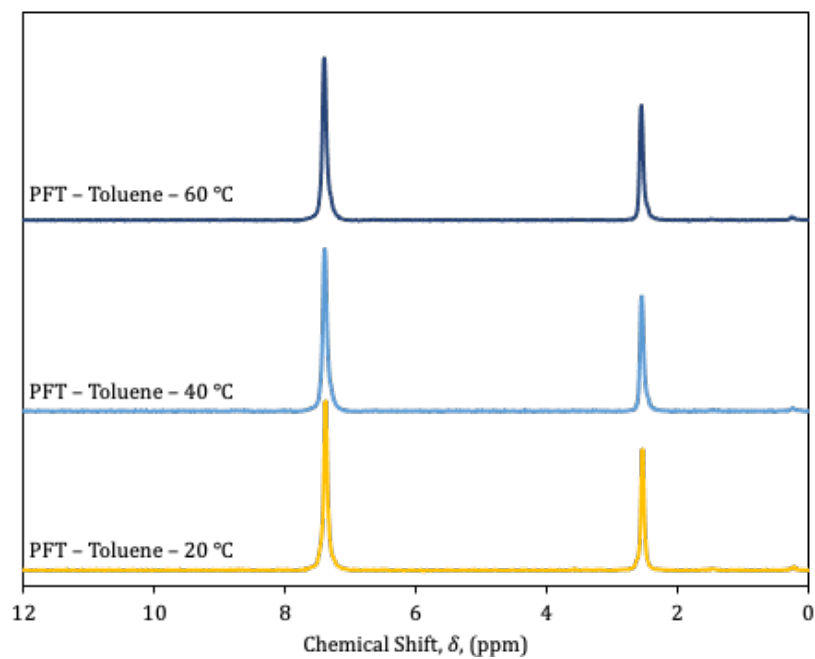


Figure A. 11. NMR spectra for PFT toluene extracts collected at different temperatures

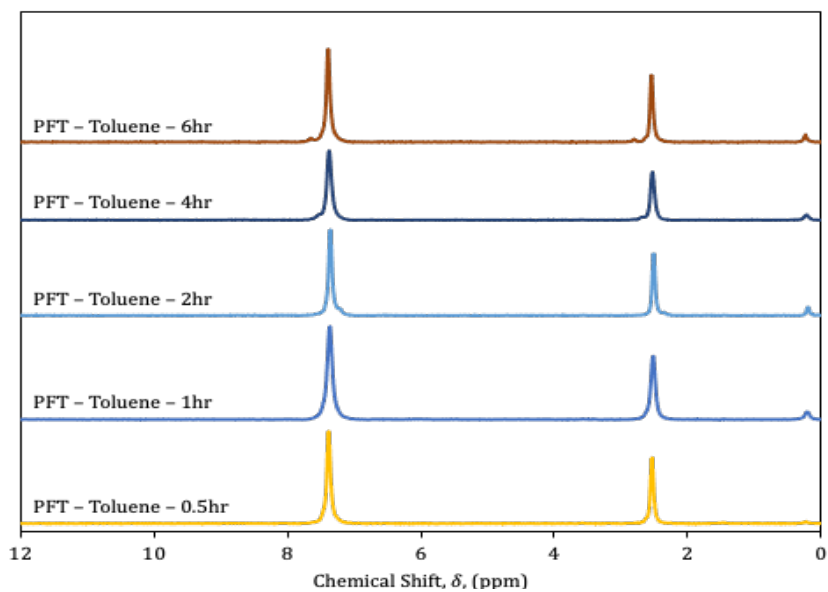


Figure A. 12. NMR spectra for PFT toluene extracts at different contact times

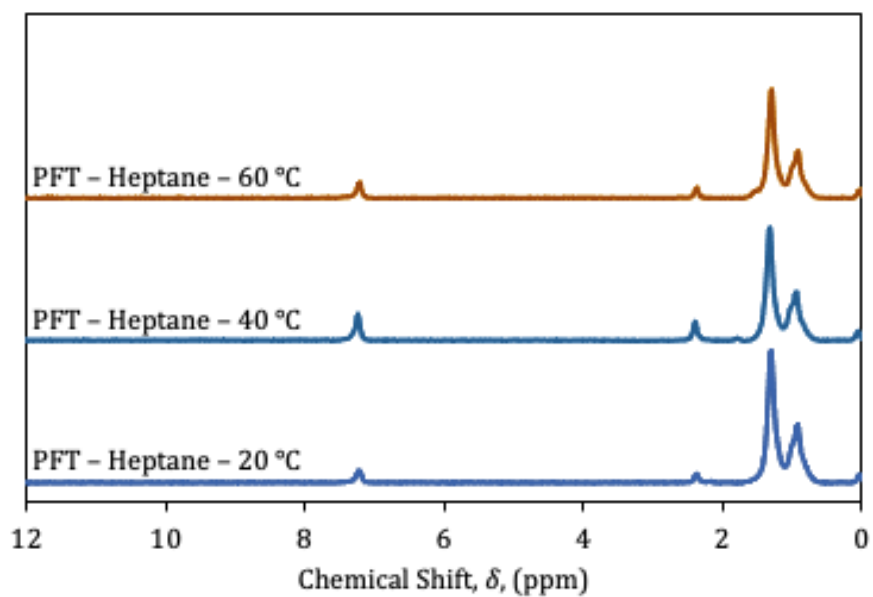


Figure A. 13. NMR spectra for PFT heptane extracts at different temperatures

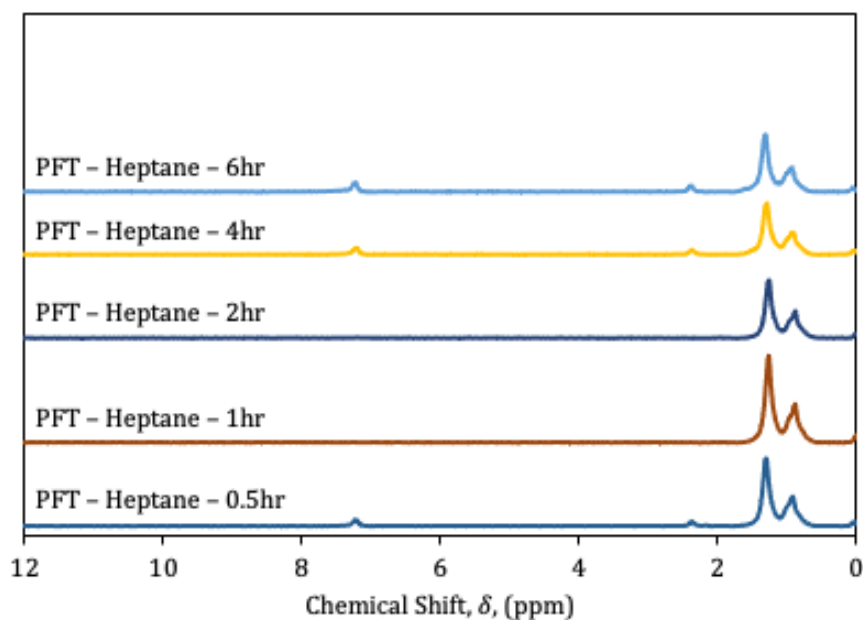


Figure A. 14. NMR spectra for PFT heptane extracts collected at different contact times.